Microalloyed Steels

[an invited review for Ironmaking and Steelmaking]

T.N. Baker

Metallurgy and Engineering Materials Research Group

Department of Mechanical and Aerospace Engineering

University of Strathclyde

Glasgow

G1 1XJ.

21 September 2015

Abstract

This review considers the compositions, the main process routes, microstructure, and structural properties of microalloyed steels. The background and brief history are followed by sections dealing with aspects of precipitation which control grain size and dispersion strengthening in ferrite-pearlite steels, the approaches to modelling thermomechanical processing and the influence of multiple additions of transition metals on properties. High strength acicular ferrite/bainite steels used for linepipe are included and lead to super bainite steels. Around 12% of the world strip production is processed by the thin slab direct charging route, which is considered in some detail. The weldability of microalloyed steels now embraces joining using friction stir welding, which is discussed.

Over the years, many approaches have been developed to predict the structural properties of microalloyed steels. They comprise several quantifiable microstructural features including atom clusters, relatively recently identified through atom probe tomography. A comprehensive collection of references is provided.

Keywords Niobium, vanadium, titanium steels ;Thermomechanical Processing; Microstructure; Structural properties; Acicular ferrite and bainitic steels; Thin slab direct charging; Friction stir welding; Components of strengthening; Reviews.

1 Introduction

This review follows two previous reviews by the present author on 'microalloyed steels'.[1,2] Since the second of these was published in 1992, an excellent book by Gladman [3] and several reviews closely related to microalloyed steels have appeared.[4-7] Also, reviews on specific elements in microalloyed steels have been published. These include the influence of additions in microalloyed steels of niobium by DeArdo[8], an overview of titanium microalloyed steels by Pickering[9] and reviews of vanadium by Langneborg et al[10, 11] and Baker[12], and of zirconium by Baker [13], together with the effects of aluminium nitride in steel by Wilson and Gladman[14]. In the main,

these publications deal with microalloyed steels having a ferrite-pearlite (FP) microstructure.

What therefore is new and justifies yet another review? In the intervening years, there has been a continual drive to produce high strength structural steels at a lower cost. Therefore microalloyed steels have progressed in several directions. A better understanding of the role of both the microalloying additions and the deformation processes, usually hot rolling, has been sought. Thermomechanical processing has been refined through a better understanding of the relationships between processing parameters, especially those involving controlled rolling, and microstructure and properties. Direct charged thin slab processing of microalloyed steels is an example of a developing route, (by 2007, 12% of the World's strip), which for some products, is more economic and has environmental advantages over conventional processes. The extension of high strength microalloyed steels into non-F-P microstructures, having yield strengths (σ_y) >500MPa, for such applications as pipe-line and automobiles is well advanced. However, the application of friction stir welding to microalloyed steels, which reduces residual stresses associated with the fusion welding processes, is at much earlier stage of commercial exploitation. At a fundamental level, the strength contributions from nano-precipitates is being investigated, which, in some cases, may change the way estimates of contributions to strength based on microstructure are summated. The modelling

of hot working processes involving microalloyed steels is a work still in progress. All these areas will be included in this review. However, with ~130,000 hits on Google for 'microalloyed steels', the work reviewed is inevitably selective. It is based on well-cited papers that the author has been aware of for some time, and recent papers that make a novel contribution to the field from the many research groups world-wide, that I follow.

2. Background

The estimated world production of steels of all classes for 2014 is about 1.65 billion tonnes, of which 50% is accounted for from China.[15] Of this total, an ~12%, equal to some 200 million tonnes, a substantial component, is made up of microalloyed steels.[16]

Compared to mild steel, with a lower yield strength, σ_y, of 150-200 MPa, current microalloyed steels have σ_y values in the range of 350 to 800MPa, with the potential to exceed 1000MPa. [17]

Microalloyed (MA) or High Strength Low Alloy (HSLA) steels prior to the 1980's, contained typically, 0.07 to 0.12% carbon, up to 2% manganese and small additions of niobium, vanadium, titanium, (all usually max. 0.1%) in various combinations.[18] (The steel compositions are given in wt.-%, throughout the paper, unless stated otherwise.) Other elements which might be present

include molybdenum, zirconium, boron, aluminium, nitrogen and rare-earth metals.

Vervynct et al [7] compiled a useful table of alloying elements normally present in microalloyed steels, which, with the addition of zirconium and boron, is reproduced in Table 1. The microalloying elements are used to refine the grain microstructure and /or facilitate dispersion strengthening through precipitation. They are normally regarded as having a low hardenability effect.[19]

Table 1 Alloying elements frequently used in microalloyed steels

Element	Wt-% in steel	Influence
strengthener		
Mn	0.5-2.0	delays austenite decomposition during accelerated cooling
		decreases ductile to brittle transition temperature
		strong sulphide former
Si	0.1-0.5	deoxidizer in molten steel
		solid solution strengthener
Al	<0.02	deoxidizer
		limits grain growth as AlN
Nb	0.02-0.06	very strong ferrite strengthener as Nb(C,N)
		delays $\gamma \rightarrow \alpha$ transformation
Ti	0-0.06	γ grain size control by TiN
		strong ferrite strengthener
V	0-0.10	strong ferrite strengthener by V(C,N)
Zr	0.002-0.05	γ grain size control [Zr(C,N)]
		strong sulphide former

N	<0.012	forms nitrides and carbonitrides with
Mo	0-0.3	promotes bainite formation ferrite strengthener
Ni	0.0.5	increases fracture toughness
Cu	0-0.55	improves corrosion resistance ferrite strengthener
Cr	0.1.25	with Cu, increases atmospheric corrosion resistance
B	0.0005	promotes bainite formation

Controlled additions of sulphur, and occasionally tellurium, are also added to improve the machinability.[19] The original aim was to develop high strength and toughness in FP steels in the as-rolled condition. Owing to their superior mechanical properties, they allowed a more efficient design, with improved performance, even under difficult environmental conditions. Furthermore, they permit reductions in component weight and manufacturing cost. For more information on the physical metallurgy of the elements of importance in microalloyed steels, attention is drawn to the book by Gladman.[3]

To avoid any confusion, the present writer prefers to avoid the use of the term 'high strength low alloy steels, HSLA steels', and use 'microalloyed steels' to describe those with micro-additions of niobium, titanium , vanadium and zirconium, either singly or in combination, forming carbides, nitrides or carbonitrides, with a face-centred cubic structure. Low alloy steels, a much earlier defined class of steels than microalloyed steels, are generally regarded as containing less than 3.5wt.% total of alloying elements, and included Cr (0.5-

2.5%),Mo ≤ 3% and V ~1%. These steels were developed as creep resistant steels, but had an upper temperature limitation < 400°C, with applications, as discussed by Oakes and Barroclough[20], in the earlier British aero gas turbines, and by Robertson[21], in coal power energy producing plants. The Cr Mo grades were normalised, while the Cr Mo V types were used in the normalised and tempered condition, to develop the alloy carbides in a bainitic microstructure, which conferred their particular properties. While the earlier microalloyed steels sought to avoid transformation to acicular ferrite and bainite, modern microalloyed steels, built upon a sounder understanding of the processing routes and the development of microstructure than was available prior to the 1980's, embrace these phases[17].

In microalloyed steels, FeNb consumption has grown threefold during the last 25 years and the most part of this growth has been noticeable over the past ten years. Fig 1 shows the trend in ferro-niobium production. Also, the development of microalloyed steels was far greater and far quicker for flat products than for long products. [22]

The material is produced preferably by a thermomechanical rolling process, also known as controlled rolling, possibly with accelerated cooling, which maximize grain refinement as a basis for improved mechanical properties. Prior to thermomechanical processing, the steel was heated into the austenite temperature range for all of the precipitates to be taken into solution; after

forming, the material must be quickly cooled to 600°C to 540 °C.[18] Medium carbon directly quenched (DC) microalloyed steels, avoiding FP microstructures, can also be forged.[23]

Microalloyed steels lie, in terms of performance and cost, between carbon steel, or mild steels and low alloy steels mentioned above. Until around 1980, low alloy steels were designed to have a yield strength between 500 and 750 MPa without heat treatment. The weldability is at least equal to that of mild steel, and can be improved by reducing carbon content while maintaining strength. Fatigue life and wear resistance are superior to similar heat-treated steels. The disadvantages are that ductility and toughness are not as good as quenched and tempered (Q&T) steels.[18]

Cold-worked microalloyed steels do not require as much cold working to achieve the same strength as other carbon steels; this also leads to greater ductility. Hot-worked microalloyed steels can be used from the air-cooled state. If controlled cooling is used, the material can produce mechanical properties similar to Q&T steels. Their machinability is better than Q&T steels because of their more uniform hardness and their FP microstructure.[18] Because FP microalloyed steels are not quenched and tempered, they are not susceptible to quench cracking, nor do they need to be straightened or stress relieved. However, because of this, they are through-hardened and do not have a softer and tougher core like Q&T steels.[18]

Current UK standards which contain specifications for microalloyed steel grades are BS EN 10025-3:2004 & BS EN 10025-4: 2004 (UK/EU). Industry-specific grades include: C38, C38 Modified (includes Tellurium), C42, C42 Modified (includes Tellurium), 49MnVS6, Vanard™ series and Hypress™ series (for narrow strip products).[18] Table 2 gives the mechanical properties for various grades of pipeline steels discussed throughout this paper.

Table 2

Mechanical properties for pipeline steels

Grade	YS (MPa)	TS (MPa)	YR (%)	El%
X65	≥448	≥ 530	≤90	≥ 24
X70	≥482	≥565	≤ 90	≥ 23
X80	≥551	620- 827	≤93	≥ 22
X100	≥690	≥760	90	
X120	≥883	≥ 1023	90	

3. History of microalloyed steels

The main development of microalloyed steels has taken place over the past 50 years, and was initially concentrated on niobium additions. The term microalloying, as applied to steels, is generally accepted as emanating from the paper by Beiser [24] published in 1959, which reported the results of small additions of niobium to commercial heats of a carbon steel. However, it has not been recognized that microalloying as such, first occurred some 35 years earlier,

when small additions of zirconium were added to plain carbon steels, and the effects reported by Field [25,26] and by Beckett [27]. Like many other scientific and engineering innovations, military conflict was also the driving force in the case of the development of zirconium steels. During the period of a few years immediately preceding the entry of the United States into the First World War in 1918, the US War Industries Board decided upon an intensive experimental programme with the aim of possible large scale production of zirconium steels suitable for light armour. However, this appeared to be discontinued when the conflict ended, and interest moved to low alloy Q&T steels, normally containing chromium, molybdenum and vanadium additions of 0.5 to 3%.

Much of the early work on the niobium microalloyed steels, which re-emerged in the late 1950's and early1960's, was concentrated in the USA and UK. In the UK, the University of Sheffield, BISRA (British Iron and Steel Association) based in Sheffield and Swinden Laboratories of the United Steel Corporation, based nearby in Rotherham, all made significant contributions. The history of this development has been well documented in an excellent review by Morrison, [5] who [28], together with Woodhead, [29] played a major part in understanding the role of niobium carbide in contributing to dispersion strengthening and grain refining of ferrite, leading to greater strength than found in mild steels. His initial paragraph, which is quoted here, sets the scene: 'In 1958, it was announced in the Journal of Metals that the Great Lakes Steel Corporation, a

division of the National Steel Corporation of the USA, had entered the market with its GLX-W series of niobium–treated steels, the first steel company in the world to do so. What made this development so special was the very small, relatively low cost addition of niobium used, 0.005 to 0.03%, and the relatively large resultant strengthening effect, combined with good toughness. Also, the niobium was added to an ordinary semi-killed C–Mn steel (mild steel or mild carbon steel) and changed its strength level from a low yield strength of around 300 MPa to a high yield strength of up to 415 MPa for the GLX-60-W grade, equivalent to a conventional alloy steel.'

History has shown that some of the major advances owe their success to the chance simultaneous appearance several, apparently disparate, facets. This was certainly the case with microalloyed steels. The marketing by the Great Lakes Steel Corporation in the USA occurred in the same decade as the series of publications by Hall [30], Petch [31] and Cottrell [32], which provided the first real understanding of the factors which control the strength, and to some extent, the toughness of crystalline material.

The Hall–Petch equation conveniently allows σ_y, the lower yield stress, (or often, in practice, the 0.2% proof stress) to be related to the ferrite grain size, d:

$$\sigma_y = \sigma_o + k_y d^{-1/2} \qquad (1)$$

where σ_o and k_y are experimental constants. The Hall–Petch equation as a basis for assessing the components of strengthening will be considered later.

Over the same period, the first high resolution (0.8nm) transmission electron microscope [TEM], the Siemens Elmiskop I, became available, and in the UK, precipitation in Q&T low alloy steels was one of the first areas studied using this new equipment. Electron micrographs had appeared in a number of papers emanating from the USA prior to this time. These were mainly concerned with steels, but apart from utilizing the higher resolution then available compared with the optical microscope, little attempt was made to extend the interpretation; this was due mainly to the studies being based on surface replicas. Following the pioneering work of Heidenreich[33] in 1949, Hirsch, Horne and Whelan[34] at Cambridge, successfully prepared thin foils of a number of alloys, including steels. The theories of kinetic and dynamic diffraction contrast were developed over a period of years, which allowed the details of features observed in foil TEM specimens, such as grain boundaries, dislocations and precipitates, to be interpreted.[35] This is well described by Hirsch[36].

Over the past two decades, the electron back scattering diffraction (ESBD) technique, originally devised for the TEM, has been widely used with an SEM to obtain information on details of grains and sub-

grains and particularly their boundaries [37], through the availability of versatile software. This has provided opportunities to quantify what were regarded formerly as difficult phases, such as bainite and MA (martensite/austenite) phase, which are important constituents in some modern high strength/high toughness microalloyed steels.

A fourth factor was the developments associated with steelmaking and hot rolling, the latter to be the main route for producing microalloyed steels. New stricter procedures were needed to ensure niobium steels in particular, achieved their potential properties. These involved a knowledge of the solubility limits of niobium carbide and nitride [3,8], to ensure that the precipitates which formed during casting, were taken into solution prior to rolling. This often involved running soaking pits at higher temperatures than normal practice. Also, it soon became apparent that the number of rolling passes and their temperature needed to be controlled, and hence the birth of 'controlled rolling' [38-40]. Within a short time, this led to the introduction of computer control in many other aspects of steel-making, and later the application of the results of academic computer modelling to aid the whole complex process of achieving a small, < 10 μm, homogeneously distributed ferrite grains.[41-43]

Fig 2 shows schematically how the microstructure and properties of plate steels changed over time with advances in alloy design and processing.[7,44]

It is obvious from Fig. 2, that the accelerated cooling after rolling was largely responsible for the very high strengths attainable, practically independent of composition. With suitable cooling practices, σ_y levels >690 MPa (X100) can be achieved in low C steels containing less than 2 wt-%Mn and with carbon equivalent and weld cracking parameter near 0.5 and 0.2 respectively.[6]

4. Chemical compositions and precipitation in microalloyed steels

DeArdo et al [6] posed the question 'what is the role of the microalloying element (MAE) in obtaining strength levels in these steels?' It is answered by considering 'the early steels (pre-1980), where air cooling of plate and high coiling temperatures of strip were used. As noted above, these were the FP steels with strengths up to ~420 MPa (X60) for gauges up to 18 mm. The most obvious contributor to strength was grain refinement, as was clearly shown by quantitative optical microscopy. There is no doubt that the MAE was responsible for this contribution through its effect on austenite conditioning. Other contributions included solid solution strengthening by the Mn, Si and others, including the MAE, when retained in solution. Equations have been published quantifying these effects.[3] The other contribution to strength, claimed by researchers studying these early steels, was dispersion hardening by transition metal carbides and nitrides.[5]

The precipitation of carbides and nitrides occur at three different stages during the processing of microalloyed steels [2,3]. Type 1 precipitates are formed during the liquid phase and during or after solidification, on the liquid-solid interface and in delta ferrite. These precipitates are very stable, and while they are normally too large to influence recrystallization of austenite, the smallest may effectively retard coarsening in austenite during reheating or during a welding cycle.[45]

Type 11 particles are precipitated in austenite after solution treatment and during hot deformation, such as controlled rolling, as the temperature is decreasing.[46] The precipitates are strain induced, and can retard the recrystallization of austenite. Grain refinement of microalloyed steels is mainly due to this group of particles. [47-49]

Finally, Type 111 particles are formed during or after the austenite to ferrite phase transformation, nucleating on the austenite/ferrite interface and in ferrite [50]. Dispersion strengthening in ferrite normally occurs through these changes and a fine precipitate dispersion is usually observed.

The carbides and nitrides of the transition metals, which precipitate in microalloyed steels, are B1 NaCl (Fm3m) type compounds. Several precipitate nucleation processes have been recognized in microalloyed steels. These include homogeneous precipitation, resulting in coherent precipitates with strain fields, leading to semi-coherent and incoherent precipitates, interphase

precipitation, heterogeneous precipitation on grain boundaries and dislocations, where the latter is often referred to as strain induced precipitation (SIP).

A pre-precipitation grouping of atoms, nano-precipitates, known as GP zones in non-ferrous alloys and also described as 'clusters' in microalloyed steels, has received increased attention over the past decade ,due to the development of atom probe tomography(APT). Several APT studies on niobium microalloyed steels have reported.[51-56] These nano-precipitates are assuming importance, due to the claim that they provide a significant contribution to the yield strength. [57] Following a 1250ºC homogenization, water quenching, and tempering at 600 ºC in a salt bath for 300s,in a steel containing controlled atomic concentrations of 500ppm Nb and 250ppm C and N, monolayer GP zones were detected by Danoix et al [53]. These were platelets comprised of niobium and nitrogen atoms, ~ 4 x 4nm in size, lying on $\{100\}_\alpha$ planes. The amount of iron and carbon in the GP zone was ~ nil. They[53] also claimed that the homogeneous nucleation mechanism for the nitrides, which nucleated heterogeneously on dislocations, was completely different from that of carbides. However, different results were obtained by Breen et al[55], who used APT to study a steel containing 0.03 C-0.007N- 0.084Nb, finish rolled at 879 ºC and coiled at 567 ºC. Samples were aged to investigate the Nb (C, N) precipitation in ferrite. Table 3 compares the nano-precipitate composition following three ageing treatments. It can be seen that the longer ageing results in more C and N atoms being trapped within the

nano-precipitate, which had a similar composition to the nominal composition of the steel. Even after ageing for 40 min at 700 ºC, the nano-precipitate size of ~2.6nm length by 2.8nm width, was still considered to be less than the critical size for coherency loss with the ferrite matrix. As most microalloyed steels are used in the as-rolled condition, it is relevant to examine how hot deformation, rather than ageing, influences the development of nano-precipitates.

Table 3

Comparing the bulk composition measurements of C, N and Nb to the nominal composition [55]

Dataset	C (at%)	N (at%)	Nb (at%)
Nominal composition	0.140	0.028	0.050
240 h @ 525°C	0.063	0.018	0.051
4 min @ 700°C	0.053	0.012	0.056
40 min @ 700°C	0.142	0.021	0.049

Bulk atomic compositions were calculated on IVAS® using background correction and decomposition of molecular ions.

Pereloma et al[51,56] used APT to compare niobium clustering in a Nb-Ti microalloyed steel, deformed above and below the non-recrystallisation temperature, T_{nr} , which represents the start of the inhibition of complete static recrystallization during cooling between rolling passes. Using a Gleeble simulator, they studied a steel containing 0.081C- 0.064Nb- 0.021Ti-0.003V-0.017N. After austenitising at 1250 ºC and roughing at 1100 ºC, samples were cooled either to 1075 or 825 ºC, deformed at a strain rate of $5s^{-1}$ to a strain of

0.75, before cooling. Similar distributions of >70nm TiN and (Ti, Nb)(C,N) were found in all specimens. 1075 ºC was too high for Nb-C clusters to form, and therefore strain induced precipitation of NbC did not occur. However, after 825 ºC deformation, a relatively high number density of Nb-C clusters occurred, as did SIP of NbC. This implies that the lower deformation temperature of 825 ºC resulted in a higher dislocation density, leading to an increase in the number of nucleation sites for Nb-C clusters. These clusters might be considered as precursors to SIP via heterogenous nucleation of NbC. The above work was extended by Kostryzhev et al[54], to include aspects of the strengthening of the steel through the possibility of clusters being cut, which is discussed below. Coherent precipitates are cut by dislocations, leading to a different strength mechanism than incoherent precipitates. This distinction becomes very important when estimating yield strength from microstructure.

Few observations of coherent precipitates in microalloyed steels have been verified. This is in part, due to the very small size at which they lose coherency. Coherency strain fields associated with transition metal carbides and nitrides have very rarely been reported for precipitates in microalloyed steels, vanadium carbonitride [2] being an exception, Fig 3. Fig 4 shows that the calculated misfit of vanadium carbide and nitride in austenite is much less than for niobium carbide and nitride [58, 59]. Estimates of the limiting size of some coherent carbides and nitrides if they precipitated in ferrite are given in Table 4, which

shows the size when coherency begins to be lost is significantly smaller for NbC than VC. The estimated V-C cluster diameter is in the range 3-13nm, which is larger than that given for NbC in Table 4, based on misfit alone.

Table 4 – Estimated limiting sizes for coherency of platelet carbides and nitrides found in ferrite in microalloyed steels

	Lattice parameter	misfits		Limiting sizes for coherency	
	'a' nm	ε_1	ε_2	x_1 nm	x_2 nm
NbC	0.4470	0.065	0.292	1.54	0.34
NbN	0.4388	0.053	0.279	1.89	0.36
TiC	0.43285	0.043	0.270	2.33	0.37
TiN	0.42540	0.062	0.326	1.45	0.31
VC	0.416	0.017	0.245	5.85	0.41
VN	0.409-0.417	0.006	0.234	8.38	0.43
ZrC	0.4698	0.097	0.322		
ZrN	0.456	0.078	0.303		

ε_1 and ε_2 are the calculated strains parallel and perpendicular to the major axis of the disc shaped particle of diameter x_1 and thickness x_2.

The data in Table 4 is based on the cube on edge orientation relationship first established by Baker and Nutting (BNOR) for tempered steels [60]:

$$(100)_\alpha \ // \ (100)_{MCN}$$

$$<011>_\alpha \ // \ {}_\alpha<010_{MCN}$$

and on the condition that coherency starts to breakdown when the strain at the particle matrix interface equals the Burgers vector magnitude of a dislocation. This is shown schematically [36] in Fig 5. The interfacial energy of B1 carbides and nitrides having the B-N orientation relationship have been studied in detail by Yang and Enomoto.[58, 59] How this affects coherency is still unclear.

Incoherent disc precipitates of VN are seen in Fig 6, where strain fields are no longer present. The fine NbC particles in Fig7, present on a replica, would provide dispersion strengthening.

Interphase precipitation occurs during the transformation of austenite to ferrite and is found, with the possible exception of ZrC and ZrN, for all the transition metal carbides and nitrides, [50] as well as silver[61] and copper [62] precipitates in steels. Dunne [62] pointed out that the many studies by Honeycombe and co-workers [50], usually with highly alloyed ternary or quaternary laboratory steels, and often in the isothermally treated condition, producing high volume fractions of precipitates, were undertaken to elucidate the fundamental mechanisms of interphase precipitation. These are summarized in terms of the morphologies which have been established:

1. interphase precipitation (planar)
2. interphase precipitation (curved)
3. continuous fibre/lath growth
4. precipitation from supersaturated ferrite.

Planar interphase precipitation is typified by parallel sheets of densely populated sheets, related to ferrite by the Baker and Nutting orientation relationship [60], and appear to have a regular spacing, Fig 8. Continuous fibres comprise parallel laths, akin to a very fine pearlite. Details of the mechanisms have been reported in many publications, including refs.1-5, 11, 50, 61, 62.

While interphase precipitation is well established in isothermally transformed steels, it appears to be less important in commercially processed Nb and Ti-Nb as-rolled microalloyed steels. For these steels, this leaves heterogeneously nucleated precipitation associated with grain boundaries, leading to grain refining, and precipitation associated with dislocations (SIP) as the main classes of precipitates. However, compared to the other microalloying elements, vanadium has a much greater solubility in austenite, and therefore remains in solution to a much greater extent during processing in the austenite range. Vanadium–Carbonitride interphase precipitates which form above 700 ºC are recognized as making an important contribution to strengthening, which becomes general V(C, N) precipitation below 700 ºC. The fibrous morphology of V(C, N) is sparse and is never a dominant microstructure. [11]

Vervynct et al [7] considered the principal function of alloying elements in F-P microalloy steels to be ferrite strengthening by grain refinement, dispersion strengthening and solid solution strengthening, all implied by Petch [31]. Solid solution strengthening is closely related to the alloy content, while grain refinement and dispersion strengthening depend on the complex interaction of

alloy composition and thermomechanical processing. For example, the strengthening effect of niobium, the most widely studied element in microalloyed steels, occurs mainly by three microstructural mechanisms: ferrite grain refinement due to austenite grain boundary pinning, retardation of recrystallization, and dispersion strengthening [6]. Each of these mechanisms will be considered more fully below. In addition, alloying elements are selected to influence the reduction in the temperature at which austenite transforms to ferrite and pearlite during cooling. In this way, a fine grained product is produced, which is a major source of strengthening and toughness.

DeArdo et. al,[6] consider that 'the year 1980 represents a bench mark in the strength of microalloyed (MA) steels. From the early days of the 1960s to approximately 1980, the steels being micro-alloyed were low hardenability steels with FP microstructures and $\sigma_y \leq 420$ MPa. These steels were used to develop the principles and interrelationships of microalloying, controlled rolling and air cooling. They were characterised by relatively higher carbon contents and moderate manganese levels, and exhibited FP microstructures after air cooling. Around 1980, both the line-pipe and the automotive industries desired strengths >420 MPa, that could be readily supplied with fine grained FP steels. Clearly, higher strength microstructures were required. The obvious choices were the lower temperature transformation products: matrices comprised of non-polygonal ferrite, acicular ferrite, the bainites and

martensite, either as monoliths or as mixtures. To achieve these microstructures, the combination of higher hardenability and high cooling rates was required. Furthermore, much additional research was needed to reach the required goals consistently and with uniform results. From the processing side, the solution to this dilemma was using water cooling after hot rolling. This was accomplished in the mid-1980s for plate processing by interrupted accelerated cooling (IAC) [63,64] and interrupted direct quenching (IDQ)[65] in plate mills, Fig 9. Runout table water spray cooling to the coiling temperature in hot strip mills had been in practice since the 1960s, but not as a microstructural control tool for increasing strength. This was because of the higher carbon contents of the steels of that era. The benefits of faster rates of cooling and lower coiling temperatures were exploited for achieving higher strengths later with steels of lower carbon contents'.

5. Controlled rolling and controlled cooling

The importance of developing a small grain size in terms of increases in both strength and toughness is evident from the initial work of Hall [30] and Petch[31] mentioned above. As stated by Llewellyn [66], 'the traditional route (prior to the 1970's) to a fine grain size in ferrite–pearlite structural steels has been to incorporate grain refining elements, such as aluminium, and then to normalize the materials from about 920°C after rolling.' He also comments on the fact

that ‘when normalizing was carried out on a niobium treated steel to improve the impact properties, the strength advantage was forfeited. There was therefore a need for an alternative route to a fine grain size in structural steel plate which would overcome both the cost and strength penalties associated with traditional normalizing. As described by Morrison[5] 'the key to obtaining a fine grain size in a low niobium steel (~0.02wt%) is the low finishing rolling temperature, which occurs naturally in thin plates and cross-country mills. Mackenzie [67, 68] collected data from 68 plates, finished rolled from 11 to 38mm, using 14 to 36 passes, which took between 3 and 6 mins in the mill, with finishing temperatures between 800 and 1100°C. He found that finishing temperatures below ~900°C gave acceptable notch ductility, equating to as-rolled plates ≤13mm in thickness. Fig. 10 shows that much greater thicknesses could be tolerated in sections due to their lower rolling rate. As far back as 1958, Vanderbeck [69] reported that ‘European steel producers were adopting lower than normal finishing temperatures during rolling, in order to refine the microstructure and improve properties’. The idea of using a rolling schedule to produce a fine grain size may have originated from so-called cross-country mills, a versatile ‘jobbing’ finishing mill, often used for producing sections or bar in a steel works,where the work-piece usually passed only once through a set of rolls, which were spread over a large area, with the final set some distance from the starting point. Thus the rolling master was always dealing with a loss

of heat, and often the steel was black on reaching the finishing stand. However, at Round Oak Steelworks in Staffordshire, it was noted that when the steel was black at the finish of rolling, the strength and toughness properties were always superior to when the steel finished red. It was on this mill that the writer undertook some of his first controlled rolling trials in 1963.

'Controlled rolling or rolling over a deliberately lowered temperature range compared with conventional hot rolling, is now a widely accepted technique for the production of microalloyed steels.' This statement by Kozasu [70, 71] is as true today as when it was first made in 1968, when the aim of controlled rolling was to produce a steel with a fine polygonal ferrite grain size. Today, this is extended to include acicular and bainitic microstructures. [17]

In his review of controlled rolling, Tamura [40] states that 'the fundamental difference between conventionally hot-rolled and controlled- rolled steels lies in the fact that the nucleation of ferrite occurs exclusively at austenite grain boundaries in the former, while it occurs in the grain interior, as well in the latter, leading to a more refined grain structure.'

Conventional controlled rolling is an example of a TMPT which manage the temperature and deformation during hot rolling, to control the austenite microstructure at the start of transformation. Here, it is essential that recrystallization of austenite is avoided. The original approach was to introduce

a high density of nucleation sites into austenite grains for nucleation of ferrite grains, by hot rolling in the austenite phase field,

After transformation to ferrite and subsequent recrystallization, as first described by Hanemann and Lücke [72], this leads to a refined microstructure. Ferrite grain refinement is due to two mechanisms: (i) fine recrystallized austenite grains formed by hot rolling at intermediate temperatures, and (ii) austenite deformation below the recrystallization temperature, which enhances the nucleation of ferrite.[70]

The first step in the controlled rolling process is to control the austenite grain size during the soaking stage. This is set by the temperature which is necessary to take into solution the microalloying particles, which have formed during cooling following solidification during casting. As is well established, the austenite grain size is related exponentially to the soaking temperature. Therefore a balance exists between the temperature necessary to dissolve the particles, the resultant austenite grain size and the economics of high soaking pit temperatures.[7,70] The importance of the correct soaking temperature for a given steel is well illustrated by Lagneborg et al [8] for Ti-V-N steels. Reducing the soaking temperature from 1250ºC to 1100 ºC reduced σ_y by ~40MPa and the ductile-brittle transition temperature by 15 ºC, due to a reduction in the dissolved amount of titanium and vanadium.

Kozasu et al [70] divided the controlled rolling process into three ranges, associated with changes in the austenite and ferrite grain structures.

1 Deformation in the austenite recrystallization temperature range.

Deformation above 1000°C normally develops coarse recrystallized austenite grains, which transform to a relatively coarse ferrite and upper bainite. The size of the austenite grain size obtained by recrystallization, decreases with increasing strain, which is introduced by the rolling reduction, and eventually reaches a limiting value.[73]

2. Deformation in the unrecrystallized range.

Deformation in the intermediate temperature range from 1000°C to 900°C refines austenite by repeated recrystallization, leading to fine grained ferrite. The austenite grains are elongated (pancaked)and deformation structures result.[74] A build-up of strain is often associated with the formation of twins or deformation bands, which increase the number of potential sites for ferrite nucleation and this, as mentioned above, is regarded as one of the most important aspects of controlled rolling.[40,75]

3. Deformation in the ($\gamma+\alpha$) two phase region.

Deformation below the recrystallization temperature produces 'warm worked' austenite, which leads to a finer ferrite grained microstructure. The third stage deformation has a much larger influence on the final mechanical properties than the first two stages. Rolling to just above the Ar_3 temperature, can result in equiaxed ferrite grains and a substructure, produced by deformation of the

recently formed grains. The transition temperature was shown to decrease in a linear manner with an increase in total reduction in ranges 2 and 3.[76]

Kozasu et al [70], do not consider rolling below A_{r1}, or the changes in microstructure in terms of the role of dislocations. This has been addressed more recently Vervynckt et al [7].

An important concept, is the non-recrystallisation temperature, T_{nr}, which represents the start of the inhibition of complete static recrystallization during cooling between rolling passes. The most common method of determining $T_{nr,}$ consists of simulating successive rolling passes and representing the mean flow stress (MFS) versus the inverse of the absolute temperature graphically for each of the simulated passes, [7] as seen in Fig 11. Here $T_{nr,}$ appears as a change in slope of the MFS curve. Vervynckt et al [7, 75] proposed extending the controlled rolling process to four regions, as defined in Fig 11. Data was obtained for a microalloyed steel containing 20ppm Ti and 18ppm N, based on a simulation of a 23 plate rolling pass schedule, with fixed interpass times of 20s and a cooling rate of 1°Cs^{-1}. In Fig. 11 (a), the flow stress increases with decreasing temperature in Region 1, while the curves change their shape entering Region11. As strain increases and temperature decreases in Region 111, the flow stress decreases, before increasing again in Region 1V. These are better interpreted in Fig. 11(b) , where the mean flow stress (MFS) is plotted against the inverse absolute temperature.

Region I corresponds to deformation at high temperature. Austenite recrystallizes completely between passes and there is no accumulation of dislocations. The increase in flow stress is solely due to the decrease in temperature.

In Region II, the change in slope indicates that dislocations are being accumulated. The flow stress increases more rapidly because of the inhibition of recrystallization between passes.

Region III is characterised by a significant decrease in MFS, and corresponds to the start of the $\gamma \rightarrow \alpha$ transformation. Here the intercritical two–phase rolling takes place.

Region IV corresponds to warm rolling in ferrite.

The intersection of the straight regression lines fitted to regions I and II defines T_{nr}, that fitted to regions II and III defines Ar_3, and that fitted to regions III and IV defines Ar_1. These are only for the conditions used here; i.e. fixed interpass times of 20s and a cooling rate of $1°Cs^{-1}$.

Hot rolling takes place on a falling temperature gradient, and the influence of the recrystallized state of austenite on the transformation behaviour and CCT curves of microalloyed steels was first investigated by Smith and Siebert.[77] They showed that the ferrite start line, Ar_3, was shifted to shorter times when austenite was in the unrecrystallised state. Mixed ferrite grain sizes were found when large strains were introduced in a temperature range in which only a fraction of the austenite grains recrystallized. The regions where

unrecrystallized grains transformed, i.e. $<T_{nr}$, usually lead to ferrite of a different grain size, from the ferrite originating from the recrystallized austenite in adjacent regions.

The state, or condition of the austenite prior to transformation, is therefore one of the major factors that determines the ferrite grain size. In addition to the grain size of austenite, the potential ferrite nucleation sites must be taken into account in any relationship with the ultimate ferrite grain size. Priestner and de los Rios [78] introduced the term S_v, which is the grain boundary surface area per unit volume of austenite, also described as the 'effective grain size', to account for the elongated grains. S_v is now often used to include boundary and intragranular nucleation sites.[71] Austenite which has a large value of S_v would, by definition, have a large capacity for nucleation of ferrite, and as has been pointed out by De Ardo [79], a low hardenability, and would be expected to develop a fine ferrite-pearlite microstructure. This concept is supported by experimental data, [78] Fig 12.

Final deformation in the low temperature austenite is the temperature range within which complete static recrystallization no longer takes place between rolling passes, leading to the retention of work hardening.

6. Basis of modelling thermomechanical controlled processing (TMCP)

Jonas and Sellars, [43] explain succinctly that 'thermomechanical controlled processing in industrial practice involves the production of specific microstructures, which are associated with particular mechanical and physical properties. In this way, TMCP differs from traditional deformation processing, which is generally concerned with reductions in thickness and with developing desirable changes in shape. TMCP involves the control and interaction of the following fundamental mechanisms: dislocation glide and climb, recrystallization, grain growth, phase transformation, precipitation, particle coarsening, particle pinning and solute drag. The interest in many of these structural changes is whether they take place dynamically (i.e. during deformation) or statically (i.e. after deformation). TMCP is concerned with the synthesis of these fundamental mechanisms. Of particular interest to microalloyed steels, is the TMCP operation concerned with grain refinement for high strength and toughness. Two contrasting, but complementary approaches have been taken; laboratory simulation and computer modelling. The former involve compression, tensile or torsion testing. Compression testers are useful for the determination of the kinetics of recrystallization or precipitation, while tensile machines are used to measure hot ductility, leading to the determination of the temperature and strain rate ranges associated with optimum workability. Computer modelling aims to quantify the fundamental mechanisms involved in TMCP, in terms of the variables of temperature, strain, strain rate and time, and to incorporate them within an overall mathematical description of industrial

forming processes. The inclusion of the parameters of microstructural features is now widely accepted as essential, both for off-line optimization of processing conditions, and for on-line control. In the case of hot rolling of steels, the modelling process involves sequential deformation passes taking place over a range of temperatures, rolling speeds, and interpass times.'

As explained by Sellars[42], 'during the hot deformation process itself, e.g. a rolling pass, work hardening takes place but it is balanced by the dynamic softening processes (i.e. during deformation) of recovery and recrystallization. These processes, which are thermally activated, lead to a flow stress that depends on strain rate and temperature, as well as strain. The microstructural changes taking place within the material result in an increase in dislocation density with strain, causing dynamic recrystallization, which takes place repeatedly as new recrystallized grains are themselves work hardened. These dynamic microstructural changes leave the metal in an unstable state and provide the driving force for static recovery and static recrystallization to take place after the deformation pass. Static recrystallization may be followed by grain growth, if the temperature is sufficiently high. Sellars [42] poses two important questions, which must be answered to apply the above principles to commercial practices: '(a) how long does recrystallization take after a deformation pass; and (b) what grain size is produced by recrystallization and grain growth? The answers determine the microstructure of the material entering the next and subsequent passes and hence influence the flow stress of

the material and the working forces required. Eventually they determine the microstructure and properties of hot worked products.' Details of the application of this approach is given by Sellars [40] and in a shorter form by Jonas and Sellars [43].

Depending on the eventual product, after casting and solidifying into an ingot, the steel is further processed by rolling (or forging). The rolling process requires the ingot to be reheated (soaked) before primary rolling to a smaller intermediate size (billet), which is cooled to ambient temperature. Normally, the steel is finish rolled in a different mill at a later time, and it is at this stage that the controlled rolling process is undertaken.

To make the forming process easier, relatively high soaking temperatures are traditionally employed for primary rolling, which causes considerable grain growth. Therefore the first step in controlled rolling is to control the austenite grain size, which increases exponentially with temperature, during reheating. The temperature should be sufficient to take into solution the microalloying elements, as discussed in detail in a later section.

From a commercial aspect, the modelling must relate to (a) the stock soaking temperature and time (b) the rolling schedule in terms of rolling velocity, deformation per pass, temperature at entry of rolling stock to each pass, interval between passes, and final rolling temperature, and (c) the cooling rate following rolling.

Vervynckt et al [7] describe T_{nr}, the non-recrystallization temperature, as representing the start of the inhibition of complete static recrystallization, during cooling between rolling passes. They also considered the experimental methods for the determination of T_{nr}, and note that most measurements of this parameter relate to plate mill schedules, which are easier to simulate by laboratory test methods due to their long interpass times of 10-20s, compared to strip mills. They consider that new experimental methods are essential to determine T_{nr} for strip mills, with their short (1s) interpass times. In microalloyed steels, the initiation of strain induced precipitation, (SIP), which is the normally considered as the nucleation of carbides, nitrides and/or carbonitrides on dislocations introduced by deformation, has the ability to suspend both static and dynamic recrystallization. In other words, SIP, strongly influences T_{nr}. He also points out that continuing deformation also leads to coarsening of existing precipitates, and that 'fresh' precipitates are generally considered to be necessary for preventing recrystallization. This effect is important in modelling of rolling operations, because the interruption of both static and dynamic recrystallization leads to increases in rolling loads, whereas the initiation of dynamic recrystallization in the absence of precipitation, results in a sudden decrease in rolling load. It should be noted that the models developed for controlled rolling processes which involve precipitation, normally do not include coherent precipitation or interphase precipitation, but only heterogeneous nucleation of particles on dislocations (SIP).

A different approach has been adopted by Matlock and Speer. [80] They started from the product, in their example, long bars, and then developed a microalloying and processing strategy for their manufacture. In this way, they considered that it was more likely that strategies which are less successful could be avoided. While this is a far less rigorous approach than the modelling described above, it does have the merit of being applicable to a very wide range of steel compositions and processes, associated with microalloying. These include thermomechanical processing of steel bars, which involves forging, and the production of reinforcing bars. Matlock and Speer [80] also considered the process route of a range of products, such as automotive springs and components for automotive engines and transmission systems, which require quenching and tempering, and high temperature carburising.

7. Solubility of particles which control grain size and provide dispersion hardening.

As mentioned earlier, the soaking temperature, prior to rough rolling, must be sufficient to take into solution the microalloying elements. In microalloyed steels, the most important particles are carbides and nitrides, of the transition metals, niobium, titanium, vanadium and to a considerably lesser extent, zirconium. These are often present as carbonitrides. In certain cases, oxides of titanium and sulphides are of importance, as are aluminium nitride precipitates.

During processing, the lowest temperature for taking into solution the particles precipitated on casting, which are later to control grain size and dispersion strengthening, is determined by their solubility in iron as a function of temperature and time. Matlock and Speer [80], in defining a strategy for the application of microalloying to a range of products, summarised the main objectives of adding niobium, titanium and vanadium to steels with a spectrum of carbon contents, relevant to long products. For example, they considered that the main precipitates were likely to be NbC, V(C,N) or TiN. NbC precipitates, which are expected at reaustenitising temperatures in virtually all heating treating applications. Solute niobium, remaining in solution in austenite, may also contribute to subsequent formation of nano-precipitates or clusters [51-57], and finer dispersion strengthening precipitates in ferrite. As discussed below, vanadium exhibits considerably greater solubility in austenite than niobium or titanium, and carbonitrides are only expected to form at the lowest austenite temperatures in alloys containing relatively high levels of vanadium, carbon and/or nitrogen. Austenite grain refinement is therefore less likely to occur in leaner alloys, but vanadium is available to precipitate in ferrite over a wide variety of steels, across the entire spectrum of carbon concentrations and processing temperatures. TiN is very stable and usually precipitates at high temperatures in the austenite phase and may be useful in resisting subsequent austenite grain coarsening, when added as a small addition.[80] The basis for most of the conclusions made by Matlock and Speer [80] lay with the solubility

equations appropriate for carbides and nitrides of niobium, titanium and vanadium in austenite.

Solubility equations allowing the temperature of compounds in a solvent to be estimated, for example, zirconium carbide in austenite [13], are normally described in the form of an Arrhenius equation. This gives the dependence of the rate constant K of chemical reactions on the temperature T (in absolute temperature, kelvins) and activation energy E_a, as shown below

$$K = A^{-Ea}/RT \qquad (2)$$

where A is the pre-exponential factor and R is the Universal gas constant.

In microalloyed steels, the microalloying element, M is often combined with an interstitial X, to give a compound, MX, some or all of which, dissolves in austenite as the temperature is raised.

$$[M] + [X] = MX] \qquad (3)$$

The rate constant K in equation (2) is now described as an equilibrium constant for the reaction given by equation [3].In practice, the concentrations of M and X are normally low, being less than 1% and therefore may be considered as having an ideal solution behaviour. M and X are expressed in terms of the weight percentage of the alloying

element present in the steel chemical composition. This allows equation (1) to be expressed as

$$\log_{10} [M][X] = k_s = -Q/RT + C \qquad (4)$$

Empirical Arrhenius equations have been determined for many of the important refractory carbides and nitrides known to form in steels, but similar equations for sulphides have not been found. Unlike the solubility equations of transition metal carbides and nitrides of niobium, titanium or vanadium in austenite, the corresponding equations of zirconium are almost entirely due to one source, and have some shortcomings.

Table 4, summarises selected Q and C values, collated from the literature, for the relevant grain boundary pinning and dispersion hardening compounds found in microalloyed steel. Taylor [81] has calculated values for carbides in ferrite. Examples of solubility diagrams for (a) NbC,(b)VN and (c)VN in austenite over the temperature range relevant to TMP, and based on the data in Table 5, are given in Fig.12**,** taken from Matlock and Speer. [80] For more details of the solubilities, the reader is referred to the reviews on the role of individual elements in microalloyed steels [8-14], and the book by Gladman[3] ,which also provides examples of some mutually soluble carbonitrides.

A comparison of these carbide and nitride solubilities is shown in Fig 13. Here, it can be seen that while zirconium carbides and nitrides show little solubility in

austenite, and often nucleate while the steel is still molten, both zirconium and titanium precipitate in austenite, as do niobium and vanadium, both as carbides and nitrides

Table 5

Selected solubility parameters in austenite of carbides and nitrides found in microalloyed steels

	Q	C	Reference
AlN	-6770	1.03	Leslie et al [82]
NbC	-6770	2.26	Irvine et al[49]
NbN	-8500	2.80	Narita[83]
TiC	-10,475	5.33	Narita[83]
TiN	-8000	0.332	S. Matsuda and N.Okumura[84]
VC	-9500	6.72	Narita[83]
VN	-8330	3.46	Irvine et al[49]
ZrC	-8464	4.26 *	Narita[83]
ZrN	-16000	4.38	Narita[83]

* use with caution[13]

In general, nitrides are more soluble in austenite than carbides, zirconium and titanium nitrides are the least soluble, while vanadium carbide is the most soluble. In ferrite, vanadium carbide is the most soluble, followed by titanium carbide and then niobium carbide, all of which, with high carbon/nitrogen ratios, could be important sources of dispersion hardening.

Narita[83] has given data on the recovery of the elements in Groups IVA and VA, which are reproduced in Table 6. Both niobium and vanadium can be seen to have a higher percent recovery than titanium and zirconium.

Table 6

Recovery of the elements in Groups IVA and VA

V: 90-100%	Ti: 50-80%	Y: 35-60%
Nb: 80-100%	Zr: 50-80%	La: 20-50%
Ta: 70-90%	Hf: 40-80%	U 20-50%

Vervynckt et al [7] considered that 'for most steel grades, T_{nr} is determined by the niobium and carbon contents. One the other hand, titanium forms a very stable compound, TiN, which may remain undissolved in austenite. This compound consequently limits austenite grain growth at relatively high soaking temperatures and also restricts nitrogen from forming Nb (C, N), enabling dissolution of NbC to occur more readily.'

A term of importance in discussing particle pinning of grain boundaries is the austenite grain coarsening temperature, $T_{c,}$ which is the

temperature where the pinning effect becomes ineffective. This condition considerably restricts grain growth. As would be expected, T_c is significantly lower than the solution temperature of the precipitate. There have been several studies [49, 84-87] of the effect of carbides and nitrides on T_c. Fig14, taken from Cuddy and Raley [86] illustrates some results which clearly show the importance of NbCN and AlN compared with VC, which is confirmed in more recent work [3]. As a result of experimental studies, linear relations were obtained between T_c and the temperature for complete solution of the microalloying carbide or nitride, T. This lead to the relationship;

$$T_c = A + B\left(Q/C - \log(M.I) - 273\right), °C \qquad (5)$$

M and I are the metal and interstitial, A and B are the intercept and slope of the line segments in Fig 14, while Q and C are constants, such as those given in Table 5.

Using this data for Q and C for AlN and NbC, the latter labelled NbCN by Cuddy and Raley[86], who give the respective constants A and B as 285°C, 460°C and 0.535,0.569, to allow the calculation of T_c. From the work of Hall [30] and Petch [31], and Zener [88], it is evident that ferrite grain size and the size and volume fraction of precipitated particles, are of seminal importance in determining the mechanical properties of polycrystals. The volume fraction of particles is initially controlled by

their solubility in austenite, where most of the deformation, which determines the final size and shape of the steel, is scheduled.

As acknowledged by Martin[89], it is well established that dispersed, hard, incoherent particles can either retard or accelerate recrystallization of a metallic matrix, and this was affirmed by the work of Docherty and Martin [90]. Zener [88] was the first to devise a relationship involving a dispersion of particles and the retarding force which they exerted on a grain boundary. This effect is known as the Zener drag after his original analysis, and was first published by Smith, Zener proposed that the driving pressure for grain growth due the curvature of the grain boundary would be counteracted by a pinning (drag) pressure exerted by the particles on the boundary. Consequently, normal grain growth would be completely inhibited when the average grain size reached a critical maximum grain radius, also known as the Zener limit, RR_c), is given by:

$$R_c = 4r/3f \qquad (6)$$

where f is the particle volume fraction and r the radius of the pinning particles.

He considered that both grains and particles could be approximated to spheres, particle volume fraction and r the radius

In its general form the Zener Equation is given as:

$$R_c = K_g r/f^m \qquad (7)$$

where K_g is a dimensionless constant and m an index for f. Several other models have been produced, collated and critically reviewed. [91-93] The model by Zener [88] the model has been shown to overestimate R when compared with

experimental data overestimate R_c [1] when compared with other data. [91-93]. The most extensive consideration of the many modifications proposed to the Zener equation has been undertaken by Manohar et al [93], who examined in detail some 32 models published up to 1987. In general, the pinning of sub-grain and high-angle grain boundaries has been shown to occur when the particle radius, r, is the size range 30-800nm, and particle volume fraction (f) less than 0.01. While data for R_c and to some extent r are available, no reliable data on volume fraction of precipitates in these steels has been published. [13]Figs 16 and 17 show the effect of particles pinning grain boundaries. There also exists a body of experimental evidence to show that in steels, particles, particularly oxides and carbides greater than 0.5μm in length, with interparticle spacings, also greater than 0.5μm, can lead to acceleration of recrystallization due to nucleation of new grains at carbide particles [94, 95] and oxide slag inclusions [96] These particles are assumed to create lattice curvature at particle–matrix interfaces in the deformed matrix, which enhances recrystallization and gives rise to accelerated recrystallization, also known as particle stimulated nucleation (PSN).[91]

8. Precipitation and recrystallization

As mentioned above, while restriction of grain growth by particle pinning initially takes place during the soaking stage of the rolling schedule, an equally

important aspect of precipitation is that during the rolling, most of which occurs in the austenite phase in niobium steels. In vanadium steels, precipitation in ferrite, also is important, Fig 18. The inter-relationship between hot deformation and concurrent precipitation has been conveniently summarized by Pandit et al [97], reproduced in part here: 'The presence of precipitates increases the non-recrystallisation temperatures (T_{nr}), which is of significance in deciding the reheating temperature for hot rolling.[98] The presence of precipitates in austenite, increases the flow stress of the material and hence the rolling loads. Niobium is the most potent of the microalloying elements in retarding austenite recrystallization through solute drag [98] and/or by strain induced precipitation. [99, 100] Fig 19 shows that only NbC can have high supersaturations over a large portion of the typical hot rolling range.[8] It is well established that the onset of precipitation is greatly enhanced by prior deformation. A comparison of the precipitation kinetics of strain induced NbC particles with those in undeformed austenite, reveals that at least two orders of magnitude difference occurs between the two, over a given temperature range.[101] This may be attributed to the presence of dislocations, deformation bands, sub-grain structure and twins, the well-known potent sites for nucleation which accelerate the precipitation process in the deformed microstructure.[101, 102] The kinetics of SIP of niobium in microalloyed steels has been extensively investigated for over 25 years by the Sellars's group, who have compared their experimental data with modelling predictions with increasing success.[41,42,101-106] Recently, Nöhrer et al[107] ,using a

quenching dilatometer and TEM and APT techniques, considered in detail the influence of deformation on the behaviour of niobium precipitation in a microalloyed steel containing: 0.20C-1.29Mn-0.029Nb-0.035Al,-0.004N, and found that this was different in the austenite and ferrite regions. The steels were solution treated at 1250ºC, cooled to a deformation temperature of 700 ºC in the austenite and ferrite region, held for 7mins to partially transform to ferrite, before being deformed to true strains of 0.7,0.2 or 0.05, at a strain rate of $0.1s^{-1}$. After a second hold, the samples were gas-quenched to RT within 5s. It was found that the niobium precipitates nucleated as carbonitrides, taking up the total available nitrogen. Following deformation, with longer dwell times, increasing carbon levels were detected in the niobium precipitates. A higher volume fraction of precipitates, with a higher carbon content, was found in ferrite compared to austenite. With increasing strain, the dislocation density increased, resulting in a higher volume fraction of strain induced niobium precipitates, not through accelerated precipitate growth.

While an abundance of research has been reported on the SIP behaviour of Nb(C,N), less consideration has been given to the SIP of TiN and V(C,N) in austenite. The evolution of SIP of vanadium precipitates in an 0.20% C steel at 600 and 700ºC was considered by Nohrer et al [108] using the same techniques mentioned above[107]. They observed that the initial V(C,N) precipitates were higher in nitrogen than carbon, and this changed with increasing dwell time and

occurred faster at 700 ºC, as in their niobium steel study.[107] Gomez et al[109] considered a more complex additions in the microalloyed steels: (a) 0.034Nb-0.004N, (b) 0.092V-0.0065N, (c) 0.018Ti-0.008N and (d) 0.037Al-0.010N, on recrystallization/precipitation interactions, by using hot torsion tests. Their results showed that steels (a) and (b) exhibited long inhibition plateaux, while steel (d) displayed a very short plateau; the steel (c) did not show any plateau. This was interpreted as indicating that niobium and vanadium precipitates (nitrides and carbides) can inhibit the static recrystallization, but this does not occur for the aluminium and titanium steels, which formed only nitrides. Recrystallization-precipitation-time-temperature diagrams showed the interaction between both phenomena, along with the SIP kinetics and precipitate coarsening. TEM studies, based on the average precipitate size, found that AlN particles (87nm) nucleated and grew faster than NbCN (22nm) or VN (10.5nm). TiN (1250nm) in this work had a size dependent only on the solution temperature of 1300ºC. The effect of a titanium addition on SIP of NbC in simulated deformed 0.047% Nb and 0.043%Nb-0.016%Ti steels was explored by Hong et al [110] using two stage interrupted compression tests. They found that the size of NbC formed in the Nb-Ti steel was smaller than in the Nb steel, and that the precipitation start time in the Nb-Ti steel was delayed compared to that of the Nb steel. After reheating the Nb-Ti steel at 1250ºC,undissolved Ti-rich (Ti,Nb)(C,N) particles were located at prior austenite grain boundaries, resulting in a finer austenite grain size of 130µm, compared with 180 µm for the Nb steel.

Medina[111] studied the influence of strain on precipitate nucleation in austenite comparing three Nb-V-N microalloyed steels. Precipitation start-time-temperature diagrams were determined by hot torsion tests, while corresponding increases in dislocation density, and the driving force for precipitation, ΔG_v , were calculated from established equations. The results show that SIP in austenite is transformed from heterogeneous nucleation on dislocation nodes, when ΔG_v is small, (-1.8 x 10^{-9} Jm^{-3}) to homogeneous nucleation as the microalloying content and therefore ΔG_v both increased (-2.48 x 10^{-9} Jm^{-3}). ΔG_v was obtained by considering that niobium forms as carbonitrides and vanadium as nitrides. However, in many cases, (Nb,V)(C,N), of varying composition, after removing from different stages in a process, have been characterised. In this case, no such work was undertaken by Medina[111]. It is important that the assumption that Nb(C, N) and VN have separate roles in this work, is confirmed experimentally.

Two more complex steels of compositions:

Nb-V 0.19C-1.5Mn- 0.44Si-0.1Cr-0.125V-0.035Nb-88ppm N- 0.008 Al

Ti-V 0.18C-1.5Mn-0.44Si-0.09Cr-0.13V-0.036Ti- 80ppmN- 0.008Al

were compared by Pandit et al [97], who carried out mechanical relaxation tests using a Gleeble 1500 thermomechanical simulator. Holding specimens at the reheating temperature of 1200°C for 5min. was sufficient to dissolve all the niobium, but only part of the titanium. Deformation was carried out in austenite, between 1090°C and 900 °C. Both Datta and Sellars [102] and Liu and

Jonas [112] suggested that SIP in deformed austenite occurs mostly on dislocations and sub-boundaries, which implies that the austenite grain size per sae, is not a dominant factor in influencing precipitation kinetics., Pandit et al [97] were able to show from their data, Fig 20, that the precipitation kinetics of the Ti-V steel was more sluggish than the Nb-V steel.

9. Multiple additions of niobium, titanium, vanadium zirconium and nitrogen in microalloyed steels

The year 1980 was considered by DeArdo et al[113] to be a watershed for microalloyed steels. Prior to 1980, microalloyed steels were of low hardenability with F-P microstructures, and after air cooling following hot rolling, had σ_y values of ~420MPa. Around 1980, both the line-pipe and automotive industries required steels with higher strengths than could readily be obtained with F-P microstructures. Increasing the microalloying content to enhance the dispersion strengthening contribution from the range 50-80 MPa, recorded for F-P steels, seemed limited. This magnitude is comparable to the strengthening conferred by solid solution strengthening, but significantly below of 100-480MPa levels which can be obtained from dislocation strengthening.[1,2,114,115]

One of the main developments which has occurred over the past 25 years to raise the yield strength, is the increasing tendency for steel-makers to alloy with

more than one of the niobium, titanium, vanadium trio of transition metals, often with a deliberate higher nitrogen levels than the normal range of 0.003-0.005%N. This has given rise fine ferrite grain sizes of <10μm, and to complex particles, which may precipitate in either or both the austenite and ferrite phases, depending on the chemical composition of the steel and the details of the TMP route adopted. However, multiple additions are not a recent move, as they were considered over 45 years ago by, for example, Heisterkamp et al.[116] They investigated 19 steels, 14 of which contained zirconium, with either single additions at levels of nominally 0.043%, 0.057%, 0.072%, or in combination with two levels of niobium, 0.020% or 0.035%. These steels were compared with five vanadium-zirconium steels arranged in two groups, one of three steels based on 0.030% V containing respectively, 0.019%, 0.035% and 0.057%Zr, and a second of two steels with 0.049%V, and 0.053%Zr or 0.092%Zr. The steels were examined in the as-rolled and normalised conditions. Little effect of zirconium additions were found on the strength of the niobium–zirconium steels, the as- rolled strip having σ_y of ~500MPa, which is ~20% greater than the 420 MPa, mentioned above. Furthermore, a decrease from 460MPa to ~420 MPa was found when a zirconium addition was present with 0.030-0.050% vanadium.

In controlled rolled microalloyed steels, some attention has been paid to the combination of additions of titanium and vanadium, titanium and niobium or

titanium and niobium and vanadium, with the expectation that the potential of each element will be fully exploited. Most of the work discussed below emphases that titanium additions are normally made as hypo-stoichiometric relative to nitrogen, i.e. < 3.4. This ratio is discussed by Crowther and Morrison [117], who explained the effect that titanium additions were observed to have with Al-V and Al-Nb microalloyed steels, particularly with regard to loss of strength. This was purported to be due to changes in the dispersion strengthening associated with modifications to niobium precipitates.

Strid and Easterling [118] used STEM-EDX microanalysis to understand the influence on microstructure, of precipitate compositions, morphologies and sizes in hot-rolled microalloyed steels containing, Ti, Ti-V, Ti-Nb, with different levels of nitrogen. They found that the median ferrite grain sizes in the Ti-Nb steels, 29µm and 32.5 µm, was greater than in the Ti (~16 µm) and Ti-V (13 µm) steels. Also, the median particle size, 19nm, of an Ti-Nb -0.010N steel containing predominantly nitrides, showed a coarser size distribution than in a Ti-Nb- 0.006N steel, where the median particle size of predominantly carbides, decreased to 10nm. Increasing the aluminium content of their Ti and Ti-V steels from 0.022 to 0.072 wt-%, resulted in an increase in the particle size from ~8nm to ~12 nm. These changes had only a minor influence on the yield strength, which reached 377MPa for the steels Ti and Ti-V additions, but was not given for those with Ti-Nb. Strid and Easterling [118] were unable to quantify the C or N levels in this work, and therefore details of the chemical

compositions of the particles was restricted to the transition metals. This problem was overcome to some extent by He and Baker [119], who were perhaps the first to use both TEM- EDX, in an EM400, and EELS in an HB5 instrument, to characterize their carbo-nitride precipitates present in a microalloyed steel. They attempted to elucidate the problems associated with additions of titanium in microalloyed steels, which had been reported to have differing effects when used with additions of niobium compared to vanadium. Following controlled rolling, three steels containing nominally 0.10C-1.4Mn -0.005N-0.017Nb, with respectively <0.005, 0.010, or 0.022Ti, were examined. For the different titanium additions, giving different Ti/N ratios, a distinct size variation of the Ti-Nb carbides and nitrides was observed, especially for the coarser particles. Fig 21(a) includes large Ti-Nb particles in an 0.01%Ti-Nb steel, with many smaller Nb-rich spheroids, while an EELS spectrum, Fig 21(b) collected from the centre of a ~20nm Nb-rich spheroid, shows the niobium, carbon, nitrogen and titanium edges.[119] Using a similar range of techniques to He and Baker[119], Subramanian and Weatherly [120] investigated the precipitation behaviour in Ti-V and Ti-Nb steels, but containing a higher carbon level of 0.426. The presence of complex precipitates in as-cast blooms was confirmed; in the Ti-V steel nitrides $(Ti_xV_{1-x})N$, were observed followed at lower temperatures by carbides (V_4C_3); in the Ti-Nb line-pipe steel processed from slabs, dense well dispersed mixed nitrides (Ti_xNb_{1-x}), on which epitaxial growth of Nb-rich mixed carbides were observed. The authors considered that epitaxial growth obviated the need

for SIP of mixed carbides. Here, the increase in the volume fraction of precipitates increased the Zener drag force on boundary mobility, thereby retarding recrystallization. Similar results were found by He and Baker [121-124] studying controlled rolled ~ 0.10 C steels containing additions of Nb-Ti-N or Nb-Ti-Zr-N. They observed NbC or Nb(C,N) caps or coatings to nucleate on (Ti, Nb)N core particles, Fig 22, which reduced the niobium available for both grain refinement and dispersion strengthening. A 0.016 Zr addition resulted in complex nitrides >100nm size, of Ti-Zr and Ti-Nb-Zr, which appeared to have no effect on <100nm Ti-Nb carbonitrides, also present. All the steels had σ_y values ~400MPa with 50J IIT of -80 to 100ºC. The presence of caps nucleating on more stable core precipitates has been reported more recently. Caps of Nb-rich (Nb,Ti)C were also observed to nucleate heterogeneously on undissolved (Ti, Nb)(C,N) core particles by Hong et al[110]and by Grajcar[125].

In other work, Beres etal [126] found a 0.03C-0.08Nb-0.01Ti 20mm thick plate steel, 'produced complex agglomerates with a cubic TiN seed crystal overgrown by a cubic NbC particle.' In some of the studies where core/caps particles were observed, the choice of reheating temperature prior to processing has been too low to take all of the core precipitate, normally titanium or zirconium based, into solution. While the resultant conglomerate may affect the rate of grain growth, in general, these particles should be avoided through relating the steel composition to higher reheating temperatures.

Courtois etal [127] ,who studied model Fe-(Nb,C) and Fe-(Nb,C,N) ferritic alloys, showed that 'the addition of nitrogen lead to a complex precipitation sequence, with the co-existence of two populations of particles, pure nitrides and homogeneous carbonitrides, respectively.' In other work, a comparison of precipitates in Nb-Ti and Nb-Ti-V microalloyed X80 pipeline steels produced as 18.4mm thick strip was undertaken by Li et al [128]. Their microstructures consisted of quasi-acicular ferrite (A-F).

Perhaps the first researchers to consider moving from F-P to A-F microstructures were Smith and Coldren [129], who investigated the microstructure and properties of thirty six laboratory steels. Among the most successful, were steels based on a composition of 0.4C-1.6Mn-0.09Nb-0.2Mo, FR at 870 ºC, spray cooled at ~22º C s^{-1} to a simulated-coiling temperature of 635 ºC, the approximate temperature for AF formation. This schedule resulted in a yield strength of ~570MPa and ½ size Charpy transition temperature of -60ºC.

Some of the more recent work, which lead to the gradual raising of the yield strength by controlled rolling microalloyed steels, was summarized by Ji et al.[130] Campos et al[131, 132] developed yield stress of 530-608MPa respectively, using nominal chemical compositions in of 0.12C-0.057Nb-0.049Ti and 0.11C-0.04Nb-0.11Ti. In addition, the precipitation behaviour in an 0.07C-0.086Nb-0.047Ti steel was investigated by Charleux et al, [133] who obtained σ_y levels of 650MPa in plate. Misra etal [134] developed a steel with σ_y of 770MPa, from a

complex steel composition of 0.06C- 0.07 to 0.09Nb- 0.065= 0.085Ti, 0.1 - 0.2Mo and 0.0005- 0.001B.

As pointed out by Ji et al [130], these highly alloyed steels detailed above, achieved their yield strength at a relatively high cost. The recent approach of Ji et al [130] compared two laboratory steels of compositions based on 0.09C-0.11Ti and 0.05C-0.025Nb-0.11Ti.Both steels reached σ_y values of >700MPa with >20% elongation and good toughness; it should be pointed out that one steel was without a niobium addition. The plate finishing rolling temperature was controlled to 910ºC and then cooled at 80 ºCs^{-1} to the coiling temperature of 620 ºC, using an ultra-fast cooling technique, producing a microstructure that was predominantly of massive ferrite and acicular ferrite, with ~3.2nm TiC precipitates in the Ti steel and ~5.0nm (Ti, Nb) C particles in the Ti-Nb steel. This kind of microstructure has been further considered in a series of papers involving Shan and co-workers[135-138], who explored the acicular ferrite (AF) route to achieving X60 to X100 pipeline steels. The laboratory developed AF pipeline steel was based on their continuous cooling transformation(CCT) diagrams of an experimental steel which was vacuum melted, reheated at 1150 $^{\circ}$C for 50 min, started rolling (T_s), at 1050 ºC and finished rolling (T_f) at 750ºC,starting from a thickness of 70 mm and reducing in seven steps to 7mm, then cooled to a finish cooling temperature (T_c) of 600ºC at a cooling rate (V_c) of 20ºC s^{-1} in order to obtain the AF microstructure. The steel was finally held at 600ºC for1 h and furnace cooled to room temperature, to simulate the coiling

process. The commercial AF pipeline steel was reheated at 1180 ºC for 230 min, and then rolled in two stages, rough-rolling and finish rolling. The rough-rolling stage for the steel reduced from a thickness of 230 to 40mm, in seven steps with T_s 1130 ºC; then the finish-rolling stage started at 1020ºC with T_f at 840°C, reducing from 40 to 7mm in another seven steps. Finally the steel was cooled to 600ºC at 20ºC s^{-1} for coiling and then air cooled to room temperature. With the laboratory steel [134], which had a nominal composition of 0.07C-0.9Mn- 0.04Nb-0.04V-0.015 Ti-0.004N, they found that the properties were dependent on T_s, T_f, T_c and V_c. Optimum mechanical properties were obtained when T_s was approximately 1100 °C, T_f 890 °C, T_c 520 °C and V_c 30 °C s^{-1}. Niobium in the steel was considered to have a stronger influence on T_s compared with vanadium and titanium, in controlling mechanical properties; Nb carbonitrides form in the range close to T_s of 1070–1120°C, V carbonitrides will mostly dissolve in γ-Fe ~900 °C while the formation temperature of Ti carbonitrides is far higher than T_s. Thus, an increase of T_s will mainly place more niobium in solution, which raises σ_y to a maximum of 561 MPa. Regression equations, which described the relationships between σ_y and El, elongation, and the processing parameters, were produced from the data obtained from the laboratory steels.

$$\sigma_y = 0.508\ Ts - 0.231\ T_f - 0.334\ T_c + 1.905 V_c + 323.6 \qquad (8)$$

R=0.94

$$El = 0.002\ Ts - 0.064\ T_f - 0.086\ T_c + 0.325 V_c + 121.8 \qquad (9)$$

R=0.98

Equations (8) and (9) can be used be used to predict σ_y and El of commercially produced pipeline steels.[135]

A comparison made between the same laboratory X90 grade acicular ferrite steel, containing 0.025C-0.058Nb/Ti and 0.0062N, with a commercial x70 grade containing 0.08C-0.095Nb/Ti and 0.005N. It was concluded that the higher σ_y (626MPa /530MPa) and better toughness (at -100ºC, 137J/ 108J) in the acicular steel resulted from its finer grain size and higher dislocation density and sub-boundary content.[138] The above laboratory X90 grade steel was processed to produce either an acicular ferrite or an ultrafine grain microstructure, which allowed a comparison to be made of the two microstructures and properties. The dispersed (Ti,Nb)(C,N) precipitates, together with a high density of tangled dislocations and the finer cleavage facet size-ferrite bundle, in the acicular ferrite steel was considered to be a better candidate microstructure for oil and gas pipeline steels than the ultrafine ferrite steel. [136] In their review, Beladi et al[139] have also considered alternative methods to develop high strength steels at a lower cost. Their most promising route to achieving this goal was by reducing the alloy content of the steel and relying on a reduction in the grain size to provide higher strength and toughness. It is pointed out[139] that the Hall-Petch equation, eqn. (1), predicts that a reduction in the average grain size from 5 to 1 μm will increase σ_y by ~350MPa. However, using conventional industrial approaches, the level of ferrite

refinement has been found historically, to be limited to 5–10 µm. Nowadays, several thermomechanical processes have been developed to produce ferrite grain sizes of ≤1–3µm, ranging from extreme thermal and deformation cycles to more typical thermomechanical processes. Of a number of routes established to achieve a fine grain size in the laboratory, dynamic strain induced transformation (DSIT) was considered by Beladi et al [139], as the most promising method for adapting to commercial practice. DSIT is based on the discovery, by Hodgson et al [140], for the formation of ultrafine grains during the hot deformation of thin strip. This development requires deformation to large strains within the Ae_3 to Ar_1 temperature range for a given alloy, followed by rapid cooling.[141, 142] The formation of ultrafine ferrite involves the dynamic transformation of a significant volume fraction of austenite to ferrite, which initially occurred at an early stage of deformation, at prior austenite grain boundaries. This was followed by intragranular nucleation, as in controlled rolling.[139] However, DSIT arises from the introduction of extensive extra intragranular nucleation sites, that are not present in conventional controlled rolling, They were found in an 0.17C-1.5Mn-0.02V steel.[143] Priestner and de los Rios [78],[144] were among the first to recognise that extra grain refinement may be possible if the transformation could be induced during the deformation process. The final microstructure of DSIT low carbon steels usually consists of fine equiaxed ferrite grains (< 2 µm) and cementite (typically 0.05-0.2 µm) in the grain interiors and at the grain boundaries, Fig 23. Most of the yield

strength values in Fig 24, collated by Beladi et al [139], lie within the 400 to 700MPa range, the upper end being beyond what most F-P microalloyed steels achieve. However, the commercial exploitation of the DSIT route is still a work in progress.[142, 145] Recently, a guide to industrial production of ultrafine grain microalloyed steel was published. [146] It is based on DSIT, using experimental data to aid the development of a multiscale computer model, which predicted the mechanical response of the microstructure in a hot rolling process. Two steel grades were examined: 0.07C-1.36Mn-0.06Nb-0.03Ti-0.098N-0.003B and 0.08C-1.67Mn-0.06Nb-0.018Ti-0.0316N-0.26Mo. Niobium was the principal alloying element used to control the dynamic transformation of austenite, while the additions of B or Mo increased significantly the hardenability, thereby expanding the thermomechanical processing window. However, while these steels can achieve higher σ_y levels than F-P microalloyed steels, they still rely on expensive alloy additions. Others claim that it is possible to obtain an ultrafine grain microstructure without such alloying[147], but it is not known if this is route is used commercially. As mentioned above, small amounts of boron when added to ultralow carbon steels, promoted bainite by suppressing the formation of polygonal ferrite.

Tamehiro et al [148], in studying TMP with accelerated cooling, considered the effect of a combined addition of boron and a grain-refining element such as niobium, titanium or vanadium in very low carbon steels, in terms of mechanical properties and microstructures. They found that, although boron, as

a single addition, has little effect on the properties, the combined addition with niobium improves the balance of strength and toughness. Niobium additions to boron steels suppressed the precipitation of Fe_{23} (C, B)$_6$ and strongly retarded the γ-α transformation, forming a fine-grained bainitic structure. Titanium has been found to have the same effect as that of niobium, but vanadium does not. The strengthening and toughening mechanism by the combined addition of niobium and boron was also investigated by examining the effect of alloying elements on the minimum recrystallization temperature of austenite during rolling, and γ-α transformation behaviour.[148]

10. High strength / bainitic/martensitic microalloyed steels

Acicular ferrite (AF) and conventional bainite (CB) have been mentioned in the previous section, but the difference between these two phases needs to be clarified.[149,150] Fig 25 shows a large austenite grain size containing a relatively high number density of intragranular nucleation sites, that leads to a microstructure consisting predominantly of AF. By comparison, a small austenite grain size, containing a relatively high number density of grain boundary nucleation sites, leads to a microstructure consisting predominantly of CB.[149] As indicated by Zhang and Boyd [150] 'CB nucleates at prior austenite boundaries and grows as packets of parallel ferrite plates, appearing as laths in 2D, which have similar crystallographic orientation and a high uniform

dislocation density. The length of the ferrite laths is limited by impingement with other packets, and carbon-enriched interlath austenite becomes a martensite-austenite (M/A) constituent. By contrast, AF can be nucleated by inclusions, grows as randomly oriented ferrite laths, or groups of laths, which contain a high dislocation density, and the MA usually occurs as discrete particles. This less organised aspect, provides the potential for AF combining high strength with high toughness, and is the reason of some, for developing acicular ferrite microstructures. [151] A crack therefore has to follow a more tortuous path through an AF microstructure, thereby leading to an improvement in toughness without compromising strength.[151, 152] Bainite has traditionally been separated into two groups, Fig 26, granular bainite, (GB), often described as lower bainite, which consists of sheaves of elongated ferrite crystals with low misorientations and a high dislocation density, containing roughly equiaxed islands of M/A micro-constituent; and lath bainite (LB), often described as upper bainite, which consists of packets of parallel ferrite laths (or plates) separated by low-angle boundaries and containing very high dislocation densities. In contrast to GB, the M/A particles retained between the ferrite crystals in LB have an acicular morphology.[153]

M/A particles can significantly affect fracture toughness, due to the brittle nature of martensite. Not only is the phase fraction of importance, but also the M/A morphology, Fig 27. Most of the detailed studies of the morphology of M/A phase have been conducted on weld HAZ microstructures, for example

refs.154-156. Li and Baker [155] reported four different morphologies of M/A particles, including blocky-like particles, or islands ,connected or nearly connected particles along prior austenite grain boundaries, elongated stringer particles along bainitic ferrite laths and M/A-C particles, consisting of M/A and a second phase, i.e. carbide and ferrite. M/A islands were reported with sizes between 0.5 and 5 μm and elongated particles were found with a length of up to 10 μm and a width between 0.2 to 2 μm. [155, 156] In addition to cracks initiated by M/A constituents, it is also reported that M/A particles can delay the growth of cracks.[156] This observation indicates a very complex behaviour of the influence of M/A particles on fracture. More recently, Reichert et al[156] have investigated the formation of M/A in X80 linepipe steel using a Gleeble simulator.

While it is accepted that bainite grows via a displacive mechanism, there is still much discussion on the diffusion or diffusionless nature of bainite. Caballero et al[157] used APT to track the atom distributions during the bainite reaction in steels with different carbon and silicon contents. The steels were transformed over a wide range of temperatures (200–525ºC) to elucidate the role of reaction rate and diffusion in the formation of bainite with and without cementite precipitation. From their studies, they concluded that the transformation is diffusionless, but carbon atoms partition and form clusters in the residual austenite (or precipitate as carbides), shortly after growth is arrested. The precipitation of carbides is therefore a secondary event.

The means of achieving these bainitic/martensitic microstructures in microalloyed steels, is by water cooling after hot rolling. For processing plate, interrupted accelerated cooling (IAC) and interrupted direct quenching (IDQ) were introduced in plate mills. [63-65] As recounted by DeArdo et al [6], 'run-out table water spray, cooling to the coiling temperature, had been in practice in strip mills since the 1960's, but not as a microstructural control tool for increasing strength.' To achieve a yield strength ~700MPa, steels should have an adequate hardenability (carbon equivalent, C.E.>0.50, Pcm >0.20) and be controlled rolled, followed by IDQ to below the bainite start, Bs, temperature of the pancaked austenite. With controlled rolled F-P steels having a maximum yield strength of <700MPa, the way forward to higher strengths lay with steels having lower transformation microstructures, such as non-polygonal ferrite, acicular ferrite, the bainites (B) and martensite (M), either individually or in combination, DeArdo et al.[6]

While processing using accelerated cooling after controlled rolling, normally had the aim of developing acicular ferrite/bainitic microstructures, other studies have been conducted on steels having sufficient alloy content to produce martensitic microstructures following DQ. Two papers published in the early 1990's provide good descriptions, and a collection of references pertinent to this route, for achieving proof stress levels of up to 1100MPa. Taylor and Hansen[158] studied the structure and mechanical properties of a series of TMP-DQ

martensitic laboratory steels, 0.1C-1.4Mn-0.5Mo-0.035Ti-0.0096N-B containing 0 to 0.24V. Titanium was added to stabilize the nitrogen as TiN. Fig 28 shows schematically the three processing routes investigated, together with reheated and quenched samples, to simulate the standard production practice for quenched-and-tempered steels. This latter process involved austenitizing at 920 ºC for 1 hr and WQ as for the DQ samples. The average cooling rate, between, 800ºC and 500ºC, at the plate centre during cooling, varied from 45 ºC/s and 52 ºCs^{-1}.

Fig29 shows that after tempering at 620 ºC for hrs, the vanadium containing steels exhibited markedly higher strengths than their vanadium free counterparts, while overall, the CR+DQ steels produced the best combination of strength and toughness. This was attributed to the precipitation during tempering of mainly spherical 2 to 4nm dia (46%V, 52% Mo, 3%Ti)carbides, providing an estimated 100MPa/0.1wt.%V, over the range of vanadium additions investigated.

The effect of variations in process route and processing variables is also well illustrated in the paper by Weiss and Thompson[159], who studied similar steels to Taylor and Hansen[158], with either 0.12 C or 0.19C and Mn1.4- Mo 0.3-B~0.002-Ti 0.02 to 0.03-N 0.006 with and without 0.06V. Their goal was to vary the condition of the austenite phase prior to quenching by changing the process route, in a similar manner to Taylor and Hansen [158], except the cooling rate

during DQ, at~25 ºCs^{-1}, was lower. Fig 29 compares both sets of data in terms of strength and toughness, which clearly show the advantage of the CR+DQ process. Here the precipitates in the 625ºC tempered state were characterized by SAED as cementite and Ti(C,N), considered to be remaining out of solution, following heating prior to rolling. As no EDX analysis was undertaken, the Ti(C,N) was probably what Taylor and Hansen[158] analysed as (V, Mo, Ti) C, as these particles in both papers, are the same size order of ~5nm. More recently, with a steel microstructure of martensite and a little acicular ferrite, Xie et al [17] obtained a yield stress of 1144MPa combined with an impact absorbed energy of ¼ size Charpy specimen of 17J at -20ºC. The laboratory steel containing 0.08 to 0.11C-0.4Si-1.0 to 1.9Mn-0.8Cr-0.12 (Nb+V+Ti)-0.0013B, was soaked at 1200ºC, air cooled to 950ºC,rolled to 6mm, FR at 840 ºC, water cooled at 80 ºC/s to ~260-280ºC, followed by furnace cooling to RT.

However, while martensitic steels achieve significantly higher strengths, but with some loss of toughness, than F-P steels, the additional alloying costs, together with those associated with processing via controlled rolling followed by quenching and tempering, which is not an on-line process for most plate thicknesses, has significant economic demerits.

The advantages of a bainitic microstructure on toughness have been discussed by Edmonds and Cochrane[160]. Over the past two decades, the formation of bainite has been recognized as a diffusion assisted, shear type (displacive)

transformation, with excess carbon partitioning by diffusion to highly concentrated islands of austenite, A, in the B-F microstructure, either within the ferrite grains or between the grains. In addition, a second form of MA is caused by incomplete transformation of A to B, but with a lower carbon content. Therefore there are two sources of MA in direct-quenched (DQ) steels; that from carbon partitioning during the B-F formation, and that associated with untransformed austenite. Due to the enrichment factor, one might expect the former to be of higher carbon content than the latter. These islands would subsequently transform to a high carbon martensite on cooling.[11, 150] Such microstructures are also known to show improved toughness.[152, 160]

The early work at BISRA, Sheffield, circa 1970, reported the advantages of superior strength, while maintaining good impact resistance, of microalloyed steels that were rapidly cooled immediately after hot deformation compared with the same steels which had been air cooled after rolling. [161-163] This change in processing route produced a different microstructure from the F-P associated with conventional controlled rolling. [63-65] These non-F-P steels were originally developed as laboratory experimental steels, at a time when both nitrogen additions $\geq$0.005 and the development of bainitic microstructures were generally regarded as deleterious to toughness. Tither et al [163] concluded that by utilizing the direct-quenching process, the near maximum secondary hardening potential of steels could be achieved.

More recently, several research groups have sought to raise the yield strength of microalloyed steels without producing deleterious effects on toughness and ductility. Steels containing separate additions of microalloyed steels containing vanadium and nitrogen, were investigated by Lagneborg et al [10, 11, 164, 165], who explored the effect of both nitrogen and cooling rate on properties. They considered a process based on a repeated recrystallization of austenite (RCR processing.) Fig 30 shows 'the steel with higher nitrogen content is significantly stronger than that with a low nitrogen processed in the same manner, although with some sacrifice of toughness. It can be seen that the strengthening potential of vanadium can be effectively utilised only at higher levels of nitrogen and that increased cooling rates have a profound effect, especially at these higher levels'.[11] In these steels, the titanium addition forming TiN, will influence the austenite grain size, while the remaining nitrogen combines with vanadium to form V(C, N), which is designed to nucleate in ferrite during cooling after rolling. The finishing accelerated cooling temperature (FACT) and cooling rate have a significant influence on the properties of microalloyed steels, normally increasing yield strength when FACT decreased to 500 ºC or lower. In Ti-V-N and Ti-V-Nb steels, as the cooling rate increased from 5ºC/s to 15 ºC/s, a greater volume fraction of both bainite and small particles with a reduced particle spacing were observed, the latter producing an increased dispersion strengthening contribution to the yield strength. [11, 166] Further exploratory laboratory work by Siwecki et al [167], was

centered on dilatometry, with the aim of producing yield strengths >600MPa in 8mm strip, directly in the mill. To stimulate bainite formation and simultaneously avoid ferrite/pearlite, a composition based on 1.4Mn-1.0Cr-0.25Mo was chosen to provide adequate hardenability combined with a cooling rate of 30 ºC s^{-1} between 600-400 ºC. Satisfying these conditions for a steel with 0.08V and 0.010-0.020N, gave yield strengths between 740 and 790MPa by the simulations. Raising the chromium level from 1% to 2%, with the same compositions, increased the yield strengths to 848-880MPa, or alternatively allowed a lower cooling rate of 20 ºCs^{-1}, which is associated with 12mm thick strip production in commercial mills, to give yield strengths reaching 780MPa. These strengths developed due to the arresting of the normal softening effect due to tempering of bainite during coiling, resulting in a ferrite lath width of 0.5 to 1.0µm, in which a high dislocation density was retained by a dense precipitation of V(C,N) in the ferrite. A recent paper from the same group [168], extended these laboratory simulations further in the full scale commercial hot rolling of 8mm thick strip to give yield/proof strengths >700MPa. These targets were all met or exceeded for the selected single trial steel composition: 0.042 C-1.55 Mn-1.0 Cr-0.30Mo-0.024Al-0.012N-0.079V. The additional requirements of good ductility (total El >11%), toughness down to ≤ -40 ºC and adequate weldability, were achieved.

A series of papers by Misra et al [17, 134, 169, 170] have made significant contributions to understanding the development of microstructures essential to

attain yield strengths eventually reaching >1000MPa. This σ_y permits the use of a reduced strip thickness in automotive weight reduction applications and in pipeline. Microalloyed steels[134] in the composition range 0.05C-1.5Mn-(0.1-0.2)Mo-(0.07-0.09)Nb-(0.065-0.085)Ti-(0.0005-0.0010)B were reheated at ~1325ºC, finished rolled at ~900 ºC and coiled at ~600 ºC to give a ferrite-bainite microstructure. The precipitates in the final state which were characterised from foils and replicas included 120-400nm (Ti,Nb) N, 10-120nm, spherical or plates (Nb,Ti)C and 3-5nm needle-like (Nb,Ti)C. It is quite possible that the precipitates were carbonitrides, as PEELS analysis was not available to analyse carbon and nitrogen in the particles. The high yield strengths of ~770MPa were attributed to the presence of a fine grain size in a mixed ferrite ~10% bainite microstructure containing an estimated dislocation density of 10^{14} m^{-2} retained by a fine dispersion of (Nb,Ti)C precipitates. The observed good toughness, of 50 J at−40 ºC, was believed to be a consequence of the fine grain sizes of 3–5 μm and a bainitic low temperature-transformation product. Another study of steels for pipelines, with similar carbon and niobium levels, a slightly lower titanium, and with 0.3-0.4Cr replacing molybdenum, included an examination of the welded steel.[169] The type and size range of precipitates was comparable to that above, [134] and found in the parent plate, HAZ and weld metal, together with small areas of degenerate pearlite/upper bainite, M and MA, all as microphases, which contributed to the yield strength of ~700MPa.

Achieving even higher yield strengths, ~1000MPa, is possible, but at an increased cost in both alloying and processing.[170] A steel with a nominal composition of 0.12C-0.5Si-1.4Mn-0.45(Mo+Nb+Ti+V)-0.00015B, was hot rolled to 6mm thick strip and coiled at 600ºC. It was then subjected to high frequency induction tempering at 600 ºC, following quenching at ~40ºCs^{-1} from 900 ºC. This produced a duplex microstructure of lath M and CB laths. <10nm (Nb, V) C and ~5nmVC particles were identified by FEG-TEM-EDX, the latter considered to precipitate in ferrite, obeying the Baker-Nutting orientation relationship. [60] Recently, a novel low carbon Nb-V-Ti-Cr microalloyed bainitic steel with yield strength of 1000 MPa and excellent low temperature toughness was successfully processed. The experimental results obtained by Xie et al [17]indicated that the steel subjected to a cooling rate of 65 ºC s^{-1} and a coiling temperature of 380-400° C (above M_s of 372 ºC), and finally furnace cooling to RT, resulted in superior mechanical properties. The ultra-high yield strength of 1058MPa was attributed to the transformation strengthening from CB and precipitation hardening from nano-scale (Nb,Ti)C precipitates. The Charpy impact absorbed energy of 24J at -20 ºC, was associated with CB and AF, together with a high fraction of large misorientation grain boundaries, obtained by controlling the coiling temperature.

Similar laboratory steels to Misra et al[170], investigated by Yi et al [171-174] , who achieved σ_y of 700MPa in bainitic high strength steel containing 0.15C-0.18Ti through conventional rolling [171], and in a steels with 0.08C and 0.06 to 0.08 Nb+ V+ Ti, rolling to 4mm strip, FRT 800ºC and cooling at 40 ºC s^{-1} to a

coiling temperature between 560 ºC and 350 ºC. The authors claimed that coherent precipitation occurred during coiling, which, along with a ferrite grain size of 2-6µm contributed to the strength. The Nb-Ti precipitates were identified by EDX.[172] However, it is unlikely that these particles were coherent, and their method of identification was not given. Later work by Yi et al [173], using a steel containing 0.04C-0.09Ti-0.2Mo, raised the yield strength to ~800MPa, through dispersion strengthening by nanometre carbides.

The quest for stronger and tougher steels has resulted in the recent application of both APT and EBSD techniques to further the understanding of non-polygonal transformation products. The transformation behaviour of a low-carbon Mo-Nb linepipe steel and the corresponding transformation product microstructures have been investigated by Cizek et al [175] using deformation dilatometry. They found that heavy deformation of the parent austenite caused a significant expansion of the polygonal ferrite transformation field in the CCT diagram, as well as a shift in the non-equilibrium ferrite transformation fields, toward higher cooling rates. Also, the austenite deformation resulted in a pronounced refinement in both the effective grain (sheaf/packet) size and substructure unit size of the non-equilibrium ferrite microstructures. This was confirmed in recent research investigating a 0.01Ti-0.039Nb-0.0046N steel by Liang and DeArdo[176] who used EBSD images to quantify grain and subgrain morphology.

11. Super-bainitic (SB) steel

A development of the bainite story which, however, is marginal but pertinent to microalloyed steels, is the development of 'super bainitic' microstructures, which can also result in strength levels of ~1000MPa. According to Garcia-Mateo et al [177], the bainite obtained by transformation at very low temperatures, is the hardest ever, has considerable ductility (almost all of it uniform), does not require mechanical processing, and does not require rapid cooling. Therefore, the steel after heat treatment, does not have long range residual stresses. Nominally, it is very cheap to produce and has uniform properties in large sections. Steel transformed into carbide free bainite can meet these criteria. SB steel comprises 50 % to 90 % bainite, the rest being austenite. The excess carbon remains within the bainitic ferrite at a concentration beyond that consistent with equilibrium; there is also partial partitioning of carbon into the residual austenite. The microstructure has very fine bainite platelets with an average bainite platelet thickness < 40nm. One composition is: 0.6-1.1C, 1.5-2.0Si, 0.5-1.8Mn, ≤ 3 Ni, 1.0 -1.5 Cr, 0.2 - 0.5Mo, 0.1-0.2V, balance iron, save for incidental impurities. The content of silicon and or aluminium, is to sufficient to render the bainite substantially carbide free. Of the various processes used, one includes the fast cooling from austenite to avoid transformation to pearlite, and transforming the steel to bainite at a temperature

in the range 190°C to 250°C, by holding between ~8 hours and 3 days. Due to the combination of ultra- high hardness and ductility, a major application for super bainite is armour, which is included in the patent. Friction stir welding is one means being explored to join SB steel plates and to other steels of other compositions. The topic of SB steels is discussed in more detail by Bhadeshia [178] and recently extended by Caballero et al [179] and Avishan et al [180], who explored and detailed the microstructures of high carbon steels, some with microalloying additions of niobium or vanadium to produce nanocrystalline bainitic ferrite, with plates a few tens of nanometers in thickness.

12. Thin slab direct charge processing

The background to the TSDC processes, also known as Thin Slab Direct Rolling (TSDR) and Compact Strip Production (CSP), which originated in 1989 in Crawfordsville, Indiana, U.S.A, has been very well described by Glodowski[181]. 'It appears that the commercial (TSDR) process preceded any academic research, and steady progress has been made over the past 25 years. Initially, the emphasis was on the obvious economic and ecological benefits gained by retaining part of the heat of casting in the slabs through to the rolling process, and casting to a "near net shape," thereby reducing the amount of hot working necessary to reduce the material to final gauge. Conventional

microalloying approaches for high-strength, low-alloy (HSLA) strip steels presented some processing complications that were new and required some alternative solutions. For many mills, the vanadium and nitrogen alloying system has proven to be highly effective and compatible with the processing peculiarities of the thin-slab-casting and direct-charging process. The thin-slab-casting, direct-charging and finish-rolling process has a number of characteristics that vary from conventional blast-furnace / BOF / slab-cast / slab-reheat / roughing-mill / finishing-mill routings. Fig. 31 shows these, plus the metallurgical mechanisms that operate at different stages of the TSDR process and ASP process.[181] First, steelmaking often uses electric-arc-furnace (EAF) melting from predominately scrap charges, and the refining process takes place in separate ladle-furnace operations. Second, the casting process involves rapid cooling, necessary for high-volume production in thin slabs from 50 to100 mm in thickness. Third, the slab is directly charged into a tunnel holding furnace without undergoing a $\gamma \rightarrow \alpha$ phase transformation. Fourth, the tunnel furnace is limited in reheating capabilities, typically from to 1100 to 1150°C maximum. Finally, the 50-mm slab will enter directly into a 5- or 6-stand finishing mill without undergoing a roughing mill reduction. When processing thicker slabs, 80-to 100-mm slab casters will have one or two roughing mills prior to a 5-stand finishing mill. In those cases, a transfer system of coil boxes or holding furnaces will be installed after the roughing mills to equalize temperatures before entering the finishing-mill stands. This step provides a

speed “break” between the start and finish rolling speeds, to allow more reasonable entry speeds in the first reduction pass. The remainder of the process, from finish rolling through a run-out table usually equipped with significant accelerated-cooling capability and into a down coiling system, will be similar to existing modern strip mills. Many of the mills have the capability to approach 1-mm final thickness, although most commonly the final gauge will be 1.5-mm or larger’. The changes in the TSDR technology over a period of 20 years to 2010, has been recounted by Klinkenberg et al [183], who also list the wide variety of steels now produced by this route.

The TSDR route has attracted a plethora of research activity over the past 15 years. Much of this has been concerned with optimizing production parameters and relating to them properties through microstructure. In particular, the evolution to precipitates associated with the various stages of the process have been investigated, and the development of coarse grained austenite received attention. These topics are considered in more detail below.

A particular theme running through an excellent review of 52 papers, published up to 2005, which are considered in some depth by Rodriguez-Ibabe[184], is the dependence on microstructure of the production parameters of TSDR technology route. He considered this route particularly attractive to microalloyed steels. This is because the microstructural development during TSDR and the mechanical properties of the final coil, differ from equivalent

steels conventionally rolled (CCR). In TSDR, slabs are thinner, compared with 200-250mm in CCR, while casting speeds are higher at 3.5-6.0m min^{-1}, compared with 0.75-1.25 m min^{-1}. Consequently, the thin slabs solidify much quicker, show less segregation, smaller inclusion sizes and a more homogeneous microstructure. Also, when scrap based electric arc furnace routes are used, thin slabs will have a very coarse as-cast γ grain size prior to hot rolling, experience a smaller total reduction during rolling, and higher nitrogen and residual element concentrations. Some of these aspects can result in a loss of microalloying efficiency as a consequence of premature precipitation before rolling. This is especially the case with titanium additions, and niobium steels must be considered with care. However, a different view was expressed by Bruns and Kasper[185], who together with Priestner and Zhou [186], published some of the earliest studies describing the laboratory simulation which resulted in the TSDR microstructural evolution of Nb-Ti microalloyed steels. The former [185] found that direct charging resulted in a greater dissolution of niobium and titanium compared with cold charging, leading to more precipitation of (Nb, Ti)(C,N), with a consequential greater strength in the final product.

A series of papers associated with Li [187-191] , also used laboratory simulation to study several vanadium based microalloyed steels which were vacuum melted, cast into moulds and controlled cooled at 3.5°Cs^{-1}, transferred to an equalisation

furnace and held at 1050, 1100 or 1200°C for between 30 and 65 min, prior to rolling to 7mm strip with 5 passes. After rolling, the strip was cooled under water sprays to simulate run-out table cooling, with a cooling rate of 18°Cs^{-1} and the aim-end water temperature was 600°C. Following cooling, the strip was immediately transferred to a furnace set at 600°C and slow cooled to simulate coiling. Samples were quenched after casting, after equalisation, after the fourth rolling pass and after coiling, to follow the evolution of both precipitation and mechanical and impact properties. Using this TSDR simulation in an investigation of the effect of a 0.008Ti addition to a 0.10Vsteel, Li et al [187] reported that for both V and V-Ti steels, the average austenite grain size in the ¼ thickness position of the as-cast ingot was about 1mm. This was reduced to a ferrite grain size of 4.8-7.2µm in the final strip. After equalisation at 1050ºC, precipitation of VN in austenite in the V steel was replaced by (V, Ti)N in the V-Ti steel. Both types of precipitates, which were in the range 2-10nm, made a contribution of >90MPa to dispersion strengthening. However, the yield strength of the V-Ti steel was lowered by the removal of a significant fraction of vanadium and nitrogen to form (V,Ti)N in austenite, thereby reducing the volume fraction of V(C,N) particles precipitated in ferrite. A similar situation occurred with V-Nb-Ti steels, with the addition of Ti resulting in a reduction of the yield strength due to precipitation in austenite of nanosized particles of (V, Nb, Ti) N, as characterized by both EDX and PEELS.[190,191] These transition

metal nitrides did not coarsen during the final stages of processing, retaining a size of ~7nm.

More recently, a TSDR process, similar to that described by Glodowski[181], called the Angang Strip Production (ASP) process, [182] has been used with medium thin slab of 170mm, by installing a roughing mill after the reheating furnace and before the finishing mill. Sha and Sun [182, 192-194] studied commercial sized slabs of an 0.04C- 0.06Nb-0.30V-0.014Ti-0.23Mo-0.0032N microalloyed steel in the as-cast condition. The slower cooling rate of the 170mm slab influenced the secondary dendrite arm spacing and the austenite grain sizes (320-2200μm) which were slightly larger compared to the microstructure of specimens taken from a corresponding TSDC route processing of 53mm thick slab (150-2000 μm). Dendritic precipitates were mainly niobium rich carbonitrides, while large cubic (150-600nm) and fine cubic (10-40nm) particles were characterized as titanium rich carbonitrides. The authors considered that vanadium was not detected in the complex precipitates due to the low nitrogen level in the steel. The refinement of the coarse grained austenite in the same steel, during roughing rolling after simulated equalisation, and more recently, after preliminary rolling in a roughing mill installed between the reheating furnace and the finishing mill, was also examined by Sha et al. [182] The microstructural homogeneity using the ASP route was found to be better than the TDSR route without additional rolling, due to a higher reheating and entry

temperatures and a larger reduction with the thicker slab. The coarse–grained austenite (~1mm) which developed during equalisation, (compared with, ~250µm in as reheated) in the Nb-V-Ti steels was modelled by Sha et al. [194] This followed the austenite grain size distribution method used by Gao and Baker [195,196] and Zhang and Baker [197], who considered abnormal austenite grain growth, an approach also developed by Uranga et al[198] for their model, which they later expanded to include the carbon and nitrogen content of microalloyed steels.[199] The modelling, involving the same processes discussed previously, [97-106] was used to alleviate microstructural heterogeneities in the final product. These heterogeneities are thought to be associated with the coarse austenite grains which developed through the processing parameters not perfectly matching, leading to un-recrystallized regions after the rolling process, particularly in niobium steels. All these authors[184, 195-199] concluded that their models highlighted production pit-falls which could be avoided, supporting the view that strict control of grain size at each stage of the TDSR process is essential.

The application of the TDSR process for thin slab production for pipeline microalloyed steels, reducing 50-90mm slab to 6 to 12.5 mm thick strip, was reported by Reip et al.[200] Two steels containing nominally 0.06C-1.35Mn-0.074V-0.04Nb-0.0065N with Steel(a) 0.01Ti, and Steel(b) 0.002Ti, were processed in a commercial caster. After processing, both steels exhibited very

good notch toughness of 200-400J/cm^2 at -40ºC and Steel (a) had σ_y of 680MPa, which was 100MPa higher than Steel (b). The excellent toughness of both steels was attributed to the fine grain sizes of 2.6µm and 6µm, respectively.

It has been showed by Lee et al [151], that increasing the dislocation density opposed the formation of acicular ferrite and bainite through a mechanical stabilization effect. The results of Reip et al[200], suggest that the exclusion of titanium in Steel (b) favours the formation of acicular ferrite and bainite. This maybe be due to the higher percentage of dissolved niobium which supports the formation of acicular ferrite and bainite, because titanium, precipitated as TiN, may provide nucleation sites for precipitation of Nb(C,N), during the final phase of rolling.[201] Further work was devoted to comparing fine scale precipitates in high strength industrially processed trial steels containing Ti-Nb and Ti-Nb-Mo-V additions. This focussed on the precipitate characterisation based on crystallography, through some careful analysis of electron diffraction patterns gained from thin foils.[202] As the nitrogen content of the steels was not given, it seems that, based on lattice parameter determination, they were all considered to be carbides.

An investigation was undertaken by Nagata et al [203] to assess the potential of obtaining and utilizing titanium nitride refinement, primarily for austenite grain size control, through the increased post solidification cooling rates associated with the TSDC process. They comparing eight commercially TSDC cast steels

with a conventionally cast (CC) steel. The steels had titanium contents in the range 0.009% to 0.048% and Ti/N ratios between 0.6 and 6. The precipitation behaviour was explored, with extensive TiN particle size distributions evaluated by TEM. Despite designing the steels to prevent precipitation in the liquid state, TiN cubic particles of ~1μm were found in some steels after casting.

The hyperstoichiometric steels (excess titanium) exhibited cubic TiN particles of mean size <40nm after casting and soaking, but showing dramatic coarsening to >90nm after hot rolling. Hypostoichiometric steels, which contain excess carbon and/or nitrogen, exhibited no coarsening in the end product. Also, comparison of the particle sizes of the TSDR and CC steels, showed a shift to larger sizes and greater relative frequency for the particles in the CC steel.

13. Weldability of microalloyed steels

The weldability of microalloyed steels is an extensive topic in its own right, and has been addressed in many publications, including several of the reviews discussed here [4, 8, 9, 11, 13] and parts of the book by Easterling [204]. As expressed by Hart [205] 'the opportunities that microalloying gives for improving weldability of microalloyed steels, by reducing carbon content was fairly quickly recognised and became another major driving force for the development and understanding.' Also, many modern steels have low sulphur, and generally

nitrogen is < 4ppm.However, rapid cooling of regions adjacent to the weld (HAZ) frequently produce martensitic hard zones leading to local increases in hardness, which can result in lower toughness. It is common practice to specify a maximum hardness that can be tolerated in the HAZ. As the hardness of martensite is related to the carbon content of the steel, this has a profound influence on hardenability. Other elements affecting hardenability are considered in the carbon equivalent (CE) equations deduced from multiple regression analysis, such as:

$$CE = C + Mn/6 + (Cr + Mo + V)/5 + (Ni + Cu)/15 \qquad (9)$$

As pointed out by Lagneborg et al [11], 'nitrogen levels in plain C-Mn steels show a strong correlation with coarse-grained HAZ toughness, where higher N-levels are clearly deleterious, showing a marked increase in Charpy T_c, which is reflected in maximum permitted contents of nitrogen in various steels specifications. However, the presence of the nitride forming elements Al, Ti, Zr, Nb, V, can mitigate considerably the negative effect of nitrogen, indicated by the relaxation of the limit of nitrogen in the presence of these elements.' Much attention has been paid to steels containing titanium and nitrogen and how these elements interact in combination with vanadium, niobium and zirconium.

In a review on the status of microalloying elements in plate used for the construction of naval ships, by McPherson[206] , it is recognized that the potential problem area tends to be the HAZ toughness. A tentative relationship exists

between the HAZ toughness effect of the microalloying element and its effect on the susceptibility to induce transverse slab cracking. Overall, it was found that the benefits improve in the order of niobium, vanadium and titanium. If cost is factored into these effects, then the microalloying element with the most potentially positive benefits is titanium. [206]

In titanium microalloyed steels, the effects of Ti and N contents in improving the HAZ toughness through the pinning of austenite grains by TiN particles has been mentioned earlier and is well established.[207-210] TiN particle size and volume fraction both influence toughness.[211,212] With hyperstoichiometric titanium additions, coarse TiN particles (side length>0.5μm), form in the liquid state, and above a critical number density can act as fracture initiation sites when ferrite grain sizes are >9 μm.[212] It is recommended that the contents of Ti and N should be kept close to the stoichiometric ratio Ti/N=3.42. Another view is that soluble nitrogen should be minimized. Mixed additions of Nb-Ti-V in microalloyed steels were considered by Adrian and Pickering [213] and by Hamada et al [214], as a function of nitrogen content. Both concluded that high nitrogen, 0.018% and 0.0084%, respectively, was advantageous, resulting in the substantial refinement of austenite grains [213, 214], and in the case of HAZ simulation, an austenite grain size of ~30μm was produced by ~10nm (Nb, Ti)N precipitates. The effects of zirconium, along with those of titanium and vanadium, on submerged arc deposits were compared by Koukabi et al [215], who concluded that vanadium had a greater effect on increasing toughness in both

the as-welded and stress relieved welds than did zirconium. It is well established that both TiN and ZrN particles have little solubility in austenite, as seen in Fig 14. Zirconium additions were expected to behave similarly to titanium, but Koukabi et al [215] found that ZrN particles did not promote acicular ferrite and the weld toughness was only slightly improved, due they considered, to the removal of the soluble nitrogen. The observations of Koukabi et al[215] were later explained by Chai et al [216], who suggested that the equilibrium number and composition of the inclusion phases changed with the zirconium addition from Ti_2O_3 to ZrO_2. When the zirconium content was lower than 0.0085%, the inclusions were mainly Ti_2O_3 and ZrO_2 , and the oxides shared the same proportion of ~0.0045%Zr content. The role played by ZrO_2 is also supported by the work of Guo et al [217].

A study by Wan et al [218] of simulated HAZ in Ti-Zr steels, also found in situ evidence for acicular ferrite nucleating on Zr-Ti oxides containing Al, Mg and Mn when the austenite grain size was large, 100-200µm, but bainitic plate packets, nucleated on different sites of smaller, ~50 µm, austenite grains.

While inclusions in steels are usually classed as oxides and sulphides, Koseki and Thewlis [219] also include large nitrides, as discussed above. Inclusions are normally regarded as being deleterious to toughness, but over the past three decades, inclusion assisted microstructure control has become a key technology in the improvement of toughness of weld and HAZ regions. In addition to pinning austenite grain boundaries, it is well documented that inclusions

nucleate intragranular acicular ferrite (AF).[219-221] As discussed previously, the development of a microstructure with a high proportion of AF is recognised as means of generating steels with high strength and good toughness. This approach had its birth in attempts to improve the microstructure of welds, where toughness problems were mitigated by inclusion nucleated AF. The formation of AF is closely related to oxygen content of the weld metal and the type, volume fraction, and size distribution of the inclusions.[221, 222] It has been reported that TiO and TiN, if oriented correctly, have good coherency with ferrite, when the two lattices exhibit a low misfit, δ.[223]

Mills et al [222] identified a titanium rich phase, which they considered to be a mixture of TiO and TiN with other phases, on the surface of a glassy manganese silicate and on galaxite (Al_2O_3,MnO). Both TiO and galaxite have a low δ, ~3%, with ferrite, which is considered the reason these phases nucleate AF. Several other phases have been collected by Koseki and Thewlis [219] showing low δ values, with <5% mismatch. In addition to low misfit, the number density of inclusions, N_{AF}, which act as AF nucleation is important.

More recently, the AF formation potency of Ti-Rare earth metal (REM)-Zr (TRZ) complex oxides have been investigated in the simulated HAZ of low carbon steel studied by Nako et al [224]. The TRZ complex oxide shows a higher AF formation potency than either titanium or aluminium oxides. AF crystals nucleate on the interface between austenite and the Zr-rich oxide phase. Good lattice coherency through the orientation relationship:

(011) AF// (011) (oxide),

[100](AF)//[01$\bar{1}$] (oxide)

between AF-TRZ, with δ calculated as 8.8%. Also N_{AF} (mm^{-2}) was 8, 14 and 42, respectively for Al, Ti and TRZ, all added alloys. These two factors, δ and N_{AF}, promoted AF nucleation on TRZ complex oxides. Also, the AF-austenite orientation relationship is that of Kurdjumov-Sachs (K-S), and the AF-TRZ and K-S 'three phase' orientation relationships is caused by variant selection of AF. This is in addition to the formation of a rational orientation relationship between zirconium-rich oxide phase and the austenite matrix during the HAZ thermal cycle. Therefore several factors must be favourable for nucleation of AF by inclusions.

While the welding of microalloyed steels by the standard techniques is well established, less has been published on the application of friction stir welding (FSW) to this group of steels.[225, 226] FSW, which was invented by TWI in the early 1990's and was originally developed for joining Al-alloys. [227-231] FSW is a solid-state joining process (the metal is not melted) that uses a third body tool to join two facing surfaces. Heat is generated between the tool and material which leads to a very soft region near the FSW tool, Fig 32. It then mechanically intermixes the two pieces of metal at the place of the joint, after which the softened metal (due to the elevated temperature) can be joined using mechanical pressure which is applied by the tool. [232] FSW is now a mature process for welding several alloys, including microalloyed steels. The

advantages of FSW include improved mechanical and metallurgical weld properties, rapid joining speeds, elimination of weld cracking and porosity, and no need for shielding gas or filler metal, together with normally resulting in lower residual stresses than fusion welding. [227-233] Also, FSW is a "green technology" in that it produces no arc radiation, no significant fumes, and no hazardous waste. The possibility of joining dissimilar metals and alloys, such as steels and aluminium is now being actively explored. [225] There are several publications describing FSW of ferritic steels, where additional advantages include lower heat inputs, with, it is claimed, fewer metallurgical changes in the HAZ, and also the potential for joining dissimilar steels. [234-236] The majority of the material joined by the FSW process has a thickness of ≤ 10mm. The plate thickness which can be welded, is limited by the length of the tool, which for BN pins, often the pin of choice for FSW of steels, is ~ 8mm. [237, 238] However, the severe stresses and high temperatures experienced by the tool materials pose a formidable challenge for the development of cost effective and durable tools for the FSW of hard alloys. As a result, the initial commercial applications of FSW to steels are likely to come from specialised, niche areas where fusion welding clearly has serious difficulties, provided the required structure and properties can be achieved by FSW.[239] While much of the earlier FSW research was concerned with details of the process and modelling of flow, [227-239] the role of microstructural evolution is now beginning to be addressed in more detail, [240-245] 'as an understanding would enable a prediction of welding properties

resulting from the microstructures'. [243] As detailed by De et al, [239] compared to fusion welding, microstructure is affected by several factors. The peak temperatures for FSW are lower, and therefore the grain size of austenite that forms in the HAZ is often smaller than after fusion welding. Also, severe deformation and flow of plasticised steel alter the stability of austenite in the TMAZ because of the stored energy, which affects its decomposition to daughter phases. In contrast, the austenite formed during cooling of molten weld metal in fusion welding is hardly affected by any stored energy. Because deformation in the stir zone (SZ) varies with position, this influences the local austenite transformation kinetics, as in thermomechanically processed microalloyed steels, the modelling of which was considered earlier. [239] Therefore microstructures are expected, and found, to vary considerably in different parts of the SZ.

EBSD produces orientation maps which provide vital information on grain misorientation and grain size from the base metal (BM), HAZ, thermomechanically affected zone (TMAZ) and the SZ of FSW. This application of EBSD has been used to good effect by Davies et al [246], studying deformation textures in FSW Ti-6Al-4V alloy, who showed that the texture of the Ti α hcp fully lamellar microstructure was inherited from the shear texture of the high temperature β phase. This does not yet appear to have been investigated for the $\gamma \rightarrow \alpha$ transformation in FSW microalloyed steels. Cho et al [243] were among the first to apply EBSD obtained with a FE-SEM, to study the

microstructural evolution of a FSW high strength linepipe steel. They found that in the SZ, the structure morphology, texture and misorientation angle were completely different from other FSW regions. Fig 33 shows the changes in grain size and the fraction of acicular ferrite across the weld section, observed in the SZ. An increase in hardness in the SZ, also recorded by Lienert et al, [234] was attributed to acicular-shaped bainitic ferrite, observed by TEM. Mirinov et al [242] found that the material in the SZ of pure iron had a prominent (112) [111] shear texture with the shear direction aligned approximately tangential with the shear surface, while the work of Cho et al [243] revealed only a weak shear texture.

A FSW method developed for thicker plate, >12mm, with applications, for example, in shipbuilding, involves passing the tool sequentially on both sides of the abutted plates.[247, 248] This gives rise to a complex interaction zone (IZ) where the deepest re-solidified metal created by the first pass is re-melted by the second pass on the reverse side of the plate, Fig 34. The HAZ's are also affected by the plate reverse side FSW pass. Baker and McPherson [249] have investigated in detail the variation of microstructure and the related microhardness in different parts of a FSW EH 46 microalloyed steel. They found a decrease in microhardness in the IZ relative to the HAZ and TMAZ. It was also noted that a significant variation in the IZ microstructure over small distances occurred, as predicted by De et al [239]. Packets of laths adjacent to polygonal ferrite grains Fig 35, some containing dislocations pinned by particles was also observed. It was considered that SIP occurred in the TMAZ. Rahimi

et al [250] used EBSD, after the manner of Gourgues et al [251] to assess the crystallographic features of the EN46 steel. Their EBSD data [250] show that the IZ underwent deformation in ferrite, since the pole figure shows bcc shear texture. Also, the IZ has ultra-fine grain size (i.e. $\leq 1\mu m$) in which the misorientation distribution fits in well with the MacKenzie distribution, implying that the ultra-fine grain ferrite is recrystallized. TEM data collected from the IZ shows dislocation cell structures which agrees well with the EBSD data. However, in the TMAZ the EBSD data show (111) pole figures in the bcc ferrite similar to (011) fcc shear texture, implying that the deformation during FSW occurred in austenite. The data also show a significantly high fraction of sub-structures that are scattered from MacKenzie distribution. These can be due mainly to low angle grain boundaries between ferrite grains that are originating from the same austenite grain. [250] The study of microstructure using TEM and related EBSD is at a relatively early stage, and it is expected more will be forthcoming in the future.

14. Strength, toughness and ductility

14.1Components of strength

For many years, the possibility of improving the properties of polycrystalline materials through understanding and quantifying the microstructural components which determine the properties, has been a major goal of materials

scientists.[30,31] This topic has been explored to a much greater depth in the case of microalloyed steels than in perhaps, any other material. One of the main reasons, has been the challenge posed by such a complex microstructure, which involves contributions from solid solution hardening, precipitate dispersion strengthening, dislocation densities, grain and sub-grain size, the Peierls-Nabarro stress and a possible texture contribution.[2, 28, 29, 252-257] In addition, the effect of the interaction of some of these components, giving rise to superposition, which is considered below, must be addressed. [114, 257]

It has long been appreciated that a fine grain size is associated with superior properties. In the 18thC, separately Reaumur, [258] and Grignon, [259] noted that, as revealed on fracture surfaces, excellent metals were distinguished from mediocre ones by the fineness of their grains. This historical background was initially described by Desch [260] more recently by Armstrong. [261]

The measurement of a fine grain size necessitated optical microscopy, which lead to the study of microstructure normally described as 'metallography'. The earliest systematic study is generally attributed to H.C. Sorby, who in 1849, extended a technique to geological specimens of meteorites, taught to him by a Manchester surgeon, W.G.Williamson. [262] Sorby adapted his techniques to the examination of iron and steel products of his native city, Sheffield. Many years later, W.L. Bragg, who had long held the view that grain size influenced the

strength of polycrystals,set Orowan in the late 1940's, with two research fellows, Hall and Petch, to systematically study this effect in mild steels. [263]

The Hall-Petch relationship, which was initially concerned with FP steels, conveniently allows σ_y, the lower yield stress, (or often in practice, the 0.2% proof stress) to be related to individual components of strengthening.

$$\sigma_y = \sigma_o + k_y d^{-1/2} \qquad (10)$$

As can be seen in Fig 36, based on the work of Morrison [264], when σ_y is plotted against a function of the grain size, $d^{-1/2}$, a straight line relationship is obtained over a range carbon contents in steels. The intercept on the ordinate axis, σ_o, and the slope of the straight line, k_y, are experimental constants. Hall and Petch proved that strengthening was therefore due to a reduction of grain size together with an increase in the factors which determined σ_o. The latter, which is often referred to as the friction stress, [29] results from the features which arrested the motion of dislocations across the grains. Problems associated with the determination of σ_o have been discussed in detail by Baker [255]. These included strain fields from misfitting solute atoms in solid solution (σ_{ss}) precipitates (σ_p) and other 'forest' dislocations (σ_d). Other factors are sub-grain sizes (σ_{sg}) and texture (σ_t) plus the basic lattice Peierls-Nabarro component, (σ_i).

The linear summation of these components leads to the relationship:

$$\sigma_o = \sigma_i + \sigma_{ss} + \sigma_p + \sigma_d + \sigma_{sg} + \sigma_t \quad (11)$$

$$\text{giving} \quad \sigma_y = \sigma_L = \sigma_i + \sigma_{ss} + \sigma_p + \sigma_d + \sigma_{sg} + \sigma_t + k_y d^{-1/2} \quad (12)$$

where σ_L refers to linear addition.

Each of these components is now considered separately.

14.1.1 Solid solution strengthening (σ_{ss})

Mechanisms of solid solution strengthening in microalloyed steels are dealt with in detail by Gladman[3]. The contribution of σ_{ss} to σ_y, based on data provided by Gladman[3], up-dated from Pickering and Gladman, [252] were obtained from regression equations, where the alloying elements are given in weight per cent, can be expressed as:

$$\sigma_{ss}\,(\text{MPa}) = 678\text{P} + 83\text{Si} + 32\text{Mn} + 38\text{Cu} + 11\text{Mo} \quad (13)$$

The low weight percentages of Ni and Cr normally present in microalloyed steels, provided no contributions to σ_{ss}.

Table 7

Atomic radius of elements used in microalloyed steels and percent difference from iron

Element	Atomic radius nm	% difference to that of the iron atom radius
Ti	0.147	+14.8
V	0.136	+ 6.2

Cr	0.128	» 0
Zr	0.160	+25.0
Nb	0.148	+15.6
Mo	0.140	+ 9.4
Hf	0.31.3	+31.3
Ta	0.148	+15.6
W	0.141	+10.2

14.1.2Dispersion strengthening (σ_p)

Detailed accounts of dispersion strengthening, otherwise known as precipitation hardening, are found in several publications [265-267], while others deal specifically with microalloyed steels. [268, 269].

As mentioned previously, while vanadium carbides can precipitate coherently in ferrite, it is generally agreed, that in commercially processed niobium microalloyed steels, the incoherent and the strain induced precipitation in austenite provide the main contributions to σ_p. In many cases, it is not possible to separate the contributions of σ_p and σ_d. This is because deformation is introduced in the temperature range where precipitation commences, and is known to lower this temperature from the situation where precipitation of the same particles starts in the absence of strain. Briefly, strengthening takes place when particles impede the motion of dislocations, [265-269] and the overall effect is mainly due to the particle radius, r, and the particle volume fraction, f.

Dislocations can shear coherent (soft) particles, and $\sigma_p \approx (fr)^{1/2}$, or dislocations can loop around the incoherent (hard) particles, where $\sigma_p \approx f^{1/2}/r$.

Goldschmidt [270] found extensive mutual solubility of all the carbides and nitrides collated in Table 5, which formed carbonitrides. Examples are the TiN-NbN system [122] and the ZrC and ZrN system. [123] The exception is VC and VN with ZrC and ZrN, attributed to the difference in the sizes of the Zr and V atoms, which are given in Table 7. This also has implications for ternary systems such as TiN-ZrN-VN and ZrN-NbN-VN, where a miscibility bay should occur, in contrast to complete solution systems such as TiN-VN-NbN, or similar mixed carbides or carbides and nitrides. Therefore in most microalloyed steels, which contain both carbon and nitrogen in their chemical composition, the strengthening precipitates will be carbonitrides of varying C/N ratios.

The Baker-Nutting orientation relationship (BNOR) was not found in the detailed and careful crystallographic study undertaken by Epicer et al. [271] They used a model Fe-V-C alloy, and found the V_6C_5 precipitates, which exhibited an ordered monoclinic form, also characterised by Hollox et al. [272] Furthermore, their survey of the literature found no conclusive evidence for the existence of precipitates with the V_4C_3 structure. [271] This is surprising, as many publications have included SAED patterns, matching the fcc:bcc BNOR [60] for transition metal carbides and nitrides, sometimes described as the Bain orientation, with the correct lattice parameters.[273-278, 280] BNOR has been shown apply to incoherent Nb, V, Ti carbides, nitrides and carbonitrides precipitated in ferrite,

including interphase precipitation. [277-284] It should be pointed out that both the composition of the model alloy studied by Epicer et al [271], and the heat treatment conditions are unrepresentative of microalloyed steels. It would be edifying if these authors applied the same rigour to vanadium carbonitrides precipitated in commercial controlled rolled microalloyed steels. Here, however, the main point is to confirm whether the V_6C_5 precipitates are sheared or looped by dislocations, as this leads to different estimates of strengthening. There is still disagreement on the subject on the role of solute atoms, particularly niobium, versus SIP of nitrides and carbonitrides, on the kinetics of austenite recrystallization, discussed previously, and also whether or not carbides, nitrides or carbonitrides form coherently or incoherently in ferrite. [51-57, 131-133] Almost invariably, particles characterised in microalloyed steels are incoherent. This is supported in a recent APT study on vanadium steels, which found 5-20nm size, randomly distributed V(C,N) precipitates, with a BNOR, in ferrite. Interphase precipitates formed in a region of higher carbon. [280]

A more detailed expression derived from the initial work of Orowan, [285] developed by Ashby [286] and others, [4] leads to an expression which allows quantification of σ_p:

$$\sigma_p \text{ (MPa)} = (0.538\ G b f^{1/2}/X) \ln (X/2b) \qquad (13)$$

where G is the shear modulus of the matrix, b is the Burgers vector of the dislocation (mm), and X the real spatial diameter of the particles (mm). The

expression assumes the particles are spherical, and geometrical factors must be introduced for plate or needle shaped particles.

For microalloyed steels, with G=80,300MPa, b=2.5 x 10^{-4}µm, Gladman[4] produced

$$\sigma_p \text{ (MPa)} = (10.8f^{1/2}/X) \ln (X / 6.12510^{-4}) \qquad (14)$$

with X in µm.

σ_p values of 50-100MPa are typical of niobium steels of the 1980's. Kostryzhev et al [54] have collated σ_p values from eight sources, reporting on Nb and NbTi microalloyed steels, which range from 20 to 230MPa, and point out that for the same steel using different TMP routes, variations up to 4.5 times have been found. However, some of this data may include a contribution from dislocation strengthening. Recently, Yen et al [281] studying interphase precipitation of TiC, estimated σ_p values to be ~300MPa, in steels with σ_y of 780MPa.

One of the main difficulties in calculating σ_p, is the estimation, based on experimental determination of the volume fraction, f, of precipitates involved. Often, extraction carbon replicas have been employed. The problem is to determine the depth of steel which has been etched to provide on the replica in 2D, the particle volume fraction distributed in 3D. A solution to the problem was given by Ubhi and Baker [287], and discussed further by Baker. [255,288] Using the extraction carbon replica technique, one study noted that few particles ≤ 4nm was recorded. [124] MacKenzie et al [289] repeated the work using a focussed ion lift out technique, followed by low ion energy milling. This allowed the

quantitative analysis of ~1nm particles of VN. How much the loss of particles between extraction carbon replicas and the above technique, in terms of volume fraction and influence on σ_p, is not known, as this work is probably the only record of this observation.

14.1.3 Dislocation strengthening (σ_d)

Motion of dislocations (mobile) is impeded by interaction with both other mobile dislocations and with immobile dislocations already present in the grains, usually described as forest dislocations. These may be present along with precipitates, as often in the case of as rolled microalloyed steels. In the former case, σ_d, can be calculated based on the equation first derived by Taylor [290]

$$\sigma_d = \boldsymbol{\alpha} G b \rho^{1/2} \qquad (15)$$

where $\boldsymbol{\alpha}$ is a constant and ρ the dislocation density. Several values of $\boldsymbol{\alpha}$ have been derived experimentally and collated by Baker. [255] The value 0.88, obtained by Roberts et al [291] is recommended.

Based on the modifications to the Hall–Petch equation, many methods have been developed to estimate the lower yield stress, σ_y, from microstructure measurements of particle size and dislocation density. These have met with some success in microalloyed steels when dislocation densities where relatively low. Modifications to Eqn. 11 have been proposed when dislocation densities

are high, $>10^{15}m^{-2}$, due to the strong precipitate-dislocation interaction resulting in super-positioning, discussed below.

14.1.4 Grain size component

Fig 36 can be used as a guide to the possible strengthening routes for microalloyed steels with a ferrite-pearlite microstructure. Thus for a grain size of 50µm, tested at 300K, the data give a corresponding σ_y of ~160MPa. For a small ferrite grain size of 5µm, σ_y increases to 350MPa, emphasising the importance of grain size as a method of increasing strength in polycrystals. Fig 36 also shows that strength can be increased by displacing σ_o to the dotted line A-B. For a grain size of 5µm, σ_y increases to 600MPa. This is achievable by controlled rolled microalloy steels. In theory, changing the slope, k_y, as shown in Fig 36 for the dashed line σ_o-C, will also increase σ_y, although this is not normally a practicable route. The Hall–Petch relation has been found experimentally, to hold for materials with grain sizes ranging from 1 mm to 1 µm. However, experiments on many nanocrystalline materials demonstrated that if the grains reached the critical grain size, which is typically around10 nm, σ_y would either remain constant or decrease with decreasing grains size.[292]

A number of different mechanisms have been proposed for this relation which fall into four categories: (1) dislocation-based, (2) diffusion-based, (3) grain-boundary shearing-based, (4) two-phase-based. [293] Manufacturing engineering

materials, such as microalloyed steels, with this ideal grain size is difficult, because only thin films can be reliably produced with grains of this size.

However, microalloyed steels comprising of sub-grains, having misorientations, θ of < 8º are well documented, and include acicular ferrite and bainitic microstructures. De Ardo et al [6] comment that 'as there are relatively few high angle boundaries, beyond the prior austenite boundaries, Hall-Petch strengthening will not be important.' However, the friction stress term σ_o, envisaged by Petch[31], included a contribution from dislocations, as seen in Eqns. 11 and 12. Equations dealing with substructures, sometimes described as cells, are available and discussed in detail by Embury[294] and Thompson[295]. Both provide a comprehensive list of references to relevant early research, extended by Castrofernandez and Sellars.[296]

σ_{sg} is usually related to the sub-grain size, l, by:

$$\sigma_{sg} = k_s l^{-m} \qquad (16)$$

and for iron alloys [255] ,when m is often taken as 1:

$$k_s \ (Nmm^{-3/2}) = 2.1\sqrt{\theta} \qquad (17)$$

θ is the sub-grain boundary misorientation in degrees. The Hall-Petch equation is just as applicable to acicular ferrite and bainitic microstructures as to ferrite-pearlite. Fig 37 from Gladman and Pickering [255] obtained from their multiple regression equation:

$$\sigma_y \ (MPa) = -191 + 17d^{-1/2} + 14.9n^{1/4} \qquad (18)$$

where d is the mean linear intercept of bainitic ferrite laths and n, the number of carbide particles per unit planar section of microstructure. The carbide inter particle spacing, λ, is related to n through:

$$\lambda^{-1/2} = 0.94 n^{1/4} \qquad (19)$$

The results from Eqn.18 are presented in Fig.37, which shows that carbide strengthening only becomes significant at finer bainitic ferrite lath sizes.

14.2 Summation of strengthening components

One of the earliest examples of successful linear additive strengthening of microalloyed steels comprising grain, subgrains and precipitation was by Mangonon and Heitmann [297], extended more recently by Morales et al [298], who considered the same method for their linepipe steel which was comprised of AF and PF microstructures.

The summation of these components leads to the relationship:

$$\sigma_y = \sigma_{Ly} = \sigma_i + \sigma_{ss} + \sigma_p + \sigma_d + \sigma_{sb} + \sigma_t + k_y d^{-1/2} \qquad (12a)$$

where σ_i has values between 40 and 74MPa at 273K.[264,299]

In a reassessment of results obtained during research on niobium steels for microstructures containing high dislocation densities, the initial comparison of the estimated, σ_{Ly}, by linear addition, and experimental data, σ_M, was poor [256]. With a second approach, taking into account superposition, [114,256] the components were divided into two groups, σ_A and σ_d, and then used in a relationship based on the square root of the sum of the squares of σ_A and σ_d,

$$\sigma_y = \sigma_R = \sqrt{(\sigma_A)^2 + (\sigma_d)^2} \quad (20)$$

where $$\sigma_A = \sigma_i + \sigma_{ss} + \sigma_p + k_y d^{-1/2} \quad (21)$$

This procedure followed the theoretical approaches combining weak and strong obstacles, described by Foreman and Makin [300] and by Kocks et al [301], who considered that in an alloy containing both forest dislocations and precipitates; these obstacles would not be distinguished by mobile dislocations. This assumes that precipitates, nucleating and growing on dislocations, would offer the same resistance to mobile dislocations, as interacting forest dislocations. Equation 20 avoids adding the contributions from both σ_p and σ_d components in a linear manner when the interaction involves superposition. A summation equation was also devised by Li et al [302], giving the yield strength, σ_C , as

$$\sigma_C = \sigma_i + \sigma_{ss} + (\sigma_d.\sigma_p) \quad (22)$$

Table 8 gives data comparing σ_y determined experimentally σ_M [114] and calculated from microstructure [114], σ_L -linear addition, σ_R - square root of the sum of the squares, σ_C–Li et al [302]

Table 8

A comparison of σ_y determined experimentally σ_M [114] and calculated from microstructure [114]

Steel	σ_M	$k_y d^{-1/2}$	σ_d	σ_p	$(\sigma_d.\sigma_p)^{1/2}$	$\sigma_i + \sigma_{ss}$	σ_R	σ_L	σ_C
	MPa	$Nmm^{-3/2}$	MPa	MPa	MPa	MPa	MPa	MPa	MPa
S1	510	294	116	85	99	118	510	613	511
S2	559	340	145	51	86	118	543	654	544

S5	668	263	486	50	156	118	649	917	537
S6	489	340	102	43	66	118	511	501	524
S7	533	340	102	38	62	118	506	598	520
S21	544	340	116	56	81	118	527	630	539
S25	671	294	479	48	152	118	664	947	564

As can be seen, comparing the data for σ_L with σ_C and σ_R, both approaches are superior to the linear summation, and σ_C data is slightly closer to σ_M when the dislocation density is lower. However, for high dislocation densities produced by, for example, low controlled rolling finishing temperatures, σ_R data for steels S5 and S25 gives a better agreement with that of σ_M. For this reason, the summation method recommended by Irvine and Baker [114] was used in recent work by Carretero Olalla et al [115] analysing the strengthening mechanisms in microalloyed line pipe steel, with satisfactory results. It is interesting to note that the difference between σ_M and σ_R values in Table 8 is 7 to 27MPa, i.e.1.0-5.1%. In general, obtaining an estimated σ_y from the microstructural features considered above to within ≤ 50MPa, i.e. ~10%, compared to σ_M is acceptable. However, the determination of σ_y only from microstructural measurements is tedious. In work where the details of individual components was of less interest, [189,303,] and the dislocation densities relatively low, the combined σ_p and σ_d was estimated using Eqn. (23),

$$\sigma_p + \sigma_d = \sigma_M - \sigma_i + \sigma_{ss} + k_y d^{-1/2} \qquad (23)$$

There are alternative ways of determining strengthening components, other than by microstructural measurements. [304] Speich [305] used resistivity measurements to follow precipitation in alloy steels during tempering treatments to good effect. The same approach was used by Hall and Baker [306] studying precipitation of vanadium carbide in controlled rolled steels. The accuracy of ± 10 %, Fig 38, was similar to that obtained based on microstructural estimates, but no less tedious, and an example of the summation of the components is given in Fig.39.

Hornbogen and Staniek [253],[307] pointed out that, whereas the breakdown of coherency to develop incoherent precipitates via partially coherent precipitates, [308] may involve the generation of dislocations, the presence of coherent precipitates alone does not. This led them to conclude that a superposition of coherent particles and dislocations was not relevant, and that linear addition of estimated strengthening components gave a satisfactory agreement with the measured yield strength.

Recently, a 3-D analytical model of precipitate strengthening with superposition laws was developed, and characterization parameters were obtained by local-electrode atom-probe (LEAP) tomography. [309] This allowed a detailed calculation of yield strength of secondary hardening at different stages of ageing due to multiple precipitates of Cu and M_2C in a BA160 steel, to be made. The model predicted σ_y as a function of aging time at 450°C within ±13% of σ_M. The authors state that this is the first time that the prediction of the yield

strength directly from the microstructure of a multiphase steel was shown to be feasible.

Another recent study systematically investigated the stress–strain behavior of ferrite and bainite with nano-sized vanadium carbides in low carbon steels. [310] The ferrite samples were obtained through austenite/ferrite transformation accompanied with interphase precipitation and the bainite samples were via austenite/bainite transformation with subsequent aging. The contributions from solute atoms and grain boundaries were simply added, whereas those from dislocations and precipitates were treated by taking the square root of the sum of the squares of two values, giving $\sigma_{N.}$ This is a different approach from that given by Eqns(20) and (21). From the data they give, σ_L compares well with σ_M for ferrite, $\leq$ 9.6% over estimate, while comparison with σ_N is 9.6%-19.2% under estimated. For bainite, $\sigma_N \leq$ 9.4% under estimate is superior to σ_L summation, which is 19-37% over estimated.[310] Kostryzev et al [311] , who used a linear addition of components to quantify the strengthening components of Nb-Ti FP thermomechanicaly processed Nb-Ti steels, also obtained disagreements between measured and calculated σ_y values, which could reach 54%. These were attributed to overestimates in solid solution and precipitation contributions, and the errors increased with decreasing deformation temperature.

Despite the detailed consideration of the models used in calculating the individual components strengthening and the care taken to ensure the highest accuracy from microstructural parameters [115, 256, 288, 309-311] such as the foil thickness required for dislocation density, determination for σ_d and precipitate volume fraction, f, needed for estimates of σ_p, no improvement on the accuracy of the estimate in σ_y from microstructural measurements has been achieved. It is apparent that the calculated σ_y has, at best, a ±90% accuracy compared with σ_M. The error is often due to the inhomogeneous microstructure and the high magnifications required to image small particles and dislocations. This has implications for the determination of ρ and f.

14.2Toughness

For many commercial applications of microalloyed steels, good toughness is the over- riding property requirement. The development of a small grain size is the only means of making a simultaneous improvement in strength and toughness. Toughness is normally considered in terms of the energy absorbed during deformation by impact, and in microalloyed steels is defined by the temperature at which the fracture mode undergoes a ductile to brittle transition, or some fixed value of absorbed energy, for example 55J, for a Charpy test-specimen of given cross-sectional area. In 1947 Barr and Tipper,[312,313] working at Colvilles in Scotland on the Liberty ships facture problems, [314] showed that the ductile-brittle transition temperature was raised by an increase in the ferrite grain size.

Influenced by this work, Petch, [315, 316] after dealing with yield and cleavage strength-grain size relationships, turned his attention to fracture toughness, and in an initial study found a similar relationship with grain size to that of strength,

$$T_c = T_o - K_y d^{-1/2} \qquad (24)$$

where T_c and K_y are constants.

This classic work did not take into account the influence of carbide films which are normally present at grain boundaries. It is generally agreed that McMahon and Cohen [317] were among the first to appreciate the importance of the role of carbide films at grain boundaries in the fracture process in carbon steels. Detailed measurements on carbide film parameters were undertaken by Mintz et al [318, 319] to obtain statistically significant quantitative data to test the models of Smith [320], Almond et al [321] and Knott and Curry.[322] This data showed that over the grain size range 1-14$mm^{-1/2}$ (d=10 µm to 500µm), the change in T_c was 160°C, whereas the greatest change that can be produced by changes in carbide thickness alone was 60°C. This data provided support for the conclusions of Almond et al.[321] The above publications were among those which included ideas leading Petch [323] to revisit the topic some 25 years later than his earlier work, and to incorporate both grain size and carbide thickness into his model. The results in Fig 40, where the cleavage strength for fracture, σ_c, is plotted against $d^{-1/2}$, for a range of carbide thicknesses, t. The line OA in Fig 41 shows that σ_c is directly proportional to $d^{-1/2}$ and unaffected by carbide. At the other extreme, with a fine grain size and a coarse carbide, where t equals 5µm, the

carbide has a dominant influence on σ_c. The region between these two extremes shows the strong influence of grain size. Petch pointed out that over the grain size range of 3 to 10mm$^{-1/2}$, i.e.100-10μm, and with some carbide refinement concurrent with grain refinement, equation (3) can normally be used. However, when the grain size is finer, (as is sometimes the case in microalloyed steels), then the equation:

$$5.5T_c = 770\text{-}46\ d^{-1/2} - \sigma_c \qquad (25)$$

gives a more accurate estimate. Using this modified Petch approach, Bingley and Siwecki [324] analysed the data from three carbon steels. They obtained a good relationship between $d_{20}^{-1/2}$, which is for the average grain size of the highest 20% in a grain size distribution, and between t_{max}, the maximum carbide thickness and d_{20}. Furthermore, they suggested that to give the best fit for their extensive set of experimental data, Harding's formula used by Petch to calculate σ_c, should be modified to:

$$\sigma_c = 520\text{-}2.5T + 20.2\ d^{-1/2} \qquad (26)$$

Bingley [325] in a more extensive paper, studying both laboratory and commercial microalloyed steels, confirmed the earlier d_{20} analysis. [324]

14.3 Ductility

Ductility at ambient temperatures is normally recorded following tensile testing, as elongation percentage and reduction of area. A multiple regression analysis of 60 casts of carbon steels containing ≤0.25%C,

some with Nb and Al additions, was undertaken by Pickering and Gladman [252] to quantify the factors which control the properties, including RA%. This analysis resulted equation 27,

$$RA\% = 7.85 + 5.4(\%Mn) - 0.53(\%pearlite) - 210\,d \qquad (27)$$

where d is the ferrite grain size in μm.

Fig42 shows the calculated RA% plotted against the observed RA%. The correlation factor is 78%.

A more recent regression analysis by Mintz et al [326] from tensile tests undertaken over a range of temperatures and strain rates, produced equation 28. This predicted a min. RA% with an accuracy of ±12% (95% confidence limit).

$$\text{Min. RA}\,(\%) = 700d^{-1/2}\,(1 - 4{\cdot}3\,s^{-1/2}) + 20\,(\log \varepsilon + 2{\cdot}5) \qquad (28)$$

d is the austenite grain size in μm, s interparticle spacing and ε strain rate.

The importance of a small ferrite grain size and limiting the grain boundary carbide thickness are well established means of controlling the toughness to acceptable levels in microalloyed steels from +100 to -100ºC. These parameters can also influence hot ductility, which is important in processing microalloyed steels. Hot ductility testing was originally undertaken by torsion testing, [327-329] as this method was considered to provide a good simulation of hot rolling. For investigating continuous casting failures and to predict the likelihood of transverse cracking during the unbending operation, hot tensile testing, often using a Gleeble machine, is the preferred method.[326, 330-335] The sample is cooled at the rate experienced by the surface of the strand during the continuous

casting operation, ~60 K min $^{-1}$ and is strained at rates between 10^{-3} and 10^{-4} s $^{-1}$, which are chosen to simulate those associated with straightening.[326] The variation in hot ductility with temperature is obtained by plotting reduction in area, RA%, versus test temperature, as in Fig 43. For both the cast and wrought states, a decrease in hot ductility, described as a ductility trough, occurs between 700ºC and ~1200ºC; intergranular fracture is observed. The ductility trough has implications both for normal continuous cast, and for thin slab cast steels. [326, 329-334] Several explanations have been suggested for the ductility trough, including failure within a thin film of ferrite at the austenite grain boundaries, or strain induced precipitation of carbonitrides, which pin austenite grain boundaries and therefore reduce boundary mobility, and in niobium steels, precipitate free zones. [329] Fig 43 taken the work of Crowther and Mintz [331], shows that refining the austenite grain size is generally beneficial to hot ductility, as it reduces the width of the trough and increases the minimum RA%. They showed that decreasing the austenite grain size from 350µm to 70 µm increased the RA by 20%.

Over many years, Mintz and co-workers have conducted extensive investigations to understand the role of the transition metals, Nb, Ti and V, together with Al, N and C, on hot ductility of steels. [326, 331, 333, 334] It is well established, that increasing the aluminium content of carbon-manganese steels causes a progressive deterioration in hot ductility.[14] During the γ→α transformation, precipitation of AlN occurs

preferentially in ferrite, especially under deformation conditions. Microvoid nucleation at the embrittling AlN particles is one explanation for the impairment of the hot ductility. Niobium steels are known to have hot ductility problems. On the other hand, aluminium additions to niobium steels are thought to refine Nb(C, N) grain boundary pinning precipitates, which mitigates loss in ductility.

Table 9

Composition in wt% of the steels considered in Fig44 [ref331]

	Steel	C	Si	Mn	P	S	sol.Al	N	Ti
1	C–Mn	0.14	0.15	1.28	0.004	0.017	0.002	0.0035	—
2	C–Mn–Al	0.16	0.23	1.40	0.002	0.014	0.028	0.004	—
3	C–Mn–Al	0.16	0.22	1.40	0.002	0.015	0.068	0.004	—
4	C–Mn–Al–N	0.17	0.24	1.50	0.002	0.015	0.030	0.007	—
5	C–Mn–Al–N	0.16	0.23	1.40	0.002	0.016	0.078	0.007	—
6	C–Mn–Ti–Al	0.15	0.20	1.25	0.003	0.018	0.03	0.004	0.02
7	C–Mn–Ti–Al	0.16	0.23	1.50	0.002	0.013	0.03	0.004	0.03
8	C–Mn–Ti–Al	0.17	0.20	1.40	0.002	0.015	0.072	0.004	0.03

Care must be taken with titanium additions. As seen in Fig 44, adding 0.02-0.03% Ti to the C-Mn steels detailed in Table 9, can have a beneficial effect on hot ductility [331], by reducing both the depth and width of the trough. This is due to the restrained effect on austenite grain growth of coarse TiN particles still remaining out of solution, after soaking at 1350 ºC. For steels 4 to 8 in Table 9, it was considered that the suppression of AlN precipitation, due to removal of nitrogen to form the more stable nitride, TiN, resulted in improved hot ductility,

Fig44. However, if due to increased cooling rates during the simulation, fine TiN particles precipitate restricting particle growth, the beneficial influence of the titanium addition is lost. Therefore, variation in cooling rates during hot tensile testing, to simulate as close as possible the conditions pertaining to the continuous casting operation, have been an important objective in this research.[326, 335] A major concern in simulating the continuous casting process with a Gleeble machine is in deciding the thermal programme which will ensure that the appropriate RA% is recorded. [336, 337] Introducing a cooling regime similar to that undergone by the strand during commercial continuous casting has been shown for low C low Ti containing C-Mn-Nb steels, always to result in an improvement in hot ductility below 900 ºC. When the test RA% is >40%, the steel should not be susceptible to this cracking problem.[335] The addition of zirconium can also reduce transverse cracking, but cannot be added to niobium grades to be used in the as-rolled or normalized conditions, since strength and toughness are impaired. However, zirconium has been successfully added to quenched and tempered grades. [338]

A general requirement of continuous cast microalloyed steels, is that while the composition is important for avoiding cracking following processing, the choice of alloying elements must be such that the strength and toughness of the final product meets specification. Where the as cast slab is to be cooled to ambient prior to reheating for controlled rolling, then many of the precipitates formed during casting will be taken into

solution, and the microstructure controlled as discussed in the previous sections. However, if the TSDC route is to be followed, where the reheating temperature and time are limited, then steel compositions may require modification. Vanadium steels, with the lowest solution temperatures of carbides, nitrides and carbonitrides of the conventional alloy transition metals used for microalloying, may have advantages over niobium steels.[11] Roy et al [339] modelled the effect of segregation on the stability of microalloy precipitates and on the size distributions at different regions (solute rich and solute depleted), which is not well understood. They compared of two as-cast slabs:

(A) 0.09C-1.42Mn-0.035Al-0.050Nb-0.019Ti-0.05V and

(B) 0.07C-1.20Mn-0.-034Al-0.041Ti. The nitrogen level was not given.

Cuboidal TiN, cruciform and cuboidal (Nb, Ti) (C,N), and spherical NbC and VC, precipitates, which had the greatest volume fraction, were characterised, and varied with position in slab (A). TiN precipitates, with various morphologies and sizes, were found in slab (B). The model proposed for micro-segregation, which was a feature of the slabs microstructure, gave a satisfactory agreement between experimental observations and predictions for precipitate size distribution and the amount of precipitates in the interdendritic and dendrite centre regions of segregated slabs. It was concluded that this type of model may help, (1) to avoid hot cracking, (2) in the selection of soaking time and

temperature and predicting austenite grain size during soaking and (3) in designing the rolling schedule for achieving maximum benefit from the microalloying precipitates. [339]

While problems deriving from residual elements is not specific to microalloyed steels, it should be touched upon. A significant proportion of recycled steel (scrap) is now part of the normal charge load during steel making, and it is accepted that the level of residuals in steels is increasing. Basic oxygen steel uses around 10-12% scrap only, while electric arc ~75% recycled scrap. Residual elements, such as copper, nickel, tin, antimony and arsenic, at trace levels have long been recognised as leading to potential hot shortness problems. They are known to concentrate in the layer of metal immediately adjacent to the oxide scale. These are of particular concern in tube-making and forging of carbon steels. This subscale enrichment can eventually lead to the precipitation of a phase which is molten at temperatures > 950ºC.

As explained in a survey by Melford[340], it is more often the interaction between a combination of trace elements which has to be understood if their net influence on high temperature mechanical properties is to be evaluated. An earlier paper [341], Melford produced a useful guide to the limiting residual contents that could be tolerated in the form of the expression:

$$Cu+6(Sn+Sb) \leq 9/E \qquad (29)$$

where E, the enrichment factor is defined by E= average concentration of residual in then subscale/ bulk residual concentration. A literature search has not produced any extension of this work to microalloyed steels.

15. Summary.

Over the 56 years, since the first publication by Beiser [24], generally acknowledged to bring niobium steels to the attention of the world, much progress has been made. The yield strength of mild steels ~250MPa was raised up to 400MPa with an addition of 0.03% Nb. The introduction of controlled rolling made these strength levels possible, together with good toughness in weldable steels. Many of the ideas of using accelerated cooling and modifying steels compositions, to produce bainitic and acicular, with strengths above 600MPa, were known from laboratory research in the 1970's. Since this time, the expansion of line-pipe production, and the automobile industry requiring high strength and toughness in thinner sheet, to name due two examples, transferred these possibilities to the production line. The use of multiple additions of niobium, titanium and vanadium, sometimes with a high nitrogen content, is now commonplace, while processing of microalloyed steels using thin slab direct charging technology is on the increase, as is the application of friction stir welding. The recognition of the role of microstructure in achieving these improved properties, has been at the root of many of these advances.

Electron microscopes, coupled with an array of analytical equipment, now allows far more detailed information to be processed quicker and with user friendly software, than even a decade ago, but at an increasing cost. While ferrite-pearlite microalloyed steels are expected to provide the bulk production, the future may see the development of a spectrum of microalloyed steels, dictated by economics, but also tailor made for the processing route. This could well be the case for both thin slab cast direct charge steels, with their restricted reheating and rolling passes, and friction stir welded steels, with very inhomogeneous microstructures in the stir zone, especially for thicker plate, where a double pass is used.

16 Postcript

The author has been involved with Microalloyed Steels for over 50 years, and been associated with many of those who have made major contributions to this field. Initially this was during time at Hinxton Hall, the Tube Investments Research Laboratory, when we were involved in 30 Oak, a steel produced by Round Oak Steelworks and purported to have a lower yield stress of 30tsi (~400MPa), which was true, at $\leq$ 10mm thickness. As an undergraduate at Sheffield University, E.O. Hall taught me physics, and J.H. Woodhead and Prof. (later Sir) R.W.K. Honeycombe, metallurgy. The latter later invited me to write a review for Science Progress, (ref.1), and I was included in those who

presented work at a celebration of his 70th birthday (ref.2). I met W.B. Morrison at Colvilles Steelworks in the mid 1960's, having previously visited Swinden Laboratories of United Steels, to talk with Prof. T. Gladman and Prof. F.B. Pickering about AlN precipitation, which I had been taught to SAED index by Prof. D.W. Pashley, who with Sir J.W. Menter, introduced me to TEM. Prof. N.J. Petch joined the Metallurgy Department of Strathclyde University in the early 1970's. We had many discussions, and he became a firm friend. Dr. N.A. McPherson, undertook PhD work with me, as did Drs N. Gao, K. He and Y. Li, who continued in the Group as post-doctoral research fellows. All of us benefited from many years of collaboration with Prof. A.J. Craven, University of Glasgow, through PEELS analysis of nanoparticles.

16. References

1. T.N. Baker: 'Microalloyed steels', Si. Prog., 1978, **65**, 493-542.
2. T.N. Baker: 'Microalloyed steels', in 'Future developments of metals and ceramics, (eds. J.A. Charles, G.W. Greenwood and G.C. Smith), 75-119, 1992, London, Inst. Mater.

3. T. Gladman: 'Microalloyed Steels', 1997, London, Inst. Mater.

4. T. Gladman: 'The physical metallurgy of microalloyed steels', Mater. Sci. Technol., 1999, **15**, 30-36.

5. W.B. Morrison: 'Microalloy steels – the beginning', Mater. Sci. Technol, 2009, **25**, 1068 - 1073.

6. A.J. De Ardo: 'Metallurgical basis for thermomechanical processing of microalloyed steels', Ironmaking and Steelmaking, 2001, **28**, 138-144.

7. S. Vervynckt, K. Verbeken, B. Lopez and J.J. Jonas: 'Modern HSLA steels and role of non-recrystallisation temperature', Inter. Mater. Revs, 2012, **57**, 187-207.

8 A.J. DeArdo: 'Niobium in modern steels', Inter. Mater. Revs., 2003, **48**, 371-402.

9. F.B. Pickering: 'Overview of titanium in microalloyed steels' in 'Titanium Technology in Microalloyed Steels', (ed. T.N. Baker), 10-43, 1997, London, Institute of Materials.

10. R. Lagneborg, T. Siwecki, S. Zajac and B. Hutchinson: 'The role of vanadium in microalloyed steels', Scand. J. Met., 1999, **28**, 186-241.

11. R. Lagneborg, B. Hutchinson, T. Siwecki and S. Zajac: 'The role of vanadium in microalloyed steels', Michael Korchynsky Symposium, MS&T Conference, pp 1-95, October 2014, Vanitec publication.

12. T.N. Baker: 'Processes, Microstructure and Properties of Vanadium Microalloyed Steels', Mater. Sci. Technol., 2009, **25,** 1083-1107.

13. T.N. Baker: 'Role of zirconium in microalloyed steels: a review', Mater. Sci. Technol., 2015, **31**, 265-294.

14. F.G. Wilson and T. Gladman: 'Aluminium nitride in steel', Inter. Mater. Revs., 1988, **33**, 221-286.

15. World Steel Production Report August 2014

16. http://www.keytometals. Total Materia.

17. H. Xie, L-X. Du, J. Hu and R.D.K. Misra: 'Microstructure and mechanical properties of a novel 1000 MPa grade TMCP low carbon microalloyed steel with combination of high strength and excellent toughness', Mater. Sci. Eng., 2014, **A612**, 123-130.

18. http://en.wikipedia.org/wiki/Microalloyed steel

19. http://www.tatasteeleurope.com

20. G. Oakes and K.C. Barraclough: 'Steels', in 'The development of gas turbine materials', (ed. G.W. Meetham) 31-61, 1981, London, Applied Science Publishers.

21. D.G. Robertson: 'Traditional low alloy steels in power plant', in. 'Coal power plant materials and life assessment', (ed. A. Shibli): 107-126, 2014, Cambridge, Woodhead Publishing,

22. http://www.metal.citic.com/iwcm/Rofes.pdf. Shanghai, November, 2006.

23. D.K. Matlock , G. Krauss, J.G. Speer: 'Microstructures and properties of direct-cooled microalloy forging steels', J. Mater. Proc. Technol., 2001, **117**, 324-328.

24. C.A. Beiser: 'The effect of small columbium additions to semi killed, medium carbon steels', ASM preprint no138, 1959, Metals Park, OH, Am. Soc. Met.

25. A.L. Feild: 'Some effects of zirconium in steel', Trans. Am. Inst. Mining Met. Engrs., 1923, **69**, 848-894.

26. A.L. Feild: 'Effect of zirconium on hot-rolling properties of high-sulfur steels and the occurrence of zirconium sulfide' Trans. Am . Inst. Mining Met. Engrs., 1924, **70**, 201-223.

27. F.M. Becket: 'Some effects of zirconium in steel', Trans. Amer. Electrochem. Soc., 1923, **43**, 261-269.

28. W.B. Morrison: 'Influence of small niobium additions on properties of carbon-manganese steels', J. Iron Steel Inst., 1963, **201**, 317-325

29. W. B. Morrison and J.H. Woodhead: 'Influence of small niobium additions on mechanical properties of commercial mild steels', J. Iron Steel Inst., 1963, **201**, 43-46.

30. E.O. Hall: 'The deformation and ageing of mild steel. 3 discussion of results', Proc. Phys. Soc, 1951, **64B**, 747-753.

31. N.J. Petch: ' The cleavage strength of polycrystals', J. Iron Steel Inst., 1953, **174**, 25-28.

32. A.H. Cottrell: 'Dislocations and Plastic flow in crystals', 1964, Oxford, Clarendon Press.

33. R.D. Heidenreich: ' Electron microscopy and diffraction study of metal crystal textures by means of thin sections', J. Appl. Phys., 1949, **20**, 993-1010.

34. P.B. Hirsch, R.W. Horne and M.J. Whelan: 'Direct observations of the arrangements and motion of dislocations in aluminium', Philos. Mag., 1956, 1, 677- 684.

35. P.B. Hirsch: 'Direct observations of moving dislocations: Reflections. Mater. Sci. Eng., 1986, **84**, 1-10.

36. P.B. Hirsch, A. Howie, R.B. Nicholson , D.W. Pashley and M.J. Whelan: 'Electron microscopy of thin crystals', 1971, London, Butterworths.

37. V. Randle: 'Microtexture determination and its applications', 2nd edn., 2008, London, Maney Publications.

38. R. Phillips and J.A. Chapman: 'Influence of finish rolling temperature on mechanical properties of some commercial steels rolled to 13/16in. diameter bars', J. Iron Steel Inst., 1966, **204**, 615- 622.

39. H. Matsubara, T. Osuka, I. Kozasu and K. Tsukada: 'Optimization of metallurgical factors for the production of high strength, high toughness steel plate by controlled rolling' Trans. Iron Steel Inst. Jpn., 1972, **12**, 435-443.

40. I. Tamura, C. Ouchi, T. Tanaka and H. Sekine: 'Thermomechanical processing of high strength low alloy steel' 1988, London, Butterworths.

41. C.M. Sellars and J.A. Whiteman: 'Recrystallization and grain growth in hot rolling', Met. Sci. 1979, 13, 187-194.

42. C.M. Sellars: 'The physical metallurgy of hot rolling' in 'Hot working and forming processes' (eds. C.M. Sellars and G.J. Davies) 3-15, 1990, London, Institute of Materials.

43. J.J. Jonas and C.M. Sellars: 'Thermomechanical Processing' in 'Future developments of metals and ceramics, (eds. J.A. Charles, G.W. Greenwood and G.C. Smith), 147-177, 1992, London Institute of Materials.

44. K.Hulka:// www.cbmm.com.br.

45.D.C. Houghton, G.C. Weatherly and J.D. Embury: 'Characterization of carbonitrides in Ti bearing HSLA steels', in 'Thermomechanical Processing of microalloyed austenite', ed A.J. DeArdo, G.A. Ratz and P.J. Wray, 267-292, 1982 Metall. Soc. AIME.

46. J.M. Gray, D. Webster and J.H. Woodhead: 'Precipitation in mild steels containing small additions of niobium', J. Iron Steel Inst., 1965, **203**, 812-818.

47. J.W. Halley, 'Grain-growth inhibitors in steel' Trans. AIME, 1946, **167**, 224-234.

48. D. Webster: 'Effect of precipitates in grain refining microalloyed steels', Rpt.MG/C/18/62, 1962, BISRA, Sheffield.

49. K.J. Irvine, F.B. Pickering and T. Gladman: 'Grain-refined C-Mn steels ', JISI, 1967, **205**, 161-182.

50. D.V. Edmonds and R.W.K. Honeycombe: 'Precipitation in iron-based alloys', in 'Precipitation processes in solids', (eds. K.C. Russell and H.I. Aaronson), 1978, 121-160.

51. E.V. Pereloma, I.B. Timokhina, K.F. Russell and M.K. Miller: 'Characterization of clusters and ultrafine precipitates in Nb-containing C–Mn–Si steels ' Scripta Mater, 2006, **54**, 471–476.

52. A. Deschamps, F. Danoix, F. De Geuser, T. Epicier, H. Leitner and M. Perez: 'Low temperature precipitation kinetics of niobium nitride platelets in Fe ', Mater. Lett, 2011, **65**, 2265–2268.

53. F. Danoix, T. Epicier, F. Vurpillot and D. Blavette: 'Atomic scale imaging and analysis of single layer GP zones in a model steel'. J. Mater. Sci., 2012, **47**, 1567–1571.

54. G. Kostryzhev, A. Al Shahrani, C. Zhu. J.M. Cairney, S.P. Ringer, C.R. Killmore and E.V. Pereloma: 'Effect of niobium clustering and precipitation on strength of an NbTi-microalloyed ferritic steel', Mater. Sci. Eng. A, 2014, **607**, 226-235.

55. A.J. Breen, K.Y. Xie, M.P. Moody, B. Gault, H-W. Yen, C.C. Wong, J.M. Cairney, and S.P. Ringer: 'Resolving the Morphology of Niobium Carbonitride Nano-Precipitates in Steel Using Atom Probe Tomography', Microsc. Microanal., 2014, **20**, 1100–1110.

56. E.V. Pereloma, A.G. Kostryzhev, A. Al Shahrani, C. Zhu, J.M. Cairney, C.R. Killmore and S.P. Ringer: 'Effect of austenite deformation temperature on Nb clustering and precipitation in microalloyed steel', Scripta Mater., 2014, 75, 74-77.

57. K.Y. Xie, T. Zheng, J.M. Cairney, H. Kaul, J.G. Williams, F.J. Barbaro, C.R. Killmore and S.P. Ringer: 'Strengthening from Nb-rich clusters in a Nb-microalloyed steel', Scripta Mater., 2012, **66**, 710–713.

58. Z-G Yang and M. Enomoto: 'Calculation of the interfacial energy of B1-type carbides and nitrides with austenite', Metall. Mater. Trans. A, 2001, **32A**, 267-274

59. Z-G Yang and M. Enomoto: 'Discrete lattice plane analysis of Baker-Nutting related B1 compound/ferrite interfacial energy', Mater. Sci. Eng. A, 2002, **A332**, 184-192.

60. R.G. Baker and J. Nutting: 'The tempering of a Cr-Mo-V-W and a Mo-V steel' in 'Precipitation processes in steels', Special report 64, 1-22, 1959, London, Iron and Steel Institute.

61. W.B. Morrison: 'Influence of silver on structure and properties of low-carbon steel', Mater. Sci. Technol., 1985, **1**, 954-960

62. D.P. Dunne: 'Interaction of precipitation and phase transformation in low alloy steels', Mater. Sci. Technol., 2010, **26**, 410-420.

63. Proc. 'Accelerated cooling of steel' (ed. by P.D Southwick), 1986, Warrendale, PA, Metallurgical Society of AIME.

64. Proc. Int. Symp. 'Accelerated Cooling of Rolled Steel,' (eds. G.E. Ruddle and A.F. Crawley), 1988, 1st edn. New York: Pergamon Press.

65. 'Physical metallurgy of direct-quenched steels', (eds. K.A. Taylor, S.W. Thompson and F.B. Fletcher), 1993, Warrendale, Penn, Minerals, Metals, Materials Soc.

66. D.T. Llewellyn: 'Steels: Metallurgy and Applications', p 73, 1992, Oxford, Butterworth-Heinemann, Ltd.

67. I.M. Mackenzie: 'Notch ductility of mild steel ship quality plate', J. West Scotland Iron Steel Inst., 1952-53, **60**, 224-258.

68. I.M. Mackenzie: 'Niobium treated carbon steels', in 'Metallurgical developments in carbon steels', Sp. Report 81, ISI, London, UK, 1963, 30-35.

69. R.W. Vanderbeck: Weld J., 1958, **37**, 114S-1I6S.

70. I. Kozasu, T. Shimizu and H. Kubota: 'Recrystallization of austenite of Si-Mn steels with minor elements after hot -rolling', Trans. Iron Steel Inst. Jpn., 1971, **11**, 367-375.

71. I. Kozasu, C. Ouchi, T. Sampei and T. Okita: 'Hot rolling as high temperature thermomechnical process' in 'Microalloying '75', 120-134, 1977, New York, Union Carbide Corporation.

72. H. Hanemann and K. Lücke: 'Rekristallisation nach warmverformung', Stahl u Eisen 1925, **45**, 1117-1125

73. R. Priestner, C.C. Earley and J.H. Rendall: Observations on behaviour of austenite during hot working of some low-carbon steels', JISI, 1968, **206**, 1252- 1262.

74. T. Tanaka, N Tabata, T. Hatomura and C. Shiga: 'Three stages of controlled-rolling process', in 'Microalloying '75', 107-118, 1977, New York, Union Carbide Corp.

75. S. Vervynckt: 'Control of non-recrystallisation temperature in high strength low alloy (HSLA) steels', PhD thesis, Ghent University, Ghent, Belgium, 2010.

76. H. Matsubara, T. Osuka, I. Kozasu and K. Tsukada: 'Optimization of metallurgical factors for production of high-strength, high toughness steel plate by controlled rolling', Trans. Iron Steel Inst. Jpn., 1972, 12, 435-443.

77. Y.E. Smith and C.A. Siebert: 'Continuous cooling transformation kinetics of thermomechanically worked low-carbon austenite', Met. Trans., 1971, **2**, 1711-1725.

78. R. Priestner and E. de los Rios:'Ferrite grain refinement by controlled rolling of low carbon and microalloyed steel', Met, Technol., 1980, **7**, 309-316.

79. A.J. DeArdo: 'Accelerated cooling: a physical metallurgy perspectuve', 1st edn. Proc. Int. Symp. 'Accelerated Cooling of Rolled Steel,' (ed. G.E. Ruddle and A.F. Crawley), 3-27, 1988, New York, Pergamon Press.

80. D.K. Matlock and J.G. Speer: 'Microalloying concepts and applications in long products', Mater. Sci. Technol., 2009, **25**, 1118-1125.

81. K.A. Taylor: 'Solubilty products of titanium carbide, vanadium carbide and niobium carbide in ferrite', Scripta Met. Mater. 1995, **32**, 7-12.

82. W.C. Leslie, R.L. Rickett, C.L. Dodson and C.S. Walton: 'Solution and precipitation of aluminium nitride in relation to the structure of low carbon steels' Trans. Am. Soc. Met. 1954, **46**, 1470-1499.

83. K. Narita: 'Physical chemistry of group-IVA (Ti, Zr), Group-VA(V, Nb, Ta) and rare earths in steel', Trans. Iron Steel Inst. Jpn, 1975, **15**, 145-152.

84. S. Matsuda and N. Okumura: 'Effect of distribution of TiN precipitate particles on austenite grain size of low-carbon steels', Trans. Iron Steel Inst. Japan, 1978, **18**, 198- 205.

85. R.K. Amin and F.B. Pickering: 'Austenite grain coarsening and the effect of thermomechanical processing of austenite recrystallization', in 'Thermomechanical processing of microalloyed austenite' (eds. A.J. DeArdo, G.A. Ratz and P.J. Wray), 1-30, 1982, Warrendale, Penn., Metallurgical. Society, AIME.

86. L.J. Cuddy and J.C. Raley: 'Austenite grain coarsening in microalloyed steels Metall. Trans, A, 1983, **14A**, 1989-1995.

87. G.R. Speich, L.J. Cuddy, C.R. Gordon and A.J. DeArdo: Phase transformations in ferrous alloys, (eds. A.R. Marder and J.I. Goldstein), 523, 1984, Warrendale, PA, TMS-AIME.

88. C. Zener in C.S. Smith: 'Grains, phases and interfaces-an interpretation of microstructure', Trans AIME. 1948, **175**, 15-51.

89. J.W. Martin: 'Micromechanisms in particle-hardened alloys', 150, 1980, Cambridge, Cambridge University Press.

90. R.D. Doherty and J.W. Martin: 'Effect of a dispersed second phase on recrystallization of aluminium-copper alloys', J. Inst. Metals, 1962-3, **91**, 332-338.

91. F.J. Humphreys and M. Hatherly: 'Recrystallization and related annealing phenomena', 2nd edn, 2004, Oxford, Elsevier Ltd.

92. R.D. Doherty, D.A. Hughes, F.J. Humphreys, J.J. Jonas, D. Juul Jensen, M.E. Kassner, W.E. King, T.R. McNelly, H.J. McQueen and A.D. Rollett: 'Current issues in recrystallization: a review', Mater. Sci. Eng. A, 1997, **238**, 219-274.

93. P.A. Manohar, M. Ferry and T. Chandra: 'Five decades of the Zener equation' ISIJ Int., 1998, **38,** 913-924.

94. D.T. Gawne and G.T. Higgins: 'Secondary recrystallization in a steel containing coarse carbides and its relation to primary recrystallization structure', J Iron Steel Inst., 1971, **209**, 562-566.

95. C. Kamma and E. Hornbogen: 'Effect of carbide particle-size on initiation of recrystallization of a hypoeutecoid steel', J Mater. Sci., 1976, **11**, 2340-2344.

96. D.T. Gawne and G.T. Higgins: 'Associations between spherical particles of two dissimilar phases', J Mater. Sci., 1971, **6**, 403-412.

97. A. Pandit, A. Murugaiyan, A. Saha Podder, A. Halder, D. Bhattacharjee, S. Chandra and R.K. Ray: 'Strain induced precipitation of complex carbonitrides in Nb-V and Ti-V microalloyed steels', Scr. Mater., 2005, 53, 1309-1314.

98. E. J. Palmiere, C.I. Garcia and A.J. DeArdo: 'Compositional and microstructural changes which attend reheating and grain coarsening in steels containing niobium' Metall. Mater. Trans., A, 1994, **25A**, 277-286.

99. J.J. Jonas and I. Weiss: 'Effect of precipitation on recrystallization in microalloyed steels', Metal. Sci., 1979, **13**, 238-245.

100. A. LeBon, J. Rofes-Vernis and C. Rossard: 'Recrystallization and precipitation during hot working of a Nb-bearing HSLA steel', Met. Sci., 1975, **9**, 36-40.

101. B. Datta, A. Valdes and C.M. Sellars: 'Mechanism and kinetics of strain induced precipitation of Nb(C, N) in austenite' Acta Metall., 1992, **40**, 653-662.

102. B. Datta and C.M. Sellars: 'Effect of composition and process variables on Nb(C,N) precipitation in niobium microalloyed austenite', Mater. Sci. Technol., 1987, **3**, 197-206.

103. B. Datta and C.M. Sellars: 'Strengthening of austenite by niobium during hot rolling of microalloyed steel', Mater. Sci. Technol. 1986, **2**, 146-153.

104. B. Datta, E.J. Palmiere and C.M. Sellars: 'Modelling the kinetics of strain induced precipitation in Nb microalloyed steels', Acta Mater. 2001, **49**, 785-794.

105. V. Nagarajan, E.J. Palmiere and C.M. Sellars: 'New approach for modelling strain induced precipitation of Nb(C,N) in HSLA steels during multipass hot deformation in austenite', Mater. Sci. Technol., 2009, **25**, 1168-1174.

106. C.M. Sellars: 'From trial and error to computer modelling of thermomechanical processing ', Ironmaking and Steelmaking, 2011, **38**, 250-257

107. M. Nöhrer, W. Mayer, S. Primig, S. Zamberger, E. Kozeschnik and H. Leitner: 'Influence of deformation on the precipitation behaviour of Nb(C,N) in austenite and ferrite', Metall. Mater. Technol. A, 2014, **45A**, 4210-4219.

108. M. Nöhrer, W. Mayer, S. Zamberger, E. Kozeschnik and H. Leitner: 'Precipitation of strain induced V precipitates at different temperatures in a 0.2 wt% C steel', Steel Res. Int. 2014, **85**, 679-688.

109. M. Gómez, L. Rancel and S.F. Medina: 'Effects of Nb, V, Ti and Al on recrystallization / precipitation interaction in microalloyed steels', Mater. Sci. Forum, 2010, **638-642**, 3388-3393.

110. S.G. Hong, K.B. Kang and C.G. Park: 'Strain induced precipitation of NbC in Nb and Nb-Ti microalloyed HSLA steels', Scr. Mater., 2002, **46**, 163-168.

111. S.F. Medina: 'From heterogeneous to homogeneous nucleation for precipitation in austenite of microalloyed steels', Acta Mater., 2015, **84**, 202–207.

112. W.J. Liu and J.J. Jonas: 'A stress relaxation method for following carbonitride precipitation in austenite at hot working temperatures', Metall. Trans. A, 1988, **19A**, 1403- 1413.

113. A.J. DeArdo, M.J. Hua, K.G. Cho and C.I. Garcia: 'On strength of microalloyed steels: an interpretative review', Met. Sci Technol., 2009, **25**, 1074-1082.

114. J. Irvine and T.N. Baker: 'The influence of rolling variables on the strengthening of niobium steels', Mater. Sci. Eng., 1984, **64**, 123-134.

115. V. Carretero Olalla, V. Bliznuk, N. Sanchez, P. Thibaux, L.A.I. Kestens and R.H. Petrov: 'Analysis of the strengthening mechanisms in pipeline steels as a function of the hot rolling parameters', Mater. Sci. Eng. A, 2014, **60**, 46-56.

116. F. Heisterkamp, D. Lauderbod. L. Meyer C. Straussburger: 'Effect of zirconium on toughness of weldable high strength structural steels containing niobium or vanadium', Stahl Eisen, 1970, **90**, 1255-1262.

117. D.N. Crowther and W.B. Morrison: 'Influence of hypo-stoichiometric additions of titanium on the properties of microalloyed structural steels', in 'Titanium Technology in microalloyed steels', (ed. T.N. Baker), 44-64, 1997, London, Institute of Materials.

118. J. Strid and K.E. Easterling: On the chemistry and stability of complex carbides and nitrides in microalloyed steels', Acta Metall., 1985, **33**, 2057-2074.

119. K. He and T.N. Baker: 'The effects of small titanium additions on the mechanical properties and the microstructures of controlled rolled niobium-bearing HSLA plate steels', Mater. Sci. Eng. A,1993, **A169**, 53-65.

120. S.V. Subramanian and G.C. Weatherly: 'Precipitation behaviour of Ti-V and Ti-Nb microalloyed steels', in 'Titanium technology in microalloyed steels', (ed. T.N. Baker), 133-149, 1997, London, Institute of Materials.

121. K. He and T.N. Baker: 'Complex carbonitrides in multi-microalloyed Ti-containing HSLA steel and their influence on the mechanical properties', in 'Titanium technology in microalloyed steels', (ed. T.N. Baker), 115-132, 1997, London, Institute of Materials.

122. K. He and T.N. Baker: 'Zr-containing precipitates in a Ti-Nb microalloyed HSLA steel containing 0.016wt% Zr addition', Mater. Sci. Eng., 1996, **A215**, 57-66.

123. K. He and T.N. Baker: 'Effect of zirconium additions on austenite grain coarsening of C-Mn and microalloyed steels', Mater. Sci. Eng. A, 1998, **A256**, 111-119.

124. T.N. Baker, Y. Li, J.A. Wilson, A.J. Craven and D.N. Crowther: 'Evolution of precipitates, in particular cruciform and cuboidal particles, during simulated direct charging of thin slab cast vanadium microalloyed steels', Mater. Sci. Technol., 2004, **20**, 720-730.

125. A. Grajcar: 'Thermodynamic analysis of precipitation processes in Nb-Ti microalloyed Si-Al TRIP steels', J. Therm. Anal. Calorim. 2014, **118**, 1011-1020.

126. M. Beres, T.E. Weich, K. Hulka and J. Meyer: 'TEM investigations of fine niobium precipitates in HSLA steel', Steel Res. Int. 2004, **75**, 753-758.

127. E. Courtois, T. Epicier and C. Scott, 'EELS study of niobium carbo-nitride nano-precipitates in ferrite', Micron, 2006, **37**, 492-502.

128. Z. Li, D. Liu, J. Zhang and W. Tian: 'Precipitates in Nb and Nb-V microalloyed X80 pipeline steel', Micros. Microanal., 2013, **19**, 62-65.

129. Y.E. Smith, A.P. Coldren, R.L. Cryderman: 'Manganese-molybdenum-niobium acicular ferrite steels with high strength and toughness, in 'Towards Improved Ductility and Toughness', 119-142, 1971 Climax Molybdenum Development Company (Japan) Ltd.

130. F.Q. Ji, C.N. Li, S. Tang, Z.Y. Liu and G.D. Wang: 'Effects of carbon and niobium on microstructure and properties for Ti bearing Steels', Mater. Sci. Technol. 2015, **69**, 695-702.

131. S.S. Campos, E.V. Morales and H.-J. Kestenbach: 'On strengthening mechanisms in commercial Nb-Ti hot strip steels', Metall. Mater. Trans. A, 2001, **32A**, 1245–1248.

132. S.S. Campos, E.V. Morales and H.-J. Kestenbach: 'A quantitative study of interphase precipitation in a commercial microalloyed steel', Mater. Sci. Forum, 2003, **426–432**, 1517–1522.

133. M. Charleux, W.J. Poole, M. Militzer and A. Deschamps: 'Precipitation behavior and its effect on strengthening of an HSLA-Nb/Ti steel', Metall. Mater. Trans. A, 2001, **32A**, 1635–1647.

134. R.D.K. Misra, H. Nathani, J.E. Hartmann and F. Siciliano: 'Microstructural evolution in a new 770MPa hot rolled Nb-Ti microalloyed steel', Mater. Sci. Eng. A, 2005, **A394**, 339–352.

135. M-C. Zhao, K. Yang and Y. Shan: 'The effects of thermo-mechanical control process on microstructures and mechanical properties of a commercial pipeline steel', Mater. Sci. Eng. A, 2002, **A335**, 14–20.

136. M-C. Zhao, K. Yang and Y. Shan: 'Comparison on strength and toughness behaviors of microalloyed pipeline steels with acicular and ultrafine ferrite', Mater. Lett., 2003, **57**, 1496-1500.

137. F-R. Xiao, B. Liao, Y-Y. Shan, G-Y. Qiao, Y. Zhong, C. Zhang and K. Yang: 'Challenge of mechanical properties of an acicular ferrite pipeline steel', Mater. Sci. Eng.A, 2006, **A431**, 41-52.

138. W. Wang, Y-Y. Shan and K Yang: 'Study of high strength pipeline steels with different microstructures', Mater. Sci Eng. A, 2009, **A502**, 38–44.

139. H. Beladi, G.L. Kelly and P.D. Hodgson: 'Ultrafine grained structure in steels using dynamic strain induced transformation processing,' Inter. Mater. Revs., 2007, **52**, 14-28.

140. P.D. Hodgson, M.R. Hickson and R.K. Gibbs: United States Patent No. 6, 027, 587, 20 February 2000**.**

141. P.D. Hodgson, M.R. Hickson, R.K. Gibbs and: 'Ultrafine ferrite in low carbon steel', Scripta Mater., 1999, **40**, 1179-1184.

142. J-K Choi, D-H Seo, J-S Lee, K-K Um and W-Y Choo: 'Formation of ultrafine ferrite by strain-induced dynamic transformation in plain low carbon steel', ISIJ Int., 2003, **43**, 746–754.

143. H. Beladi, G.L. Kelly, A. Shokouhi and P.D. Hodgson: 'The evolution of ultrafine ferrite formation through dynamic strain-induced transformation', Mater. Sci. Eng. A, 2004, **A371**, 343–352.

144. R. Priestner: 'Origin of fine-grained ferrite in steels rolled under controlled rolled conditions', Rev. Metall. 1975, **72**, 285-296.

145. Z. Yang and R. Wang: 'Formation of ultra-fine grain structure of plain low carbon steel through deformation induced ferrite transformation', ISIJ Int. 2003, **43**, 761-766

146. K. Muszka, D. Dziedzic, L. Madej, J. Majta, P.D. Hodgson and E.J. Palmiere: 'The development of ultrafine-grained hot rolling products using advanced thermomechanical processing'. Mater. Sci. Eng. A, 2014, **A610**, 290–296.

147. H. Yada, Y. Matsumura and K. Nakajima: United States Patent No. 4,466,842, 1984.

148. H. Tamerhiro, M. Murata, R. Habu and M. Nagumo: 'Optimum microalloying of niobium and boron in HSLA steel for thermomechanical processing', Trans. Iron Steel. Inst. Jpn., 1987, **27**, 120-129.

149. H.K.D.H. Bhadeshia: 'Bainite is steels', 1992, London, The Institute of Materials.

150. R.Y. Zhang and J.D. Boyd: 'Bainite Transformation in Deformed Austenite', Metall. Mater. Trans. A 2010, **41A**, 1448-1459.

151. C. Lee, H.K.D.H. Bhadeshia and H. Lee: 'ffect of plastic deformation on the formation of acicular ferrite', Mater. Sci. Eng. A, 2003, **A360**, 249-257.

152. O. Grong and D.K. Matlock: 'Microstructural development in mild and low-alloy steel weld metals', Int. Met. Rev., 1986, **31**, 27-48.

153. C.L. Davis and J.E. King: 'Cleavage initiation in the intercritically reheated coarse-grained heat-affected zone: Part I. fractographic evidence', Metall. Mater. Trans., 1994, **25**, 5663-5673.

154. Y. Li, D.N. Crowther, M.J.W. Green, P.S. Mitchell and T.N. Baker: 'The effect of vanadium and niobium on the properties and microstructure of the intercritically reheated coarse grained heat affected zone in low carbon microalloyed steels', ISIJ Int., 2001, **41**, 46-55.

155. Y. Li and T.N. Baker: 'Effect of morphology of martensite-austenite phase on fracture of weld heat affected zone in vanadium and niobium microalloyed steels', Mater. Sci. Technol., 2010, **26**, 1029-1040.

156. M. Reichert, T. Garcin, M. Militzer, W.J. Poole: Formation of martensite/austenite (M/A) in X80 linepipe steel', Proc. of 9th International Pipeline Conference, IPC2012, Calgary, Alberta, Canada, 2012, ASME, 1-7.

157. F.G. Caballero, M.K. Miller and C. Garcia-Mateo 'Opening previously impossible avenues for phase transformation in innovative steels by atom probe tomography', Mater. Sci. Technol., 2014, 3**0**, 1034-1039

158. K.A. Taylor and S.S. Hansen: Effects of vanadium and processing parameters on the structures and properties of a direct-quenched low- carbon Mo-B steel', Metall. Trans., A, 1991, **22A**, 2359-2374.

159. R.K. Weiss and S.W. Thompson: 'Strength differences between direct-quenched and reheated-and-quenched plate steels', in 'Physical metallurgy of direct-quenched steels', (eds. K.A. Taylor, S.W. Thompson and F.B. Fletcher), 107-138, 1993, Warrendale, PA, Minerals, Metals, Materials Society.

160. D.V. Edmonds and R.C. Cochrane: 'Structure-property relationships in bainitic steels', Metall. Trans. A 1990, **21A**, 1527-1540.

161. G. Tither and J. Kewell: 'Properties of directly quenched and tempered structural steel plate', J. Iron Steel Inst., 1970, **208**, 686-694.

162. G. Tither and J. Kewell: 'Microstructure and mechanical properties of some direct-quenched and tempered low- carbon steel', J. Iron Steel Inst., 1971, **209**, 482-484.

163. G. Tither, J. Kewell and M.G. Frost: 'Improved properties of directly quenching', 'Effects of second-phase particles on the mechanical properties of steel', 157-165, 1971, London, The Iron and Steel Institute.

164. T. Siwecki, A. Sandberg, W. Roberts and R. Lagneborg: 'The influence of processing route and nitrogen content on microstructure development and precipitation hardening in vanadium microalloyed steels', in 'Thermomechanical processing of microalloyed austenite', (eds. A.J. DeArdo, G.A. Ratz and P.J. Wray), 163-192, 1982, Warrendale, PA., The Metallurgical Society of AIME.

165. S. Zajac, T. Siwecki, B. Hutchinson and M. Attlegård: 'Recrystallization controlled rolling and accelerated cooling for high strength and toughness in V-Ti-N steels', Metall. Trans. A. 1991, **22A**, 2681-2694.

166. T. Siwecki, B. Hutchinson and S. Zajac: 'Recrystallization controlled rolling of HSLA steels' in 'Proc. Microalloying -95', 1995, 197 211, Warrendale, PA, ISS-AIME.

167. T. Siwecki, J. Eliasson, R. Lagneborg and B. Hutchinson: 'Vanadium Microalloyed Bainitic Hot Strip Steels', ISIJ Int., 2010, **50**, 760-767.

168. B. Hutchinson, T. Siwecki, J. Komenda, J. Hagström, R. Langneborg, J.-E. Hedlin and M. Glagh: 'New vanadium-microalloyed bainitic 700MPa strip steel product', Ironmaking and Steelmaking, 2014, **41**, 1-6.

169. S. Shanmugam, N.K Ramisetti, R.D.K. Misra, J. Hartmann and S.G. Jansto: 'Microstructure and high strength-toughness combination of a new 700 MPa Nb-microalloyed pipeline steel', Mater. Sci. Eng., 2008, **478**, 26-37.

170. Z.J. Xie, Y.P. Fang, G. Han, H. Guo, R.D.K. Misra and C.J. Shang: 'Structure–property relationship in a 960 MPa grade ultrahigh strength low carbon niobium–vanadium microalloyed steel: the significance of high frequency induction tempering' Mater. Sci. Eng. A, 2014, **A618,** 112-117.

171. H.L. Yi, L.X. Du, G.D. Wang and X.H. Liu: 'New Ti-bearing high strengthened steel', J. Mech. Eng., 2008, **44**, 50–54.

172. H.L. Yi, L.X. Du, G.D. Wang and X.H. Liu: 'Development of Nb-V-Ti hot-rolled high strength steel with fine ferrite and precipitation strengthening', J. Iron Steel Res. Int., 2009, **16**, 72-77.

173. H.L. Yi, Y. Xu, Z.G. Xu, Z.Y. Liu and G.D. Wang: 'Microstructure and properties of low cost 780 MPa hot-rolled high- strength steel', Mater. Mech. Eng., 2010, **34**, 37–39.

174. H.L. Yi, Z.Y. Liu, G. D. Wang and D.I. Wu: 'Development of Ti-microalloyed 600 MPa hot rolled high strength steel', J. Iron Steel Res. Int., 2010, **17**, 54-58.

175. P. Cizek, B.P. Wynne, C.H.J. Davies and P.D. Hodgson: 'The effect of simulated thermomechanical processing on the transformation behavior and microstructure of a low-carbon Mo-Nb linepipe steel', Metall. Mater. Trans. A, 2015, **46A**, 407–425.

176. X. Liang and A.J. DeArdo: A study of the influence of thermomechanical controlled processing on the microstructure of bainite in high strength plate steel', Metall. Mater. Trans. A, 2014, **45A**, 5173-5184.

177. C. Garcia-Mateo, F.G. Caballero and H.K.D.H. Bhadeshia: 'Development of Hard Bainite', ISIJ Int., 2003, **43**, 1238–1243.

178. H.K.D.H. Bhadeshia: 'Large chunks of very strong steel', Mater. Sci. Technol. 2005, **21**, 1293-1302.

179. F.G. Caballero, C. Garcia-Mateo and M.K. Miller: 'Modern steels at atomic and nanometre scales', Mater. Sci. Technol., 2015, **31**, 764-772.

180. B. Avishan, S. Yazdani, F.G. Caballero, T.S. Wang and C. Garcia-Mateo: 'Characterisation of microstructure and mechanical properties in two different nanostructured bainitic steels', Mater. Sci. Technol., 2015, 31, 1508-1520.

181. R.J. Glodowski: 'Experience in Producing Vanadium Microalloyed Steels Thin-Slab-Casting Steel Technology', in International. Symp. 'Thin-Slab Casting and Rolling', Guangzhou, China, December 3-5, 2002, 329-339, Chinese Society for Metals.

182. Q.Y. Sha, Z.Q. Sun and L.F. Li: 'Refinement of coarse grained austenite in Nb-V-Ti microalloyed steels during roughing rolling', Ironmaking and Steelmaking, 2015, **42**, 74-80.

183. C. Klinkenberg, C. Bilgen, T. Boecher and J. Schlüter: '20 years of experience in thin slab casting and rolling state of the art and future developments', Mater. Sci. Forum, 2010, **638-642**, 3610-3615.

184. J.M. Rodriguez-Ibabe: 'Thin Slab Direct Rolling of Microalloyed Steels', Mater. Sci. Forum, 2005, **500-501**, 49-62.

185. H. Bruns and R. Kaspar: 'Direct charging of thin slabs of a cold formable HSLA steel', Steel Res. 1997, **68**, 215-219.

186. R. Priestner and C. Zhou: 'Simulation of microstructural evolution in Nb-Ti microalloyed steel during hot direct rolling', Ironmaking Steelmaking, 1995, **22**, 326-332.

187. Y. Li, D.N. Crowther, P.S. Mitchell, and T.N. Baker: 'The evolution of microstructure during thin slab direct rolling processing in vanadium microalloyed steels', ISIJ Int., 2002, **42**, 636-644.

188. Y. Li, J.A. Wilson, D.N. Crowther, P.S. Mitchell, A.J. Craven and T.N. Baker: 'The effects of vanadium, niobium, titanium and zirconium on the microstructure and mechanical properties of thin slab cast steels', ISIJ Int., 2004, **44**, 1092-1102.

189. T.N. Baker, Y. Li, J.A. Wilson, A.J. Craven and D.N. Crowther: 'Evolution of precipitates, in particular cruciform and cuboid particles, during simulated direct charging of thin slab cast vanadium microalloyed steels', Mater. Sci. Technol., 2004, **20**, 720-730.

190. Y. Li, J.A. Wilson, A.J. Craven, and T.N. Baker: 'Dispersion strengthening in vanadium microalloyed steels processed by simulated thin slab casting and direct charging - Part 1 - processing parameters, mechanical properties and microstructure', Mater. Sci. Technol., 2007, **23**, 509-518.

191. J.A. Wilson, A.J. Craven, Y. Li, and T.N. Baker: ' Dispersion strengthening in vanadium microalloyed steels processed by simulated thin slab casting and direct charging - Part 2 - chemical characterisation of dispersion strengthening precipitates', Mater. Sci. Technol., 2007, **23**, 519-527.

192. Q.Y. Sha and Z.Q Sun: 'Grain growth behaviour of coarse-grained austenite in a Nb-V-Ti microalloyed steel', Mater. Sci. Eng. A, 2009, **A523**, 77-84.

193. Q.Y. Sha and Z.Q Sun: 'Microstructure and precipitation in as cast low carbon Nb-V-Ti microalloyed medium thin slab', Ironmaking and Steelmaking, 2010, **37**, 320-325.

194. Q.Y. Sha and Z.Q. Sun: 'Prediction of grain growth of coarse-grained austenite in Nb-V-Ti microalloyed steel', Mater. Sci. Technol., 2011, **27**, 1408-1411.

195. N. Gao and T.N. Baker: 'Austenite grain growth behaviour of microalloyed Al-V-N and Al-V-Ti-N steels', ISIJ Int., 1988, 38, 744-751.

196. N. Gao and T.N. Baker: 'The evaluation of austenite grain size and particle size of microalloyed steels', in 'Proc. Conf. HSLA Steels 2000', (eds. G. Li, F. Wang, Z. Wang, and H. Zhang), 187-194, 2000, Beijing, The Metallurgical Press.

197. J. Zhang and T.N. Baker: 'Effect of equalisation time on the austenite grain size of simulated thin slab direct charged (TSDC) vanadium microalloyed steels' ISIJ Int., 2003, 43, 2015-2022.

198. P. Uranga, A.I. Fernández, B. López and J.M. Rodriguez-Ibabe: 'Modeling of austenite grain size distribution in Nb microalloyed steels processed by thin slab casting and direct rolling (TSDR) route', ISIJ Int., 2004, **44**, 1416-1425.

199. P. Uranga, B. López and J.M. Rodriguez-Ibabe: 'Role of carbon and nitrogen content on microstructural homogeneity in thin slab direct rolled microalloyed steels', Ironmaking and Steel Making, 2009, **36**, 162-169.

200. C.P. Reip, S. Shanmugam and R.D.K. Misra: 'High strength microalloyed C Mn(V-Nb_Ti) and CMn(V-Nb) pipeline steels processed through CPS thin-slab technology: microstructure, precipitation and mechanical properties,' Mater. Sci. Eng. A, 2006, **A424**, 307-317.

201. C. Klinkenberg, K. Hulka and W. Bleck: 'Niobium carbide precipitation in microalloyed steel', Steel Res. Int., 2003, **75**, 744-752.

202. Z. Jia, R.D.K. Misra, R. O'Malley and S.J. Jansto: 'Fine-scale precipitation and mechanical properties of thin slab processed titanium-niobium bearing high strength steels', Mater. Sci. Eng. A, 2011, **A528**, 7077-7083.

203. M.T. Nagata, J.G. Speer and D.K. Matlock: 'Titanium nitride precipitation in thin-slab cast high-strength low-alloy steel', Metall. Mater. Trans., 2002, **33A**, 3099-3110.

204. K. Easterling: 'The introduction to the physical metallurgy of welding', 2nd. edn, 1992, Oxford, Butterworth Heinemenn Ltd.

205. P.H.M. Hart: 'The influence of vanadium-microalloying on the weldability of steels', Welding Cutting, 2003, **55**, 204-210.

206. N.A. McPherson: 'Through process considerations for microalloyed steels used in naval ship construction', Ironmaking and Steelmaking, 2009, **36,** 193-200.

207. T.J. George and J.J. Irani: 'Control of austenite grain size by additions of titanium', J. Aust. Inst. Met., 1968, **13**, 94-106.

208. S. Kanazawa, A. Nakashima, K. Okamota and K. Kanaya: 'Improvement of weld fusion zone toughness by fine TiN', Trans. Iron Steel Inst. Jpn, 1976, **16**, 486-495.

209. S. Matsuda and N. Okumura: 'Effect of distribution of TiN precipitate particles on the austenite grain size of low carbon low alloy steels', Trans. Iron Steel Inst. Jpn, 1978, **18**, 198-205.

210 P.H.M. Hart and G. Ferguson: 'The role of titanium on the weldability of microalloyed structural steels', in 'Titanium Technology in Microalloyed Steels', (ed. T.N. Baker), 169-179, 1997, London, Institute of Materials.

211. S.F. Medina, M.I. Vega, M. Gómez and P.P. Gómez: Influence of the size and volume fraction of TiN particles on hot strength and dynamic recrystallization in structural steels', ISIJ Int., 2005, **45**, 1307-1315.

212. J. Du, M. Strangewood and C.L. Davis: 'Effect of TiN particles and grain size on the Charpy impact transition temperature in steels', J. Mater. Sci. Technol, 2012, **28**, 878-888.

213. H. Adrian and F.B. Pickering: 'Effect of titanium additions on austenite grain growth kinetics of medium carbon V-Nb steels containing 0.008-0.018%N', Mater. Sci. Technol., 1991, **7**,176-182.

214. M. Hamada, Y. Fukada and Y-I Komizo: Microstructure and precipitation behaviour in heat affected zones of C-Mn microalloyed steel containing Nb, V and Ti.', ISIJ Int.1995, **35**, 1196-1202.

215. A.H. Koukabi, T.H. North and H.B. Bell: 'Properties of submerged arc deposits – effects of zirconium, vanadium and titanium-boron', Met. Constr. 1979, **7**, 639-642.

216. F. Chai, C.F. Yang, H. Su, Y.Q. Zhang, Z. Xu and Y.H. Yang: 'Effect of Zr addition to Ti-killed steel on inclusion formation and microstructural evolution in welding induced coarse-grained heat affected zone', Acta Metall. Sin. (Eng. Lett.), 2008, **21**, 220-226.

217. A. M. Guo, S.R. Li, J. Guo, Q.F. Ding, K.M. Wu and X.L. He: 'Effect of zirconium addition on the impact toughness of the heat affected zone in a high strength low alloy pipeline steel', Mater. Charact., 2008, **59**, 134-139.

218. X.L. Wan, K.M. Wu, K. C. Nune, Y. Li and L. Chung: 'In situ observation of acicular ferrite formation and grain refinement in simulated heat affected zone of high strength low alloy steel', Sci. Technol. Weld Join., 2015, **20**, 254-263.

219. T. Koseki and G. Thewlis: ‘Inclusion assisted microstructure control in C–Mn and low alloy steel welds’, Mater. Sci. Technol., 2005, **21**, 869-879.

220. J.R. Garland and P.R. Kirkwood: ‘Towards improved submerged arc weld metal’, Met. Constr., 1975, **7**, 275-283 and 320-330.

221. G.S. Barritte and D.V. Edmonds: ‘Microstructure and toughness of HSLA steel weld metals’, Proc. Int. Conf. on Advances in the physical metallurgy and applications of steel', 126-135; 1982, London, The Metals Society.

222. A.R. Mills, G. Thewlis and J.A. Whiteman: ‘Nature of inclusions in steel weld metals and their influence on formation of acicular ferrite’, Mater. Sci. Techno., 1987, **3**, 1051-1061.

223. N. Mori, H. Homm, S. Okita, and K. Asano: 'The behaviour of B and N in notch toughness improvement of Ti-B bearing weld metals', IIW Document IX-1158-80, Internal. Inst. Weld., London, 1980.

224. H. Nako, Y. Okazaki and J.G. Speer: ‘Acicular ferrite formation on Ti-rare earth metal–Zr complex oxides’, ISIJ Int., 2015, **55**, 250-256.

225 Stir Welding of Dissimilar Alloys, Sci. Technol. Weld Join., 2010, **15**, 266-336.

226 Friction stir welding of steels, Sci. Technol. Weld Join., 2010, **15**, 646-711.

227. W.M. Thomas, E.D. Nicholas, J.C. Needham, M.G. Murch, P. Temple- Smith and C.J. Dawes: ‘Improvements relating to friction stir welding’, International Patent application no. PCT/GB92/02203 and GB Patent application No. 9125978·8 and US Patent application no. 5,460,317, December 1991

228. W.M. Thomas, C.J. Dawes: ‘Friction stir process welds aluminum alloys’, Weld. J., 1996, **75**, 41-45.

229. G. Cam: ‘Friction stir welded structural materials: beyond Al-alloys’, Internl. Met. Revs., 2011, **56**, 1-48.

230. Y.S. Sato, T.W. Nelson, C.J. Sterling: ‘Recrystallization in type 304L stainless steel during friction stirring’, Acta Mater, 2005, **53**, 637-645.

231. M. Root, D.P. Field, T.W. Nelson: ‘Crystallographic texture in the friction-stir-welded metal matrix composite Al6061 with 10 Vol Pct Al_2O_3’, Metall. Mater. Trans. A., 2009, **40A**, 2109-2014.

232. http://en.wikipedia.org/wiki/Friction¬stir¬welding

233. W.M. Thomas, P.L. Threadgill and E.D. Nicholas: ‘Feasibility of friction stir welding steel’, Sci. Technol. Weld Join., 1999, **4**, 365-372.

234. T.J. Lienert, W.L. Stellwag, B.B. Grimmett and R.W. Warke: ‘Friction stir welding studies on mild steel- process results, microstructures, and mechanical properties are reported’, Weld. J, 2003, **82**, 1S-9S.

235. M. Gosh, K. Kumar, R.S. Mishra: ‘Analysis of microstructural evolution during friction stir welding of ultrahigh strength steels’, Scr. Mater., 2010, **63**, 851-854.

236. J. Young, D.P. Field and T.W. Nelson: ‘Material flow during friction stir welding of HSLA 65 steel’, Metall. Mater. Trans. A, 2013, **44A**, 3167-3175.

237. P.J. Konol, J.A. Mathers, R. Johnson and J.R. Pickens: ‘Friction stir welding of HSLA-65 steel for shipbuilding’, J. Ship Prod., 2003, **19**, 159-164.

238. A.I. Toumpis, A.M. Galloway, L. Arbaoui and N. Poletz: 'Thermomechanical deformation behaviour of DH36 steel during friction stir welding by experimental validation and modelling', Sci. Technol. Weld Join., 2014, **19**, 653-663.

239. A. De, H.K.D.H. Bhadeshia and T. DebRoy: 'Friction stir welding of mild steel: tool durability and steel microstructure', Mater. Sci. Technol., 2014, **30**, 1050-1055

240. Y. Morisada, T. Imaizumi and H. Fujii: 'Clarification of material flow and defect formation during friction stir welding', Sci. Technol. Weld. Join. 2015, **20**, 130-137.

241. A. Ozekcin, H.W. Jin, J.Y. Koo, N.V. Bangaru, R. Ayer, G. Vaugn, R. Steel and S. Packer: 'A microstructural study of friction stir welded joints of carbon steels', Inter. J. Offshore Polar Eng., 2004, **14**, 284-288.

242. S. Mironov, Y.S. Sato and H. Kokawa: 'Microstructural evolution during friction stir-processing of pure iron' Acta Mater. 2008, **56**, 2602–2614

243. H-H. Cho, S.H. Kang, S-H. Kim, K.H. Oh, H.J. Kim, W-S. Chang and H.N. Han: 'Microstructural evolution in friction stir welding of high-strength linepipe steel', Mater. Des. 2012, **34**, 258–267.

244. H. Aydin: 'Relationship between a bainitic structure and the hardness in the weld zone of the friction-stir welded X80 API-grade pipe-line steel', Mater. Technol., 2014, **48**, 15-22.

245. X. Yu, B. Mazumder, M.K. Miller, S.A. David and Z. Feng: 'Stability of Y–Ti–O precipitates in friction stir welded nanostructured ferritic alloys', Sci. Technol. Weld. Join. 2015 **20**, 236-241.

246. P.S. Davies, B.P. Wynne, W.M. Rainforth, M.J. Thomas and P.LO. Threadgill: 'Development of microstructure and crystallographic texture during stationary shoulder friction stir welding of Ti-6Al-4V', Metall. Mater. Trans. A 2011, **42A**, 2278-2289.

247. S.J. Barnes, A. Steuwer, S. Mahawish, R. Johnson and P.J. Withers: 'Residual strains and microstructure development in single and sequential double sided friction stir welds in RQT-701 steel', Mater. Sci. Eng. A, 2008, A4**92**, 35-44.

248. N.A. McPherson, A.M. Galloway, S.R. Cater, M.M. Osman: 'A comparison between single and double sided friction stir welded 8mm thick DN36 steel plate, in 'Trends in welding research', Proc. 19th Int. Conf., 2013, 284-290.

249. T.N. Baker and N.A. McPherson: 'Microstructure and Properties of Double-side Friction Stir Welded EN46 Ship Steel', Mater. Sci. Technol., 2015, in press.

250. S. Rahimi, B.P. Wynne and T.N. Baker: 'Evolution of Microstructure of Friction Stir double- sided welded EH46 steel', Scr. Mater. 2015, in press.

251. A-F Gourgues, H.M. Flower and T.C. Lindley: 'Electron backscattering diffraction study of acicular, bainite and martensite steel microstructures', Mater. Sci. Technol., 2000, **16**, 26-39.

252. F.B. Pickering and T. Gladman: 'An investigation into some factors which control the strength of carbon steels', in 'Metallurgical developments in carbon steels', Sp. Report 81, ISI, London, UK, 1963, 11-20.

253. E. Hornbogen and G. Staniek: 'Grain-size dependence of the mechanical properties of an age-hardening Fe-1 % Cu-alloy', J. Mater. Sci., 1974, **9,** 879-886.

254. T. Gladman and F.B. Pickering: 'The effect of grain size on mechanical properties of ferrous materials' in 'Yield, Flow and Fracture of Polycrystals', (ed. T.N. Baker),141-198, 1983, London, Applied Science Publishers.

255. T.N. Baker: 'Determination of the friction stress from microstructural measurements', in 'Yield, Flow and Fracture of Polycrystals', (ed. T.N. Baker), 235-273, 1983, London, Applied Science Publishers.

256. T.N. Baker: 'Subgrain and dislocation strengthening in controlled-rolled microalloyed steels', in 'Hot working and forming processes' (eds. C.M. Sellars and G.J. Davies) 32-37, 1990, London, Institute of Materials.

257. W.B. Morrison, R.C. Cochrane and P.S. Mitchell: 'The influence of precipitation mode and dislocation substructure on the properties of vanadium- treated steels', ISIJ Int. 1993, **33**, 1095-1103.

258. R.A.F. de Reaumur: 'On methods of recognizing defects and good quality in steel and on several ways of comparing different grades of steel', in 'L'Art de Convertir le Fer Forge en Acier, (Paris, 1722) 63-106; transl. A.G. Sisco (Chicago, 1956)', 176-204.

259. P.C. Grignon: 'On the metamorphoses of iron', in 'Memoires de Physique sur l'Art de Fabriquer de Fer' (Paris. 1775), 56-90, transl. P. Boucher and C.S. Smith, in 'Sources for the history of the science of steel' 1532-1786 (The Society for the History of Technology and the M.I.T. Press, Cambridge, MA, 1968) pp. 125-164.

260. C.H. Desch: 'Metallography', 3rd edn, 1-9, 1922, London, Longman, Green and Co.

261. R.W. Armstrong: 'Engineering Science Aspects of the Hall-Petch Relation', Acta Mech., 2014, **225**, 1013-1028.

262. A.G. Quarrell: 'Metallography – a hundred years after Sorby', 'Metallography 1963', Spec. rept. **80**, 1-36, 1963, Iron and Steel Institute.

263. R.W. Armstrong: '60 Years of Hall-Petch: past to present nano-scale connections', Mater. Trans. 2014, **55**, 2-12.

264. W.B. Morrison: 'Effect of grain size on stress-strain relationship in low- carbon steel', Amer. Soc. Q., 1966, **59**, 824-829.

265. A. Kelly and R.B. Nicholson: 'Precipitation hardening', Progress in Mater Sci.,1963, 10, 149-391.

266. L.M. Brown and R.K. Ham: 'Dislocation-particle interactions', in ' Strengthening methods in crystals',(eds. A. Kelly and R.B. Nicholson), 12-135, 1971, London, Applied Science Publishers.

267. V. Gerold: 'Precipitation hardening' in 'Dislocations in solids', (ed. F.R.N. Nabarro), 219-260, 1979, Amsterdam, North-Holland Publishing Company.

268. T. Gladman, B. Holmes and I.D. McIvor: 'Effects of second-phase particles on strength, toughness and ductility', in 'Effects of second-phase particles on the mechanical properties of steel', 68-78, 1971, London, The Iron and Steel Institute.

269. T. Gladman: 'Precipitation hardening in metals', Mater. Sci. Technol., 1999, **15**, 30-36.

270. H.J. Goldschmidt: 'Interstitial Alloys', 238-239, 1957, London, Butterworths.

271. T. Epicier, D. Acevedo and M. Perez: 'Crystallographic structure of vanadium carbide precipitates in a model Fe-V-C steel', Philos. Mag., 2008, **88**, 31-45.

272. G.E. Hollox, J.W. Edington and R.B. Scarlin: 'Indentity of vanadium carbide precipitates in Fe-1V-0.02Nb-0.2C and Ni-4V-0.4C alloys', JISI,. 1971, **209**, 839-841.

273. E. Tekin and P.M. Kelly: 'Secondary hardening of vanadium steels', JISI, 1965, **203**, 715-720.

274. E. Smith: 'An investigation of secondary hardening of a 1 percent vanadium-0.2 percent carbon steel', Acta Metall. 1966, **14**, 583-593.

275. A.T. Davenport: 'Occurrence of 'arced' reflections in diffraction patterns from a vanadium steel', JISI, 1968, **206**, 499-501.

276. A.T. Davenport and R.W.K. Honeycombe: 'Precipitation of carbides at gamma-alpha boundaries of alloyed steels', Proc. Roy. Soc. A, 1971, **A332**, 191-205.

277. F.A. Khalid and D.V. Edmonds: 'Interphase precipitation in microalloyed engineering steels and model alloy', Mater. Sci. Technol., 1993, **9**, 384-396.

278. E.V. Morales, J. Gallego and H-J Kiestenbach 'On coherent carbonitride precipitation in commercial microalloyed steels', Philos. Mag. Lett., 2003, **83**, 79-87.

279. H-J Kiestenbach, S.S. Campos and E.V. Morales: 'Role of interface precipitation in microalloyed hot strip steels', Mater. Sci. Technol., 2006, **22**, 615-626.

280. M. Nöhrer, S. Zamberger, S. Primig and H. Leitner: 'Atom probe study of vanadium interphase precipitates and randomly distributed vanadium precipitates in ferrite', Micron, 2013, **54-55**, & 57-64.

281. H.W. Yen, C.Y. Chen, T.Y. Wang, C.Y. Huang and J.R. Yang: 'Orientation relationship transition of nanometre sized interphase precipitated TiC carbides in Ti bearing steel', Met. Sci. Technol., 2010, **26**, 421-430.

282. Y.-J. Zhang, G. Miyamoto, K. Shinbo and T. Furuhara: 'Effects of α / γ orientation relationship on VC interphase precipitation in low-carbon steels', Scr. Mater. 2013, **69**, 17-20.

283. M.-Y. Chen, M. Gouné, M. Verdier, Y. Bréchet and J.-R. Yang: 'Interphase precipitation in vanadium-alloyed steels: strengthening contribution and morphological variability with austenite to ferrite transformation,' Acta Mater., 2014, **64**, 78–92.

284. S. Freeman: 'Interphase precipitation in a titanium steel', in 'Effects of second-phase particles on the mechanical properties of steel', 152-156, 1971, London, The Iron and Steel Institute.

285. E. Orowan: 'Internal stresses in metals and alloys ', Inst. Met. 1948, 451-457.

286. M.F. Ashby: 'The hardening of metals by non-deforming particles', Zeit. Metallkd., 1964, 55, 5-17.

287.H.S. Ubhi and T.N. Baker: 'Artefacts and their influence on the analysis of small particles in extraction replicas', Analytical Electron Microscopy With High Spatial Resolution, 135-145, 1988, Institute of Metals, London.

288. T.N. Baker: 'Quantitative metallography using transmission electron microscopy', in 'Quantitative microscopy of high temperature materials' (ed., A. Strang and J.Crawley), 161-189, 2001, London, IOM Communications Ltd.

289. M. Mackenzie, A.J. Craven and C.L. Collins: 'Nanoanalysis of very fine VN precipitates in steel', Scr. Mater. 2006, **54**, 1-5.

290. G.I. Taylor: 'The Mechanism of Plastic Deformation of Crystals', Proc. Roy. Soc. A, 1934, **A145**, 362-388.

291. W. Roberts, S. Karlsson and Y. Bergstron: 'Rate of dislocation multiplication in polycrystalline iron', Mater. Sci. Eng., 1973, **11**, 247-254.

292. H. Conrad, and J. Narayan: 'On the grain size softening in nanocrystalline materials', Scripta Mater. 2000, **42**, 1025–30.

293. C. Carlton and P.J. Ferreira: 'What is Behind the Inverse Hall–Petch Behavior in Nanocrystalline Materials?' Acta Mater. 2007, **55**, 3749-3756.

294. J.D. Embury: 'Strengthening by dislocation substructure', in 'Strengthening methods in crystals', (eds. A. Kelly and R.B. Nicholson), 331-402, 1971. London, Applied Science Publishers Ltd.,

295 A.W. Thompson: 'Substructural strengthening mechanisms', Metall. Trans. A, 1977, **8A**, 833-842.

296. F.R. Castrofernandez and C.M. Sellars: 'Relationship between room-temperature proof stress, dislocation density and subgrain size', Philos. Mag. 1989, **60**, 487-506.

297. P.L. Mangonon Jr. and W.E. Heitmann: 'Subgrain and precipitation-strengthening effects in hot-rolled, columbium-bearing steels', in 'Proc.Microalloying 75', Washington, DC, October 1977, Union Carbide, USA, 59-70.

298 E.V. Morales, R.A. Silva, I.S. Bott and S. Paciornik: 'Strengthening mechanism in a pipeline microalloyed steels with a complex microstructure', Mater. Sci. Eng A, 2013, **A585**, 253-260.

299. H. Kimura: 'Mechanical properties of high purity iron and its dilute alloys', Mater. Trans. Jap. Inst. Met. 1999, **40**, 1025-1031.

300. A.J.E. Foreman and M.J. Makin: 'Dislocation movement through random arrays of obstacles', Philos. Mag., 1966, 14, 911-924

301. U.F. Kocks: 'Alloy superposition of alloy hardening, strain hardening and dynamic recovery' Proc. 5th Int. Conf. 'Strength of Metals and Alloys', (eds. P. Haasen, V. Gerold and G. Kostorz), 1661-1680, 1980, Oxford, Pergamon Press.

302. J. Li, F.Y. Sun and W.C. Xu: 'On the evaluation of yield strength for microalloyed steels', Scr. Metall. Mater. 1990, **24**, 1393-1398.

303. W.B. Morrison, R.C. Cochrane and P.S. Mitchell: 'The influence of precipitation mode and dislocation substructure on the properties of vanadium-treated steels', ISIJ Int., 1993, **33**, 1095-1103.

304. R.J. Glodowski: 'An empirical prediction model of the incremental strengthening of ferrite /pearlite steels with additions of vanadium and nitrogen, with emphasis on the effective nitrogen level', Int. J. Metall. Eng., 2013, **2**, 46-61.

305. G.R. Speich: 'Tempering of low-carbon martensite', Trans. Metall. Soc. AIME, 1969, **245**, 2553-2564.

306. W.G. Hall and T.N. Baker: 'Electrical resistivity and length changes during precipitation in Fe-V-C alloy', Met. Sci., 1981, **15**, 447-454.

307. G. Staniek and E.Hornbogen: 'Combination of precipitation and grain boundary hardening', Scr. Metall. 1973, **7**, 615-619.

308. G.C. Weatherly: 'Loss of coherency of growing particles by prismatic punching of dislocation loops', Philos. Mag. 1968, **17**, 791-799.

309. J.-S. Wang, M.D. Mulholland, G.B. Olson and D.N. Seidman: 'Prediction of the yield strength of a secondary-hardening steel', Acta Mater., 2013, **61**, 4939-4952.

310. N. Kamikawa, K. Sato, G. Miyamoto, M. Murayama, N. Sekido, K. Tsuzaki and T. Furuhara: 'Stress strain behavior of ferrite and bainite with nano-precipitation in low carbon steels', Acta Mater. 2015**, 83**, 383-396.

311. A.G. Kostryzhev, O.O. Marenych, C.R. Killmore and E.V. Pereloma: 'Strengthening mechanisms in thermomechanically processed NbTi-microalloyed steel', Metall. Mater. Trans. A, 2015, 46A, 3470-3480.

312 W. Barr and C.F. Tipper: 'Brittle fracture in mild steel plates', J. Iron Steel Inst., 1947, **157**, 223-238.

313. M. Militzer: 'Thermomechanical Processed Steels', in 'Comprehensive Materials Processing, Vol 1, Conventional and specialized materials', (ed. S. Hashmi), 191-216, 2014, Oxford, Elsevier.

314. https://en.wikipedia.org/wiki/Liberty-ship

315. N.J. Petch: 'The fracture of metals', Prog. Met. Phys., 1954, **5**, 1-52.

316. N.J. Petch: The ductile-cleavage transition in alpha iron', in Proc. Swampscott Conf. on 'Fracture' (eds. B.L. Averback, D.K. Felbeck, G.T. Hahn and D.A, Thomas), 54- 64,1959, New York, Wiley.

317. C.J. McMahon and M. Cohen:'Initiation of cleavage in polycrystalline iron 'Acta Metall., 1965, **13**, 591-604.

318. B. Mintz, W.B. Morrison and R.C. Cochrane: 'Influence of grain boundary carbide thickness and grain size on the impact properties of steel', Proc. Conf. Advances in Physical Metallurgy and Applications in Steels, 222-228, 1981, Metals Soc., London.

319. B. Mintz, W.B. Morrison and A. Jones: Influence of carbide thickness on impact transition-temperature of ferritic steels', Met. Technol., 1979, **6**, 252-260.

320. E. Smith: 'The nucleation and growth of cleavage microcracks in mild steel' in Conf. Proc. 'Physical Basis of Yield and Fracture' 36-46, 1966, Oxford, UK, Institute of Physics.

321. E.A. Almond, D. Timbres and J.D. Embury: Proc. 2ndInternal Conf. on Fracture (ed. P.L. Pratt), 253,1969, New York, Chapman and Hall.

322. D.A. Curry and J.F. Knott: 'Effects of microstructure on cleavage fracture stress in steel', Met. Sci., 1978, **12**, 511-514.

323. N.J. Petch: 'The influence of grain-boundary carbide and grain-size on the cleavage strength and impact transition temperature of steel', Acta Metall. 1986, **34**, 1387-1393.

324. M.S. Bingley and T. Siewecki: in Proc.8 th Int. Conf. Strength of Metals and Alloys (eds. P.O. Kettunen, T.K. Lepisto and M.E. Leohtonon) Pergamon Press, Oxford, 1988, 1191-1196.

325. M.S. Bingley: 'Effect of grain size and carbide thickness on impact transition temperature of low carbon structural steels', Mater. Sci. Technol., 2001, **17**, 700-714.

326. B. Mintz, S. Vue, and J.J. Jonas: 'Hot ductility of steels and its relationship to the problem of transverse cracking during continuous casting', Int. Mater. Revs. 1991, **36**, 187-217.

327. R.L. Robbins, O.C. Shepard, O.D. Sherby: 'Role of crystal structure on the ductility of pure iron at elevated temperature' JISI, 1961, **199**, 175-180.

328. C. Rossard and P. Blain: 'A method of simulation by torsion to determine the influence of hot rolling conditions on the structure of steel', Rev. Métall. 1962, **59**, 223-236.

329. R.L. Robbins, O.C. Shepard, O.D. Sherby: 'Torsional ductility and strength of iron-carbon alloys at elevated temperature', ASM Trans. Quart., 1967, **60**, 205

330. B. Mintz and J.M. Arrowsmith: Hot ductility behaviour of C-Mn-Mn-Al steel and its relationship to crack propagation during straightening of continuously cast strand', Met. Technol., 1979, **6**, 24-32.

331. D.N. Crowther and B. Mintz: 'Influence of grain size on hot ductility of plain C-Mn steels', Met. Sci. Technol., 1986, **2**, 951-955.

332. B. Mintz and J.M. Arrowsmith: 'Influence of microalloying additions on hot ductility of steels', in 'Hot working and forming processes' (eds. C.M. Sellars and G.J. Davies), 99-103, 1990, London, Institute of Materials.

333. J.R. Wilcox and R.W.K. Honeycombe: 'Influence of prior precipitation on hot ductility of C-Mn-Nb-Al steels', in 'Hot working and forming processes' (eds. C.M. Sellars and G.J. Davies), 108-112, 1990, London, Institute of Materials.

334. B. Mintz and D.N. Crowther: 'The influence of small additions of Ti on the hot ductility of steels', in 'Titanium technology in microalloyed steels', (ed. T.N. Baker), 98-114, 1997, London, Institute of Materials.

335. K.M. Banks, A. Tuling, C. Klinkenberg and B. Mintz: 'Influence of Ti on hot ductility of Nb containing HSLA steels', Mat. Sci. Technol., 2011, **27**, 737-545.

336. A.M. El-Wazri, F. Hassani, S. Yue, E. Es-Sadiqui, L.E. Collins and K. Iqual: 'The effect of thermal history on the hot ductility of microalloyed steels', ISIJ Int., 1999, **39**, 256-262.

337.C. Spanbury and B. Mintz 'Influence of undercooling thermal cycle on hot ductility of C–Mn–Al–Ti and C–Mn–Al–Nb–Ti steels', Ironmaking and Steelmaking, 2005, **32**, 319-324.

338. T.H. Coleman and J.R. Wilcox: 'Transverse cracking in continuously cast HSLA slabs – influence of composition', Mater. Sci. Technol., 1985, **1**, 80-83.

339. S. Roy, S. Patra, S. Neogy, A. Laik, S.K. Choudharey and D. Chakrabarti: 'Prediction of inhomogeneous distribution of microalloy precipitates in continuously cast high strength low alloy steel slab', Met. Mater. Trans. A, 2012, **43A**, 1845-1860.

340. D.A. Melford: 'The Influence of Residual and Trace Elements on Hot Shortness and High Temperature Embrittlement', Philos.Trans., 1980, **295**, 89-103.

341. D.A. Melford: 'Influence of antimony and arsenic on surface hot shortness in copper-containing mild steels', JISI, 1966, **204**, 495-496.

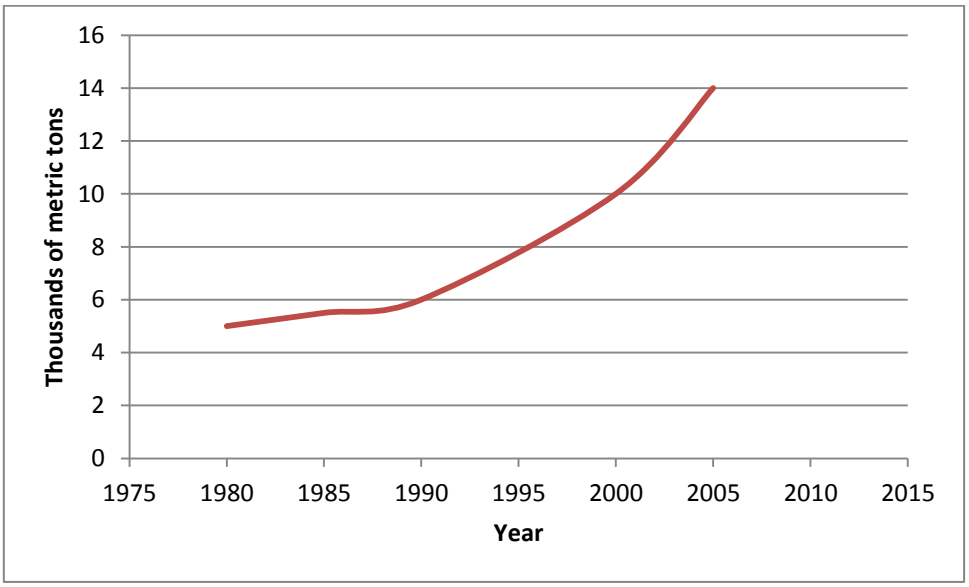

Fig 1 Ferro-Niobium (FeNb) consumption in West Europe (EU15) CBMM-NPC data.[15]

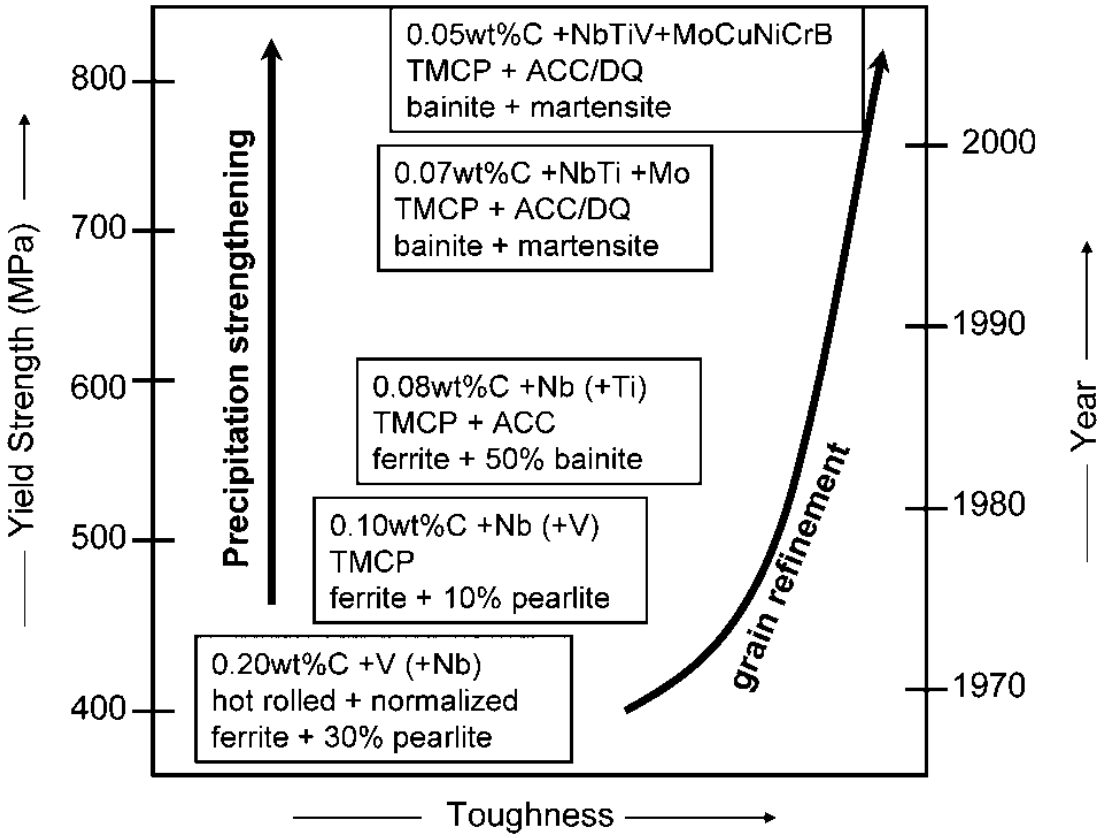

Fig 2 Development of pipeline steels as an example of HSLA steel research (TMPC: themomechanical controlled processing; ACC: accelerated cooling; DQ: direct quench) [7, 44]

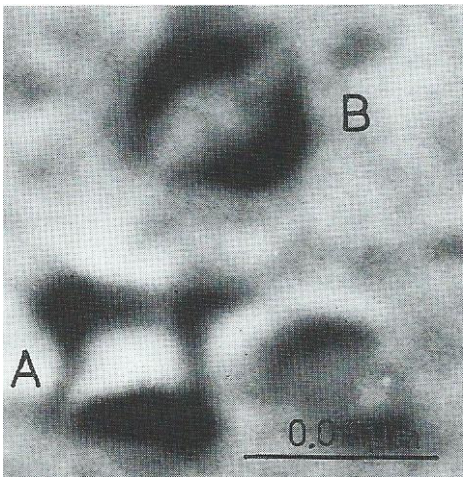

Fig 3 TEM micrograph of coherency strain fields associated with vanadium carbide particles.

A – double arrowhead strain field contrast of disc particle.

B – double lobe strain field contrast of spherical particle.[2]

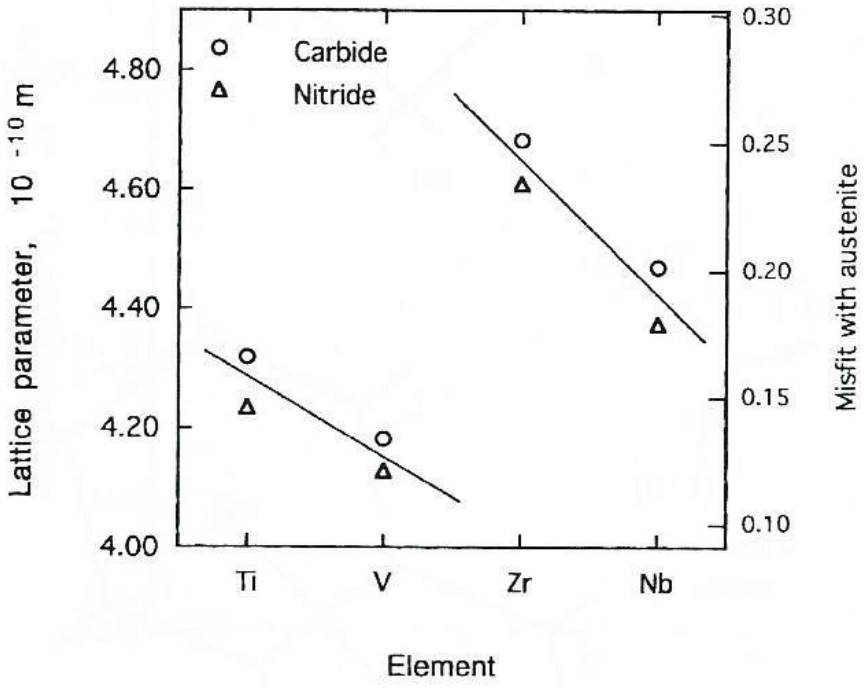

Fig 4 Variation of lattice parameters and misfit with austenite of some transition metal carbides and nitrides found in microalloyed steels [58]

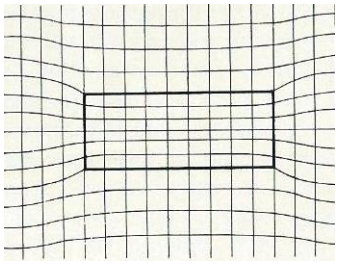

(a)

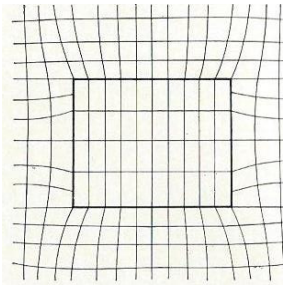

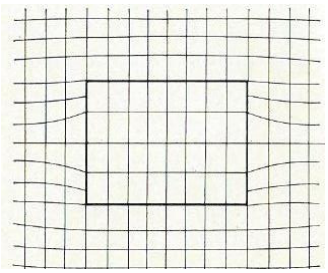

(b) (c)

Fig 5 (a) Cross section of disc-shaped coherent particle with small negative mismatch, (b) cross section of disc-shaped coherent particle with small positive mismatch, (c) cross section of disc-shaped with positive misfit normal to the plane of the disc.[36]

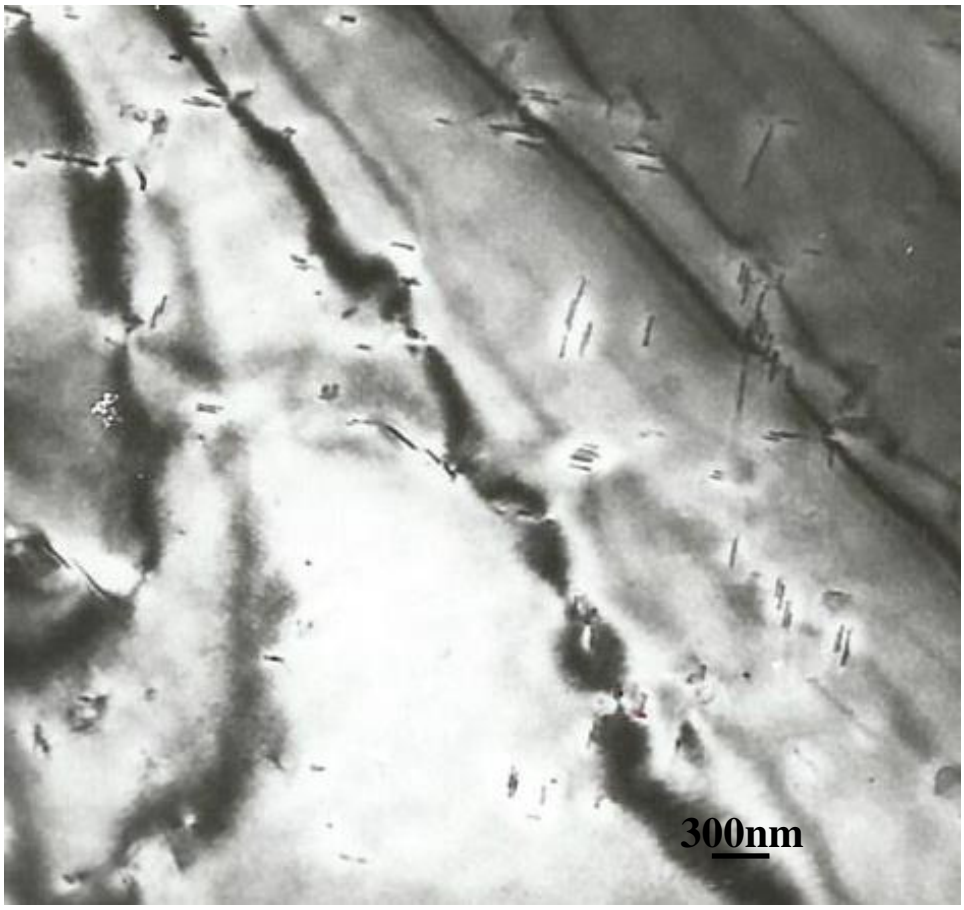

Fig 6 Incoherent vanadium nitride disc precipitates mainly in section.[1]

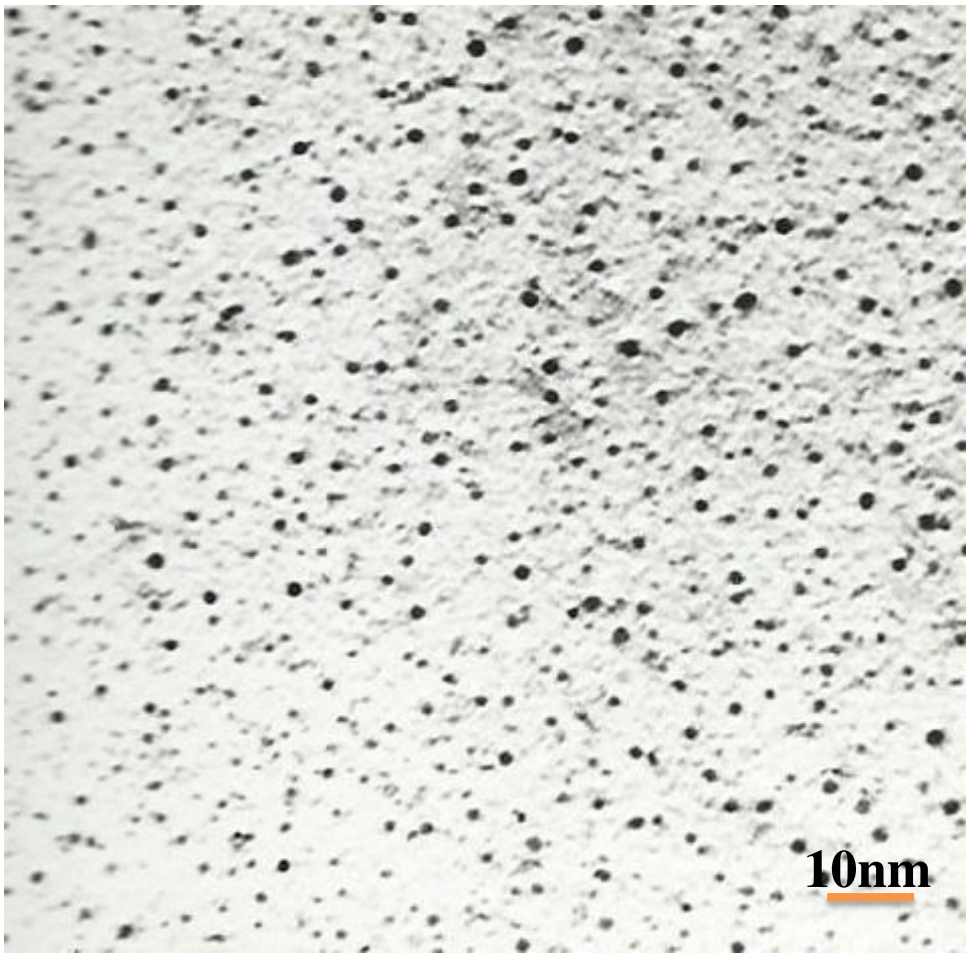

Fig 7 TEM micrograph of carbon replica which has extracted ~ 2nm particles.[114]

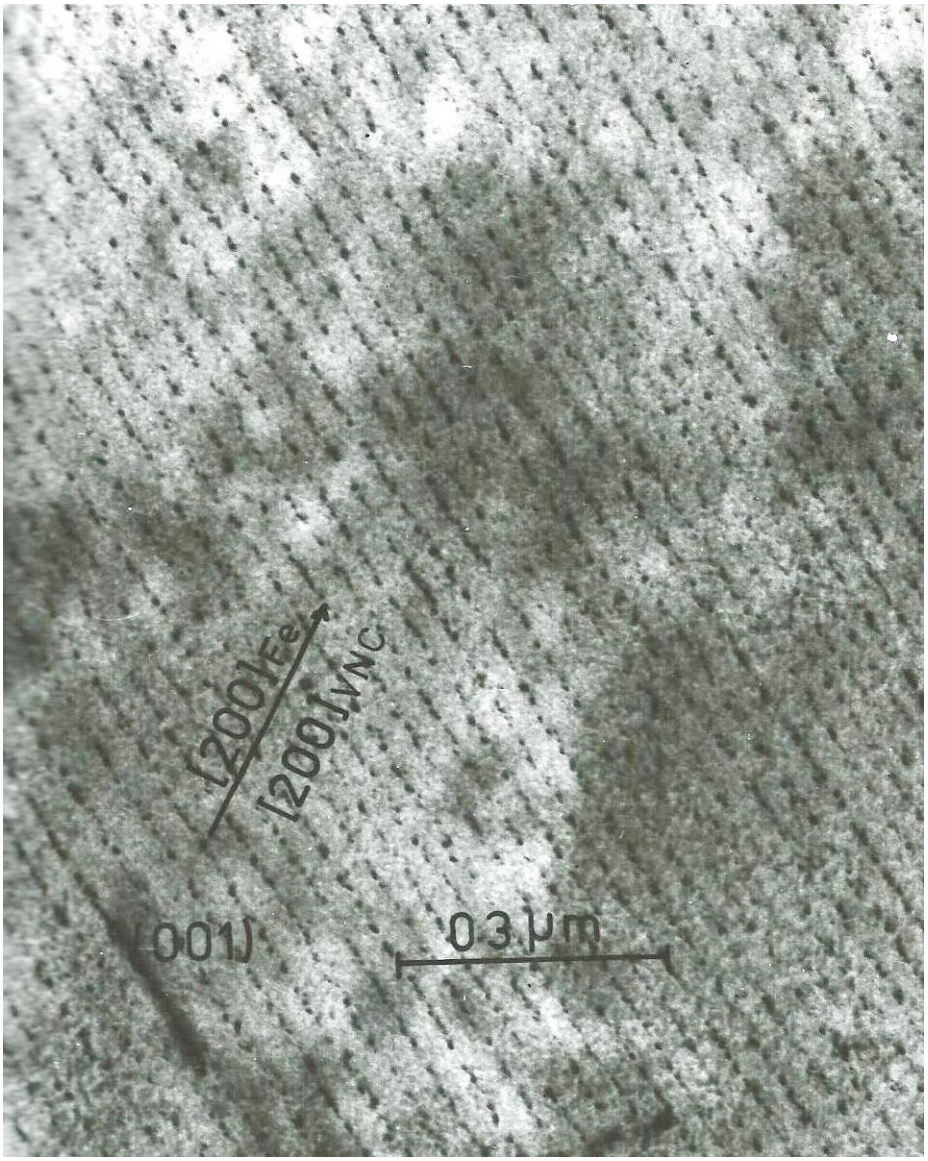

Fig 8 Interphase precipitation in a vanadium microalloy steel [1]

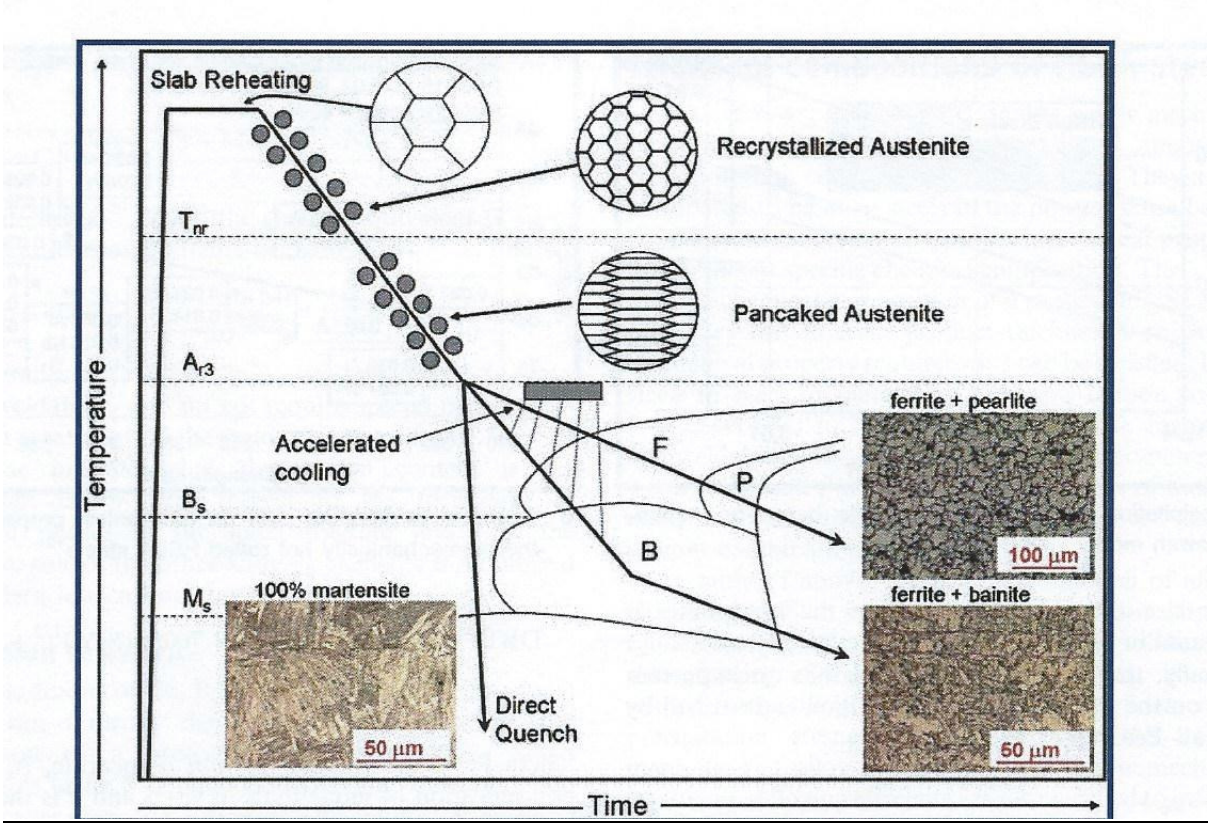

Fig 9 Schematic diagram of thermomechanically controlled processing (TMCP) and microstructures that result from this process.[7]

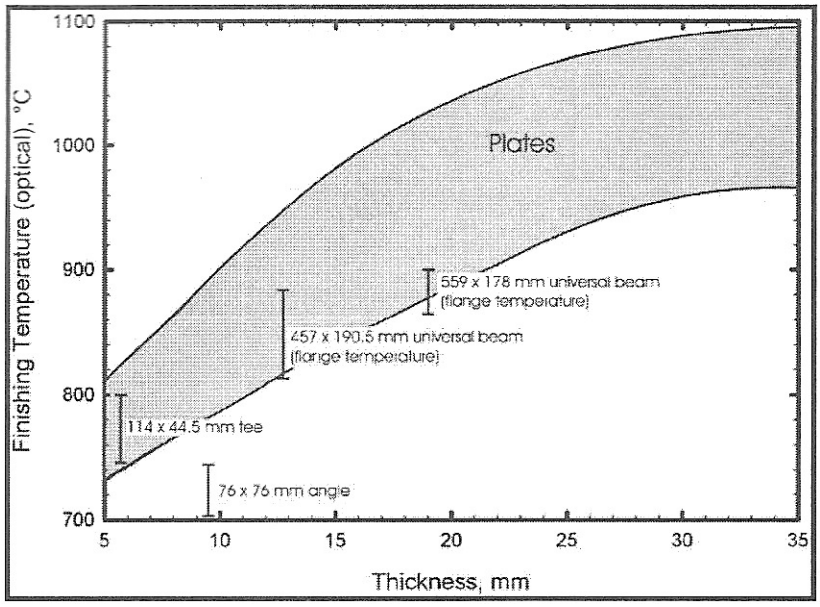

Fig 10 General relationship between thickness and finishing temperature of rolling for plates and sections [5, 67, 68]

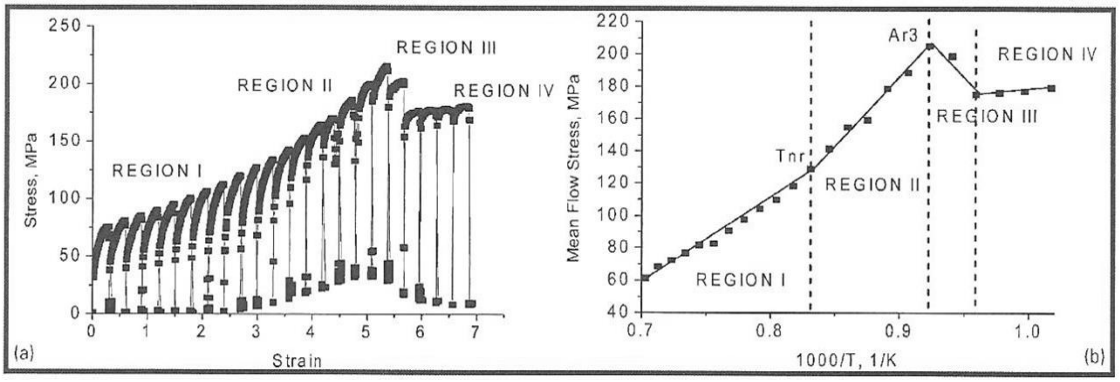

Fig. 11 (a) stress-strain curve obtained from multi-deformation test on microalloy steel, (b) mean flow stress verses absolute temperature.[7, 75]

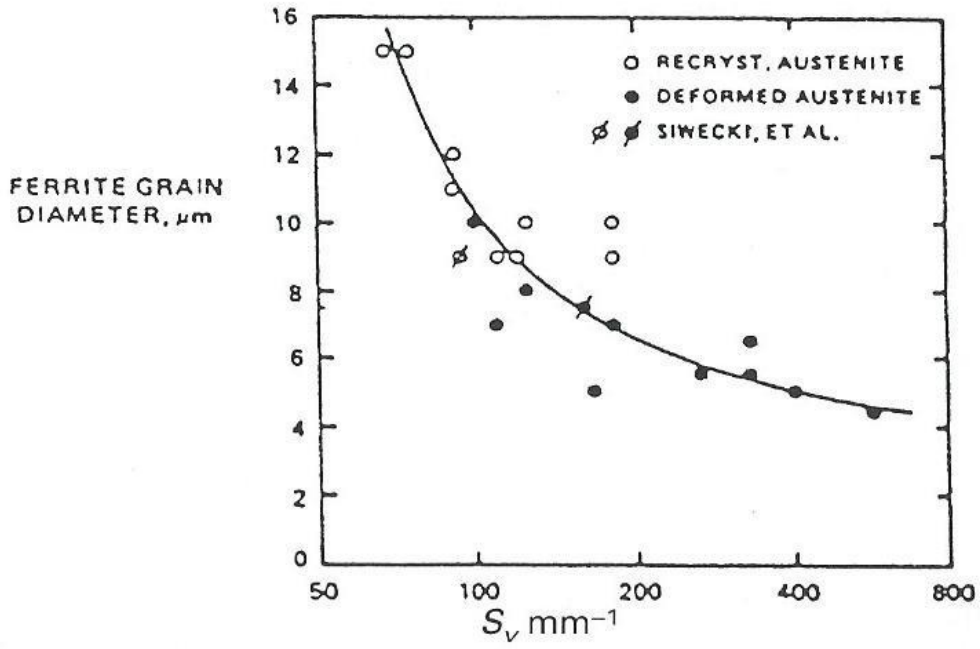

Fig 12 Ferrite grain sizes produced from recrystallized and unrecrystallized austenite at various S_v values (after Priestner and Rios [78])

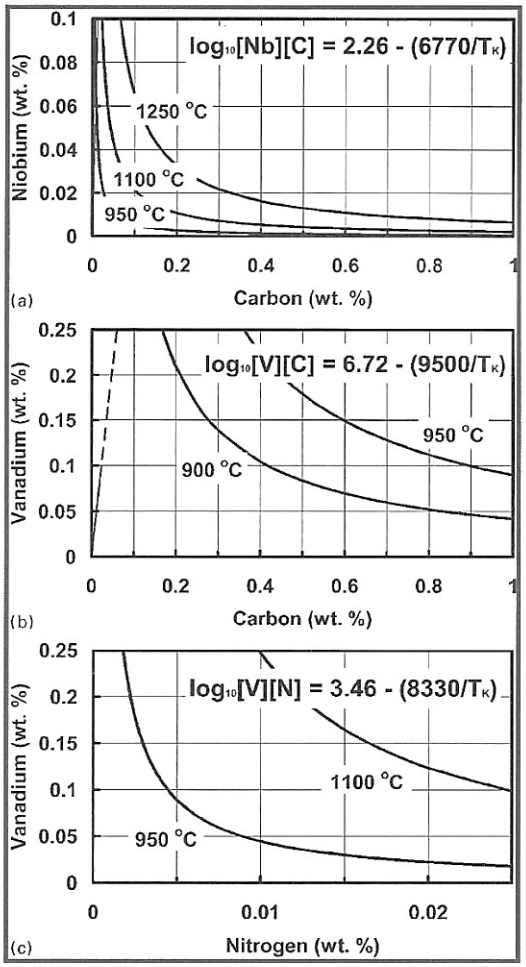

Fig.13 Calculated solubility curves at temperatures associated with thermomechanical processing for a NbC, b VC and c VN.[80]

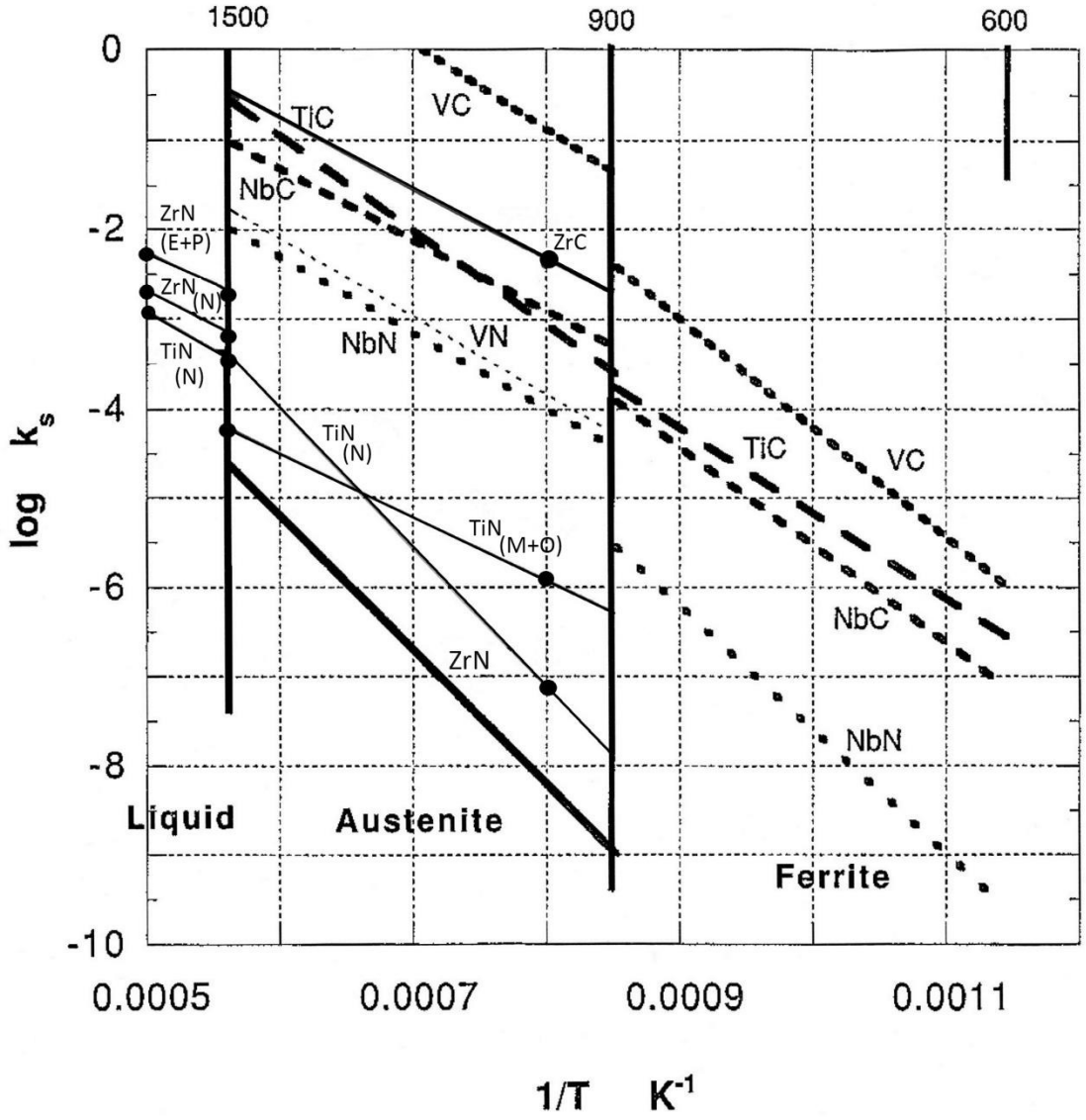

Fig14 Comparison of solubility products of carbides and nitrides in microalloyed steels: top horizontal axis is ºC: after Gladman[3]

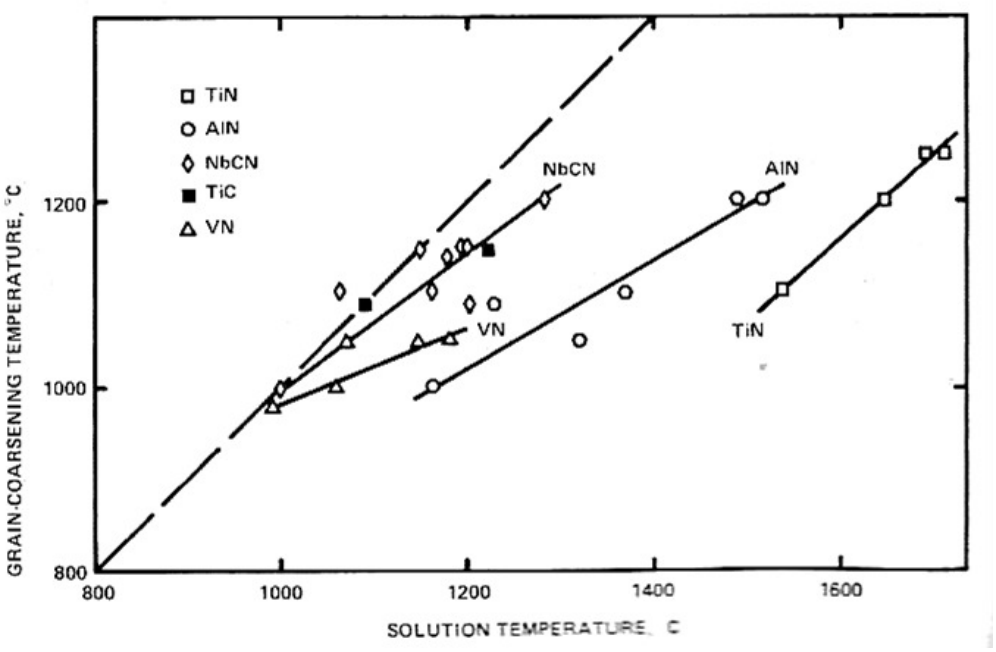

Fig 15 Relation between observed grain-coarsening temperature of austenite and computed temperature for complete dissolution of microalloying carbides and nitrides in austenite.[86]

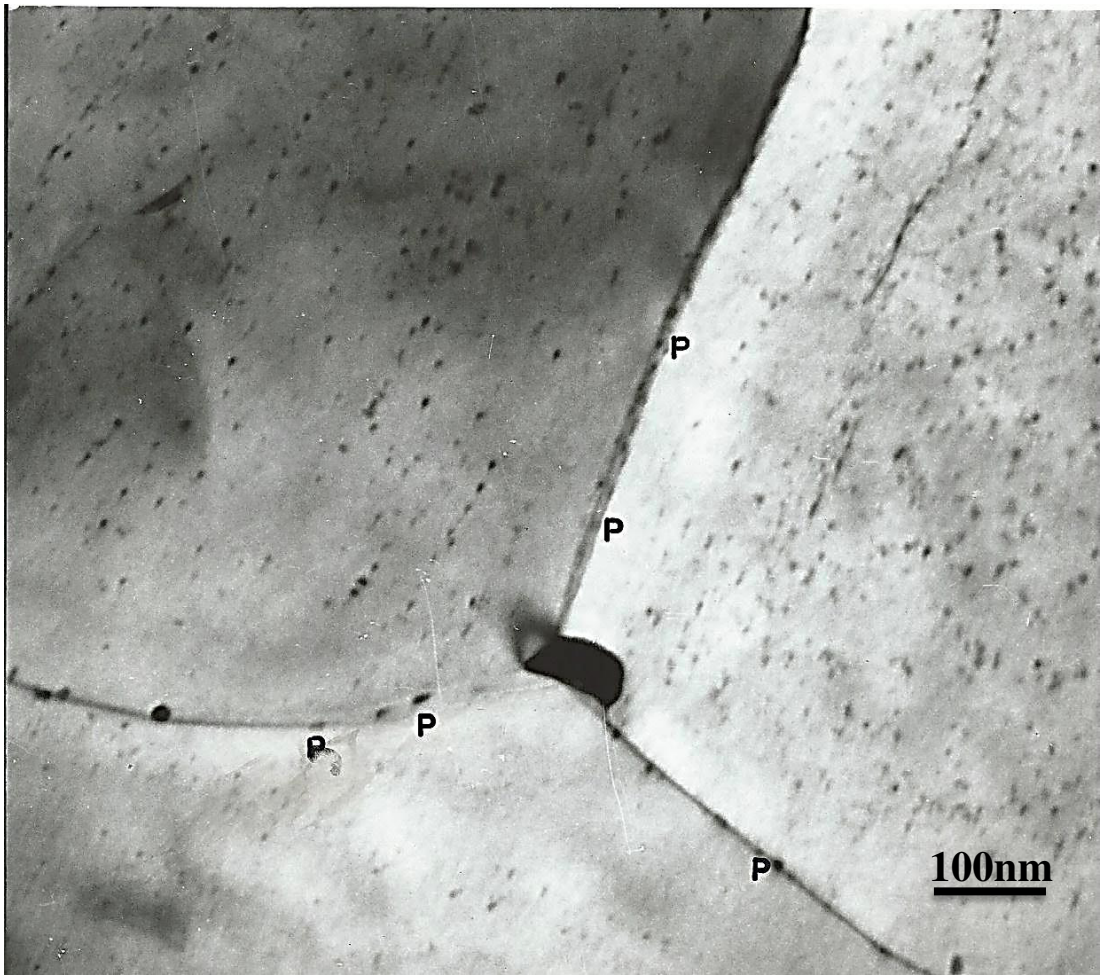

Fig 16 Thin foil of vanadium microalloyed steel, with 80nm long prior austenite grain boundary particle at triple intersection of boundaries and smaller precipitates, ~20nm, at P, on the boundaries. Also, smaller particles within the grains, some associated with out of contrast dislocations.

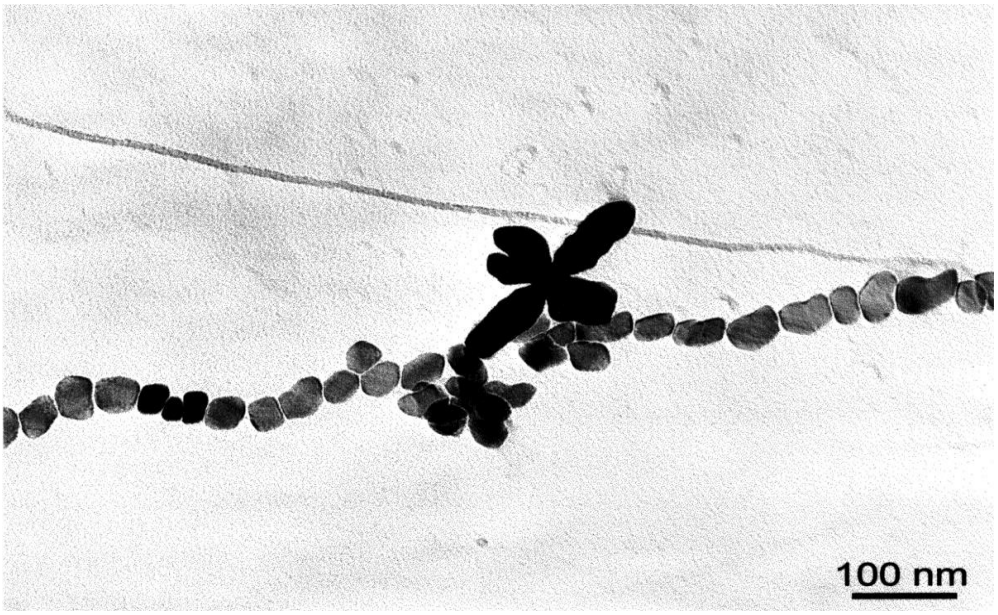

Fig 17 Carbon replica of vanadium carbonitride particles nucleated on a grain boundary.

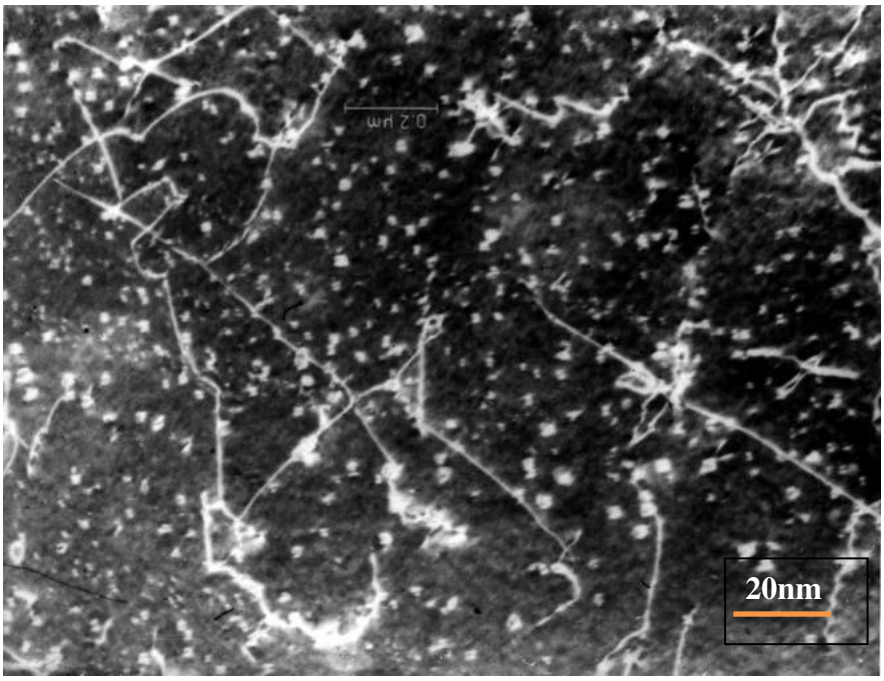

Fig 18 Dark field transmission electron micrograph showing dislocations interacting with precipitates in a microalloyed steel.

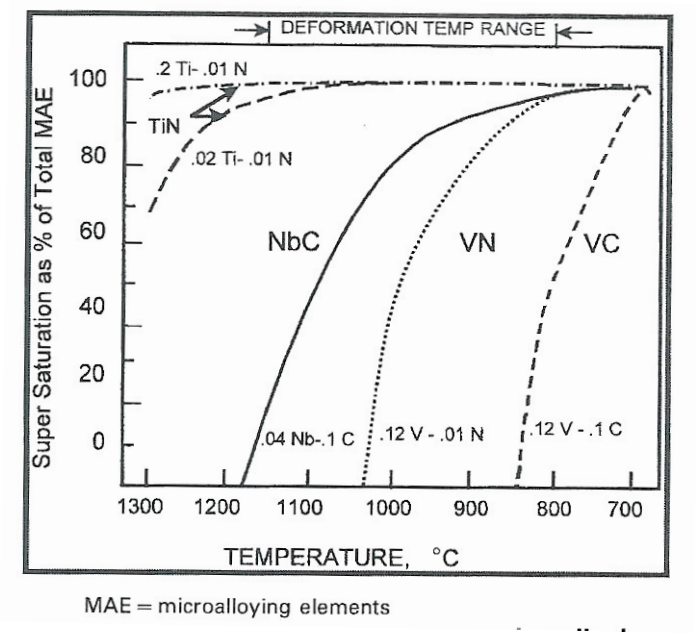

Fig 19 Precipitate potential for various microalloying systems. [6]

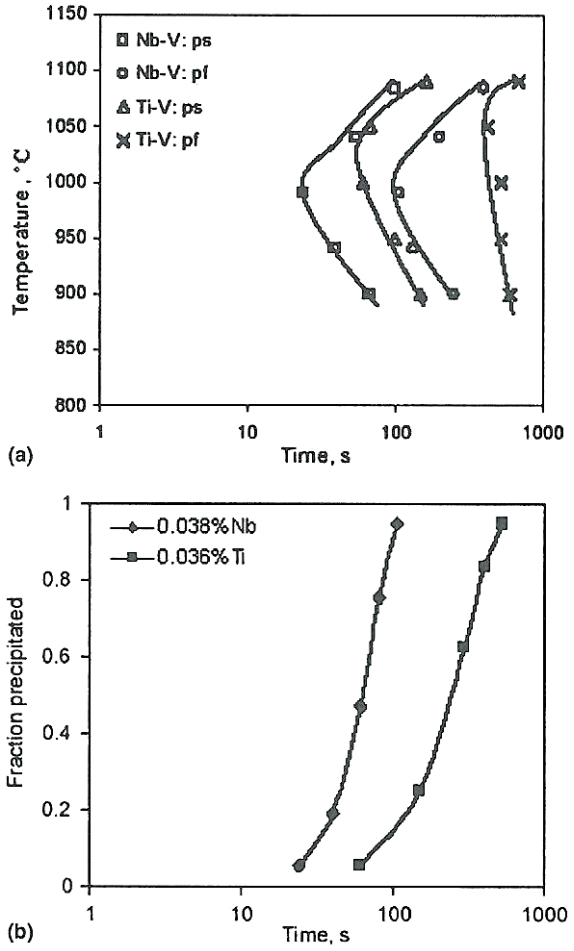

Fig 20 Comparison of precipitation kinetics for Nb-V and Ti-V steels. [97]

(ps -precipitate start, pf-precipitate finish)

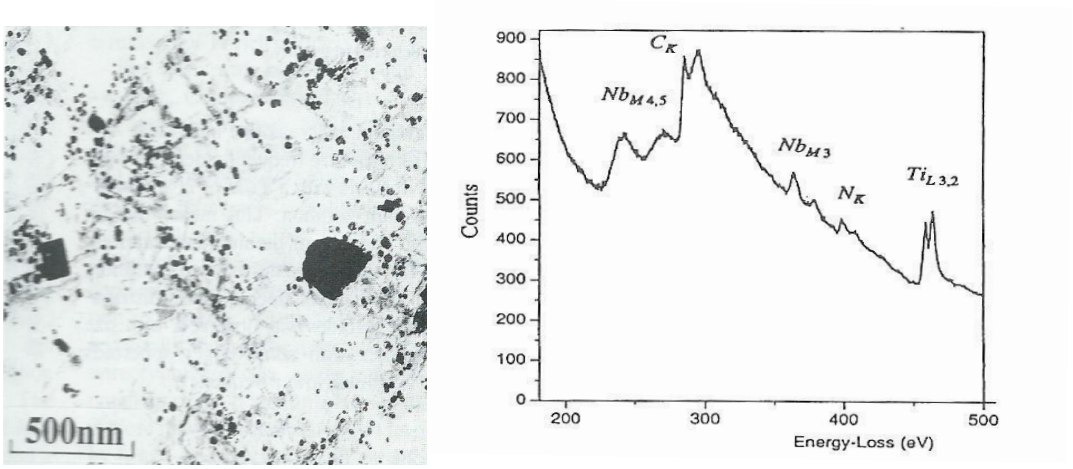

(a) (b)

Fig 21 (a) Ti-Nb particles in 0.01%Ti-Nb steel, with smaller Nb-rich spheroids.

(b) An EELS spectrum collected from the centre of a ~20nm Nb-rich spheroid showing the niobium, carbon, nitrogen and titanium edges.[119]

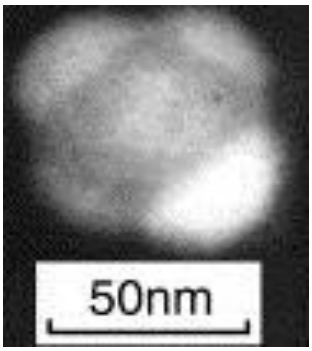

(a)

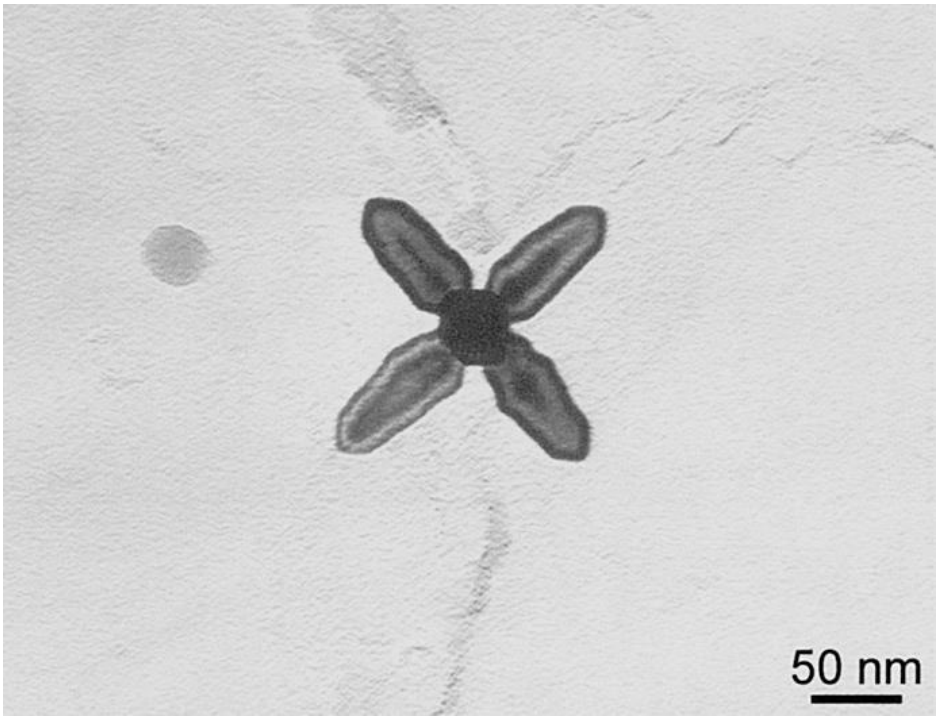

(b)

Fig 22 (a) Four caps formed on the sides of a cuboid core with the probability that there are also caps on the top and bottom faces.
(b) Cruciform particle with four arms nucleating and growing from a core.

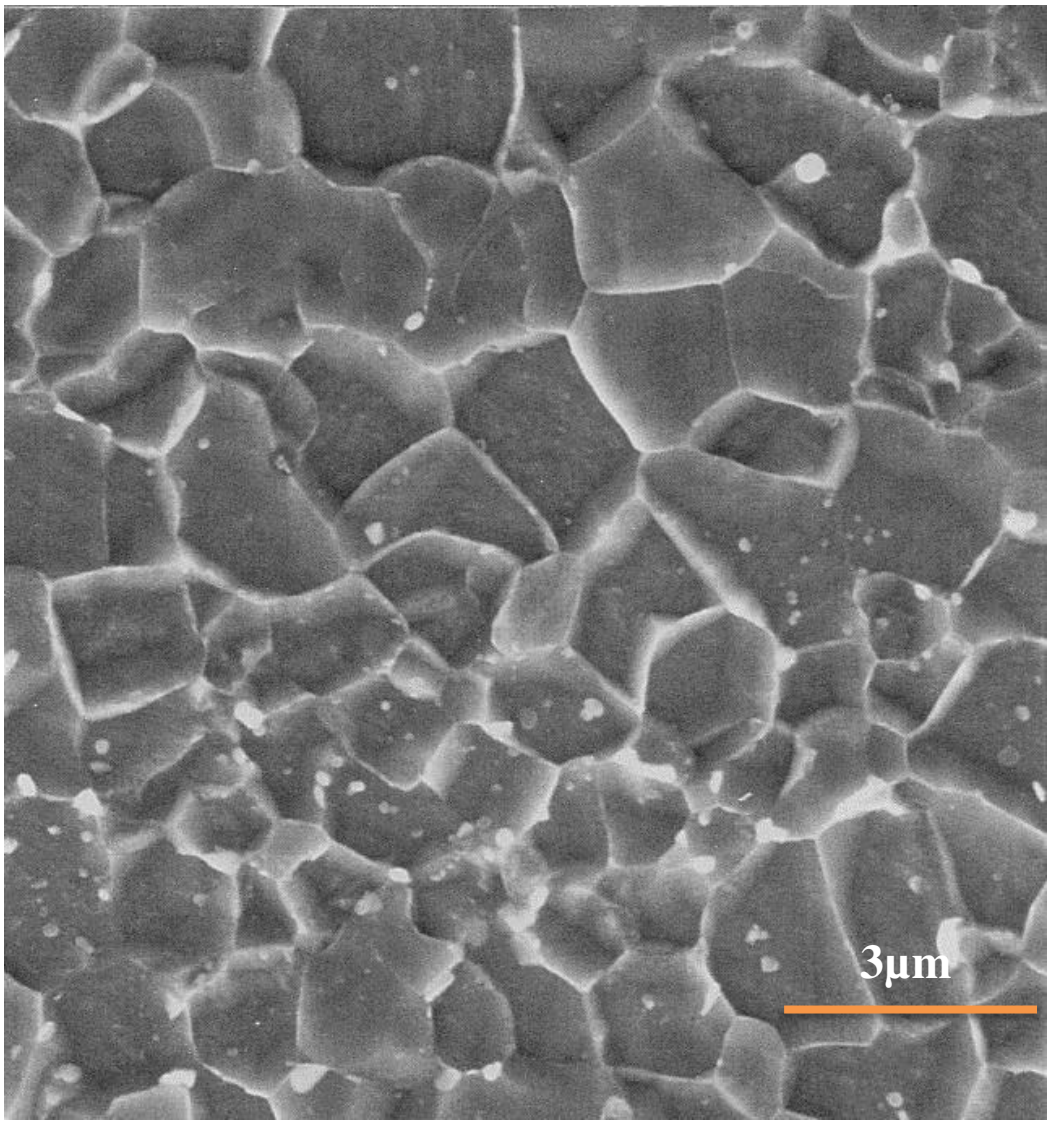

Fig 23 Ultrafine ferrite on rolled strip surface in low carbon steel formed through DSIT route using single pass rolling. [after Hodgson et al [141]]

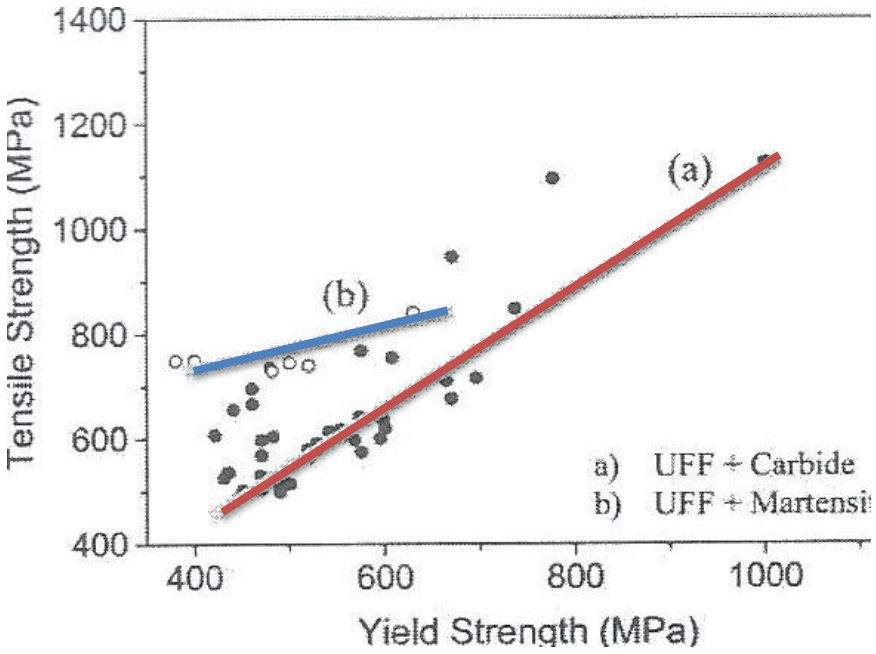

Fig 24 Effect of microstructure on mechanical properties of UFF steels produced through the DSIT mechanism. After Beladi et al.[139]

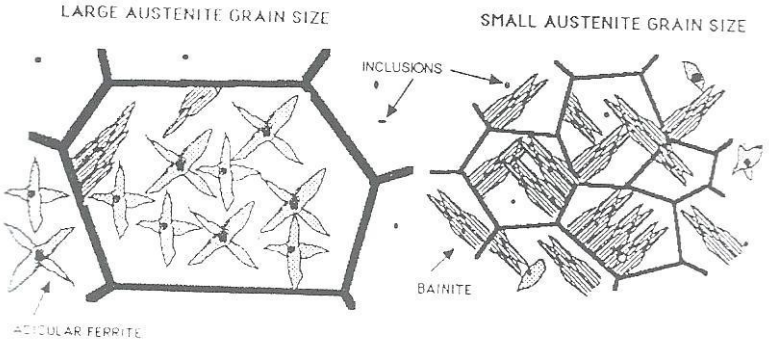

Fig 25 Effect of austenite grain size in determining whether the microstructure is predominantly acicular ferrite or bainite.[149]

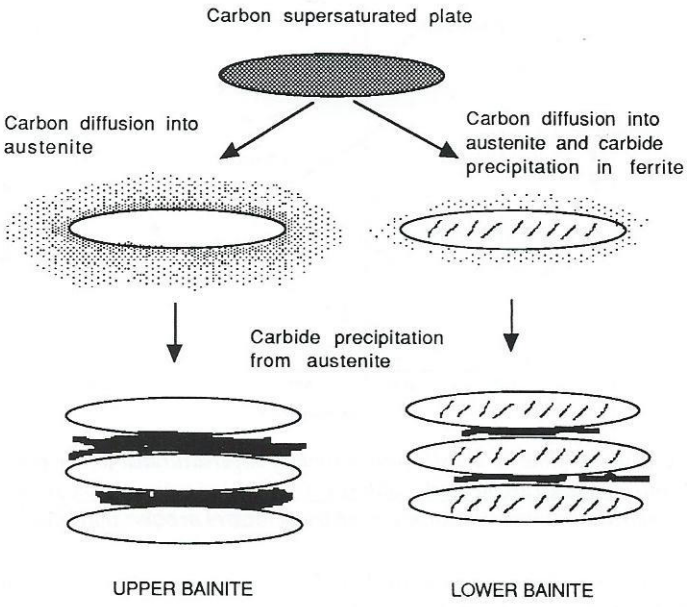

Fig 26 Schematic representation of the transition between upper and lower bainite.[149]

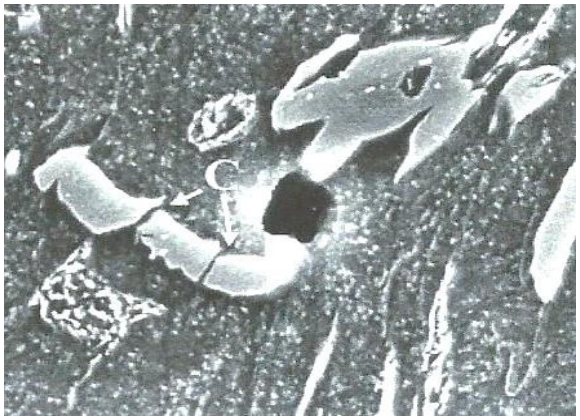

(a)

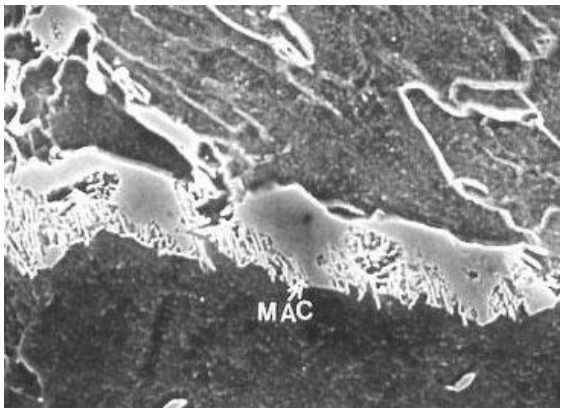

(b)

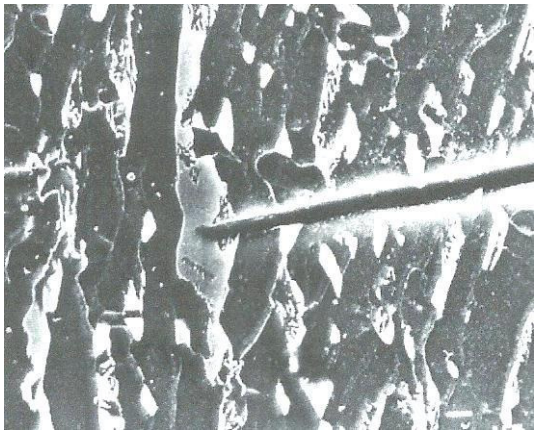

(c)

Fig 27 SEM micrographs of simulated ICCGHAZ microstructures (a) showing void between two closely spaced MA particles: two cracks at C have not propagated. (b) MA + upper bainitic structure (c) crack stopped by MA particle.[155]

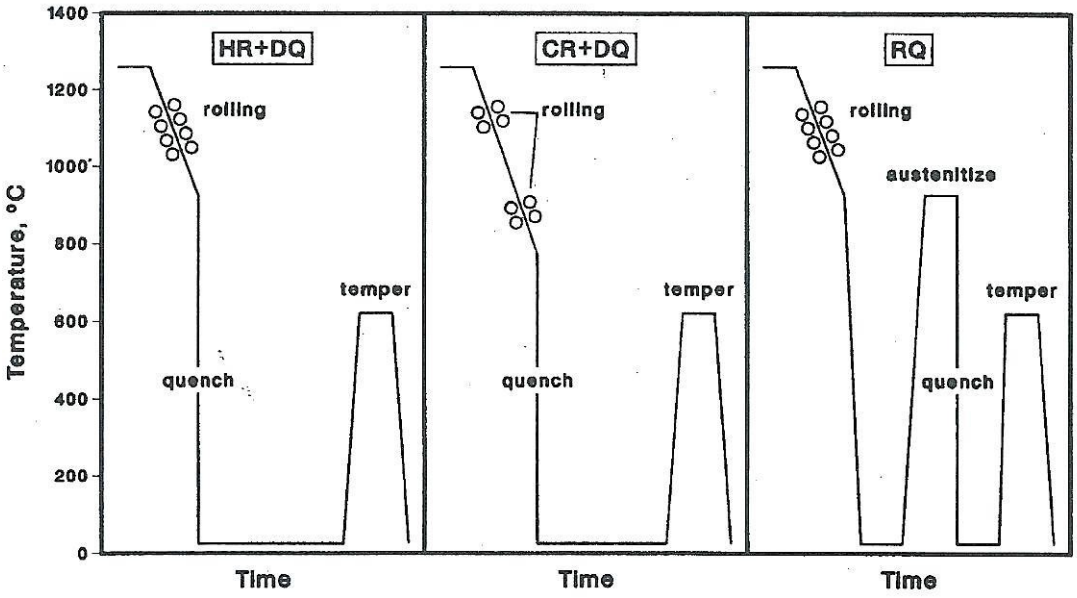

Fig 28 Schematic temperature/time profiles for hot-rolled and direct quenched (HR+DQ), control-rolled and direct quenched (CR+DQ) and reheat-quenched(RQ) laboratory plates[158]

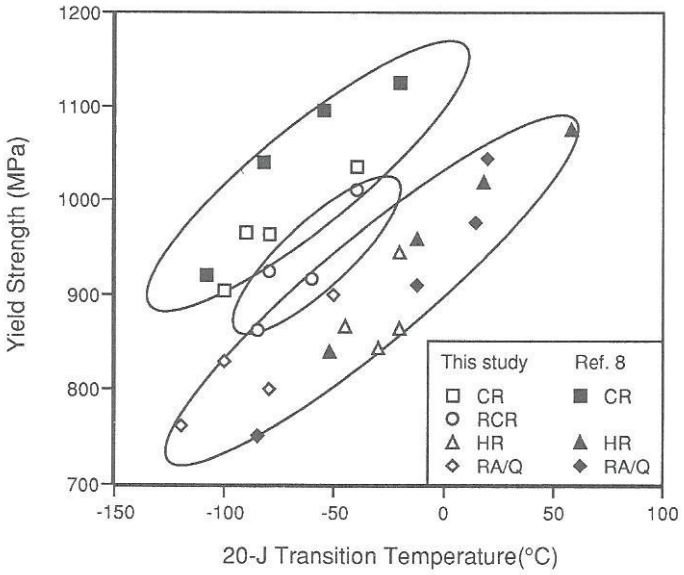

Fig 29 Yield strength /20JTT combinations for samples tempered at 620/625ºC.[159]

Ref 8 (in the box) refers to the work of Taylor and Hansen.[158]

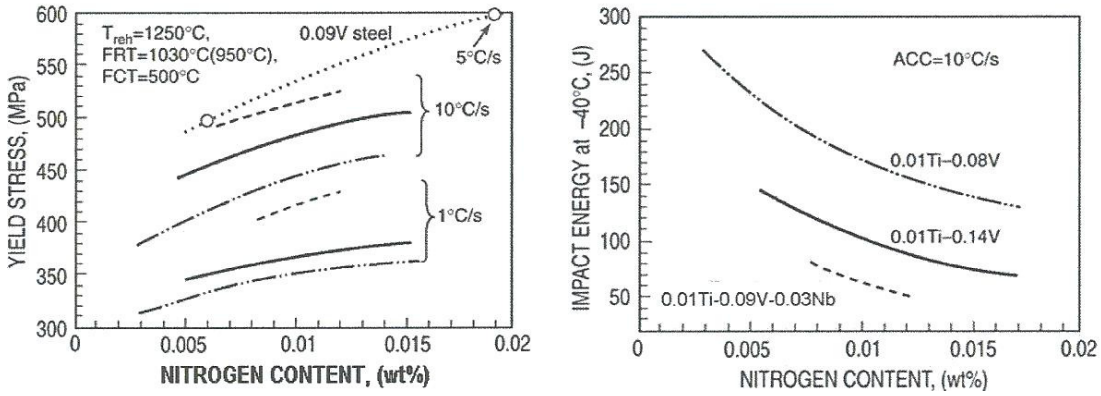

Fig 30 Effect of nitrogen, vanadium and cooling rate on the yield stress and impact toughness of Ti-V-Nb-N steels after rapid cooling process.[11]

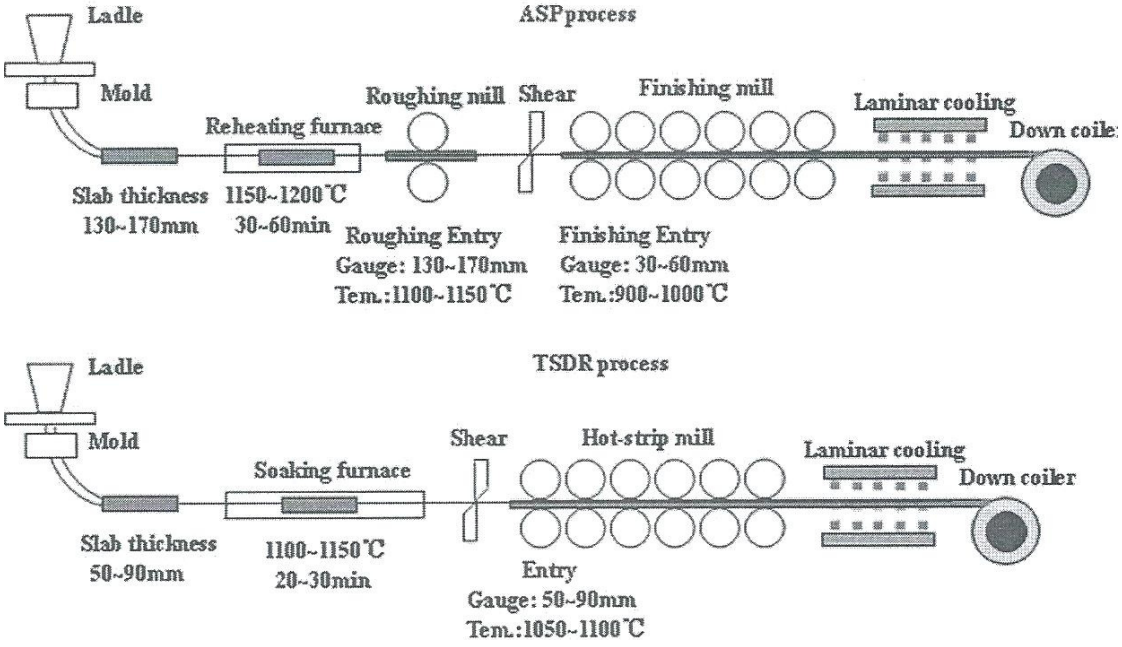

(a)

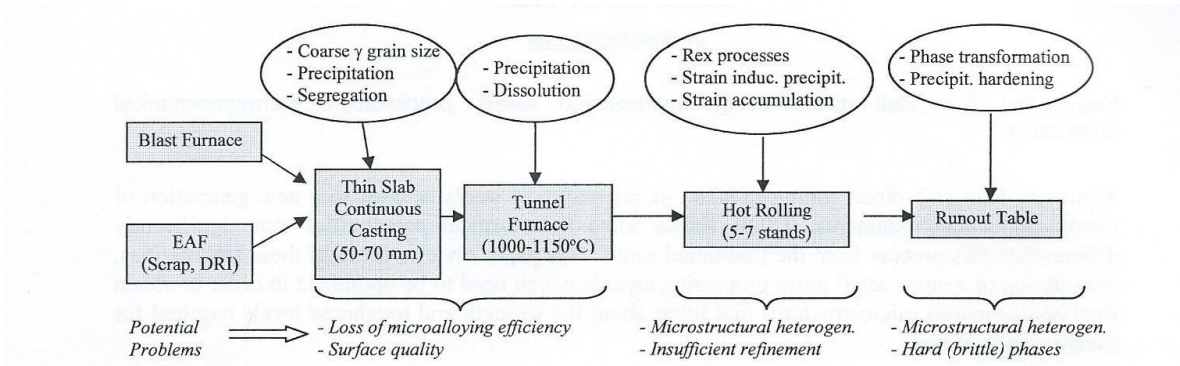

(b)

Fig 31 (a) Schematic diagram showing process route to simulate thin slab direct-charging by ASP and TDSR routes. [182]

(b) Scheme showing the metallurgical mechanisms at the different stages of the TSDR process plus the potential problems related to microalloying.[181]

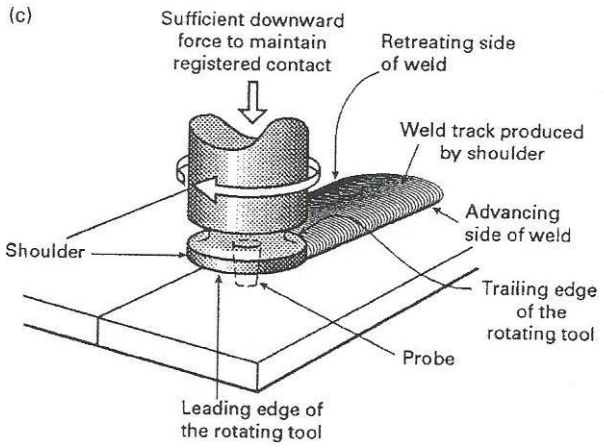

Fig 32 Schematic diagram of friction stir butt welding [233]

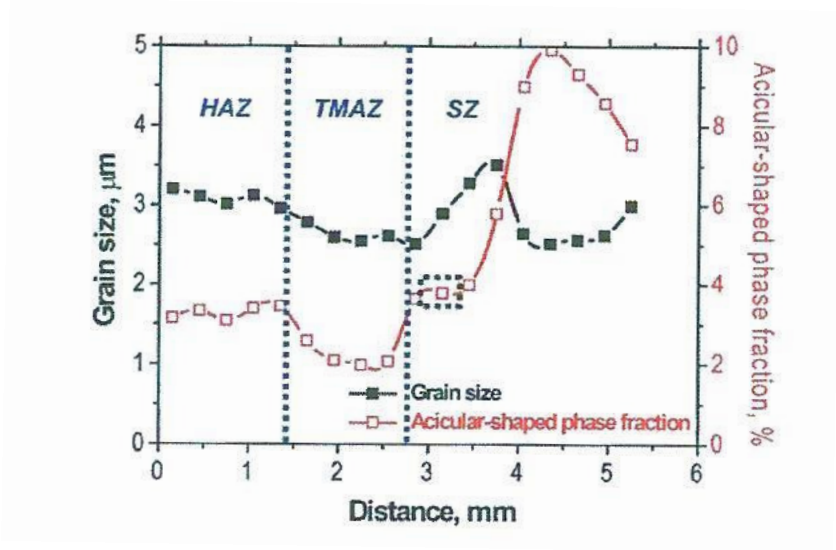

Fig 33 Profiles of grain size and acicular –shaped phase fraction [243]

(a)

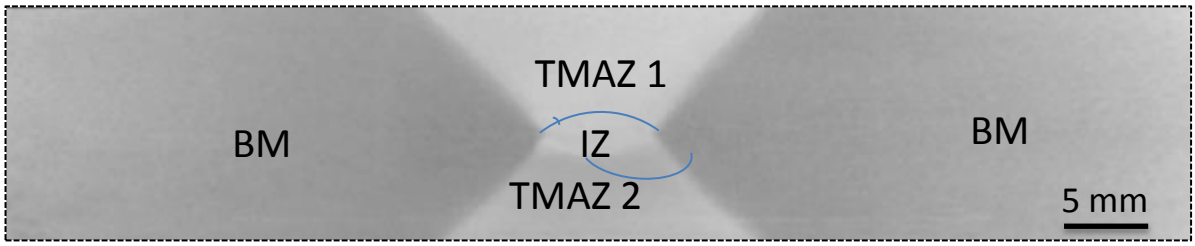

(b)

Fig 34 Macrographs of transverse sections of FSW

(a) single pass DH36 steel[238]

(b) double pass EH 46 steel [249]

BM-base metal, TMAZ – thermomechanical additive zone, IZ – interference zone

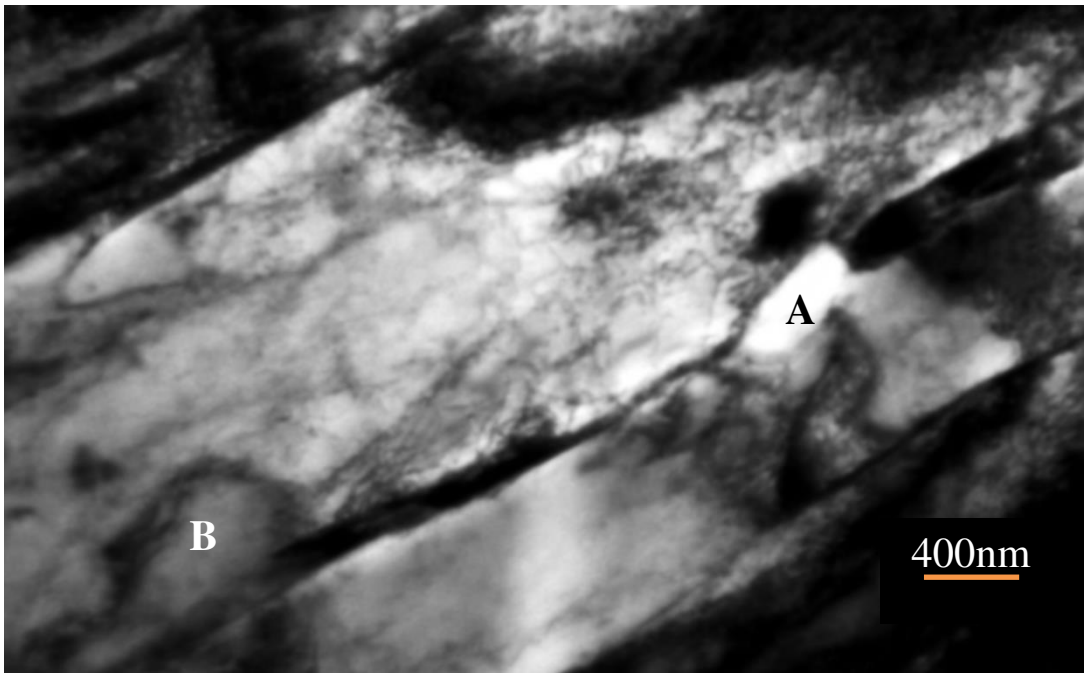

Fig 35 TEM micrograph of IZ of double-sided FSW EH 46 microalloyed steel, showing laths containing pinned dislocations and precipitates growing from the lath boundaries at A and B. [249]

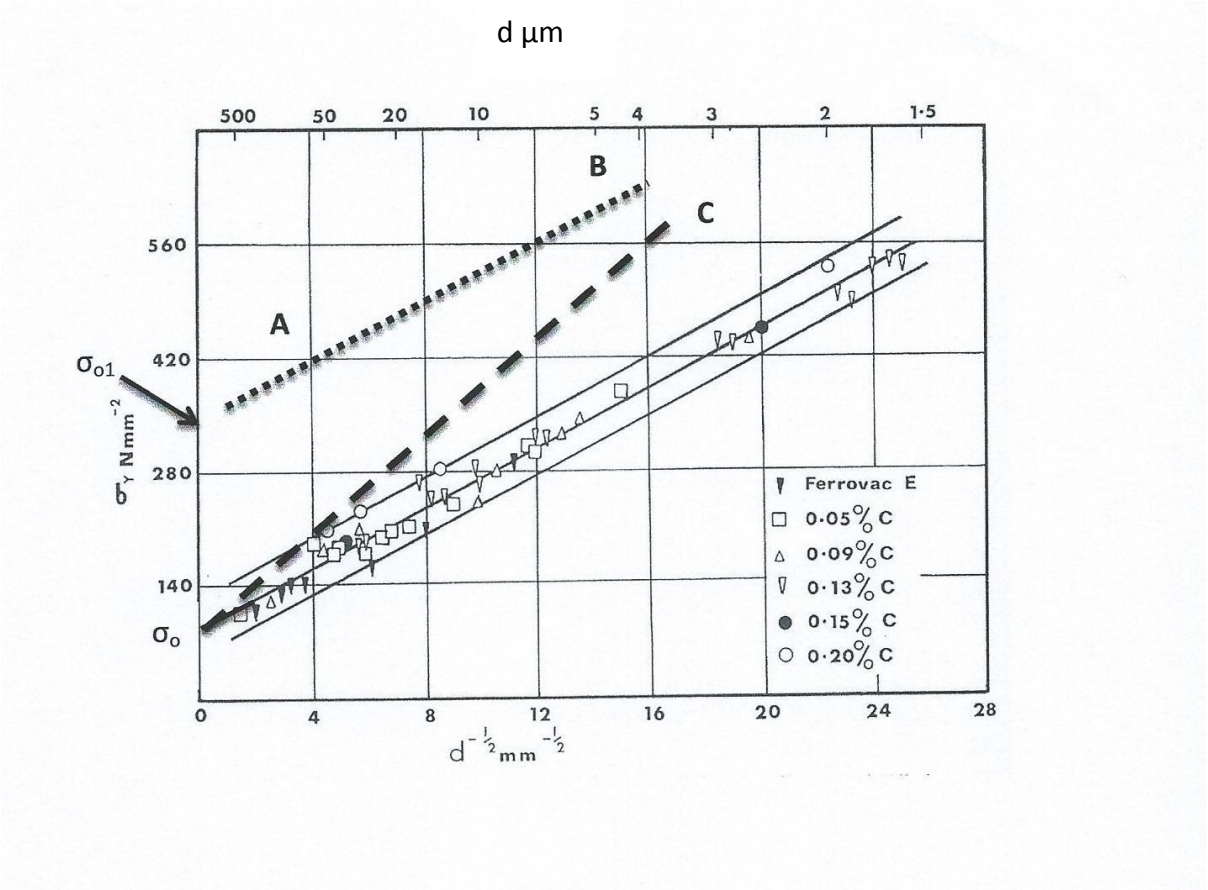

Figure 36 Relationship between lower yield stress, σ_y, and grain size, d, expressed as $d^{-1/2}$for steels containing different carbon levels. The dotted line A-B shows the situation when σ_o is increased to σ_{o1} through a dispersion strengthening component, while the dashed line CD shows the situation when k_y is increased. After Morrison[264]

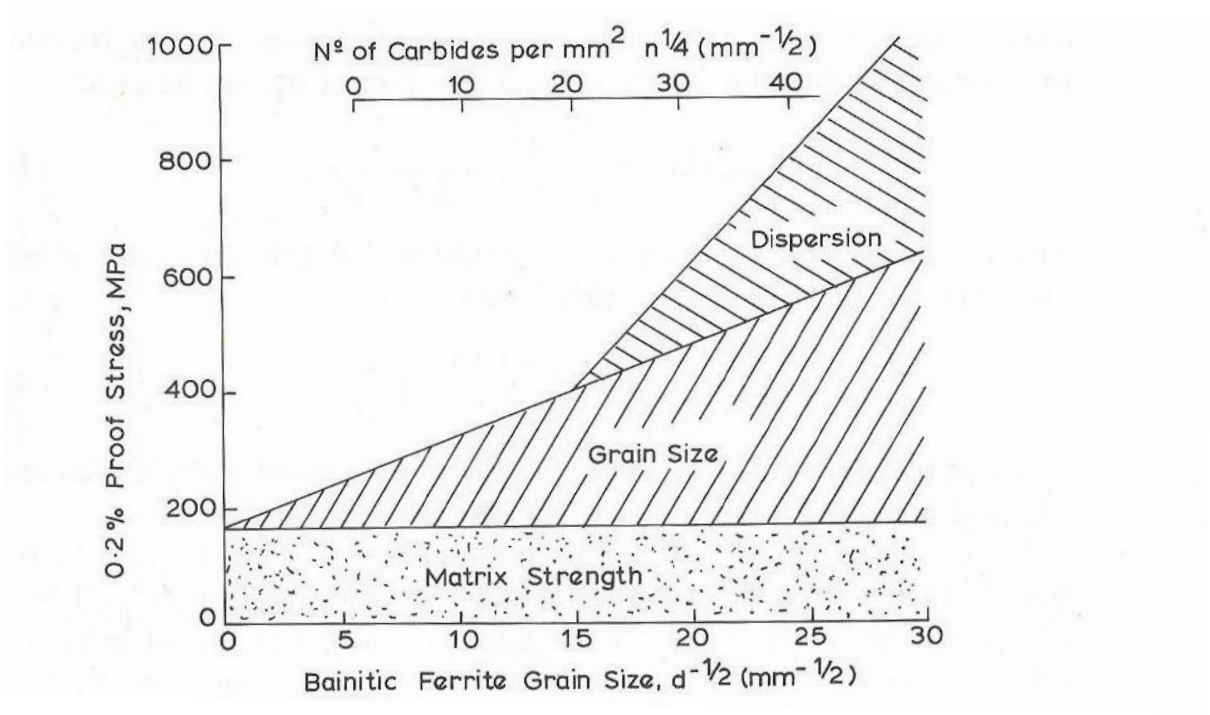

Fig 37 Strengthening effects in low carbon bainite [254]

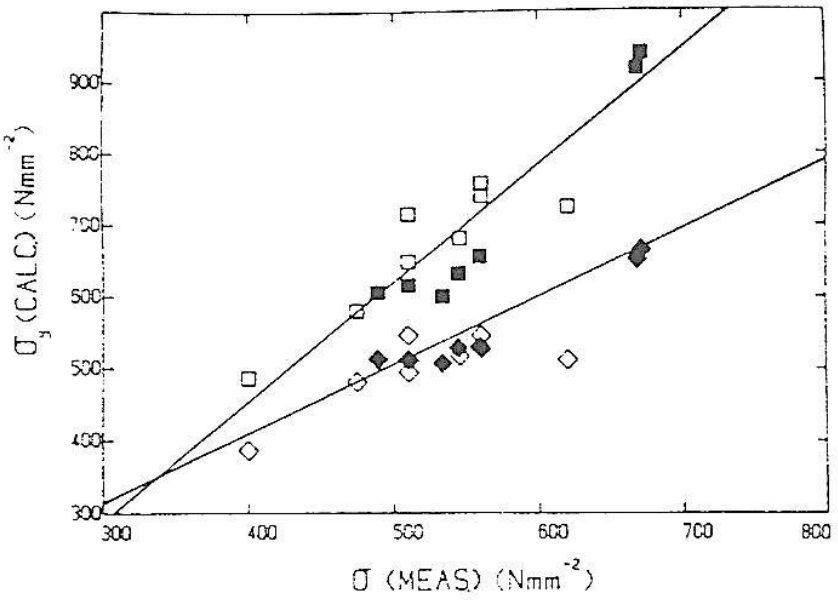

Fig 38 A comparison of measured and calculated yield stress data [2]

♦ σ_L^{114} ■ σ_R^{114} □ σ_L^{256} ◊ σ_R^{256}

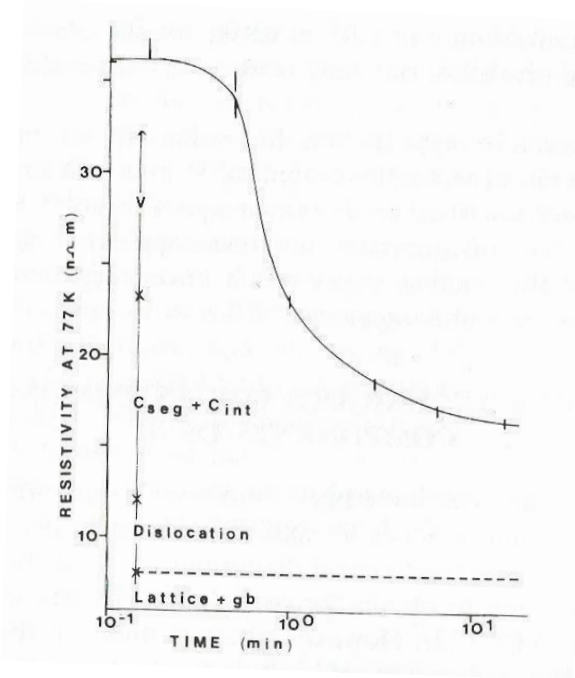

Fig 39 A comparison between the calculated resistivity contributions for an Fe-C-V alloy, totalling 32nΩm, and an experimental value of 36 nΩm.[255]

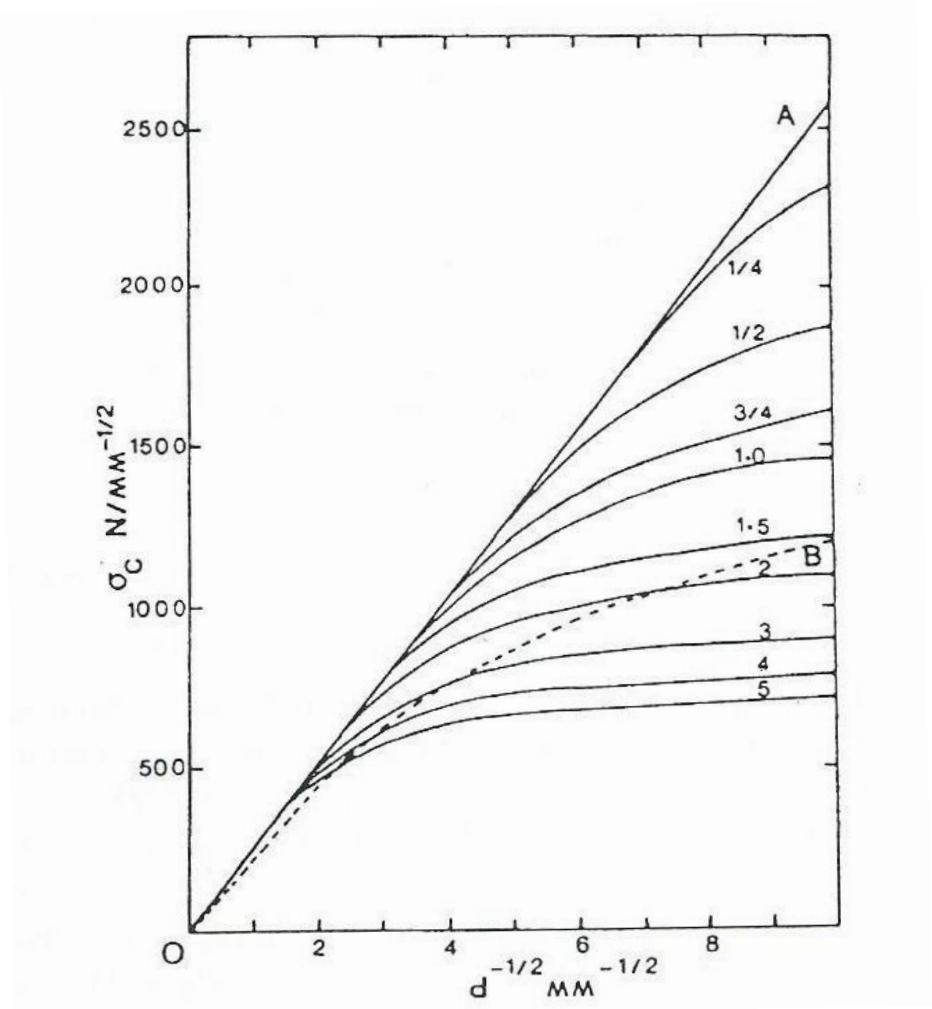

Fig 40 The cleavage strength for fracture at yield, σ_c, versus $d^{-1/2}$ for various carbide thicknesses, t, µm. [323]

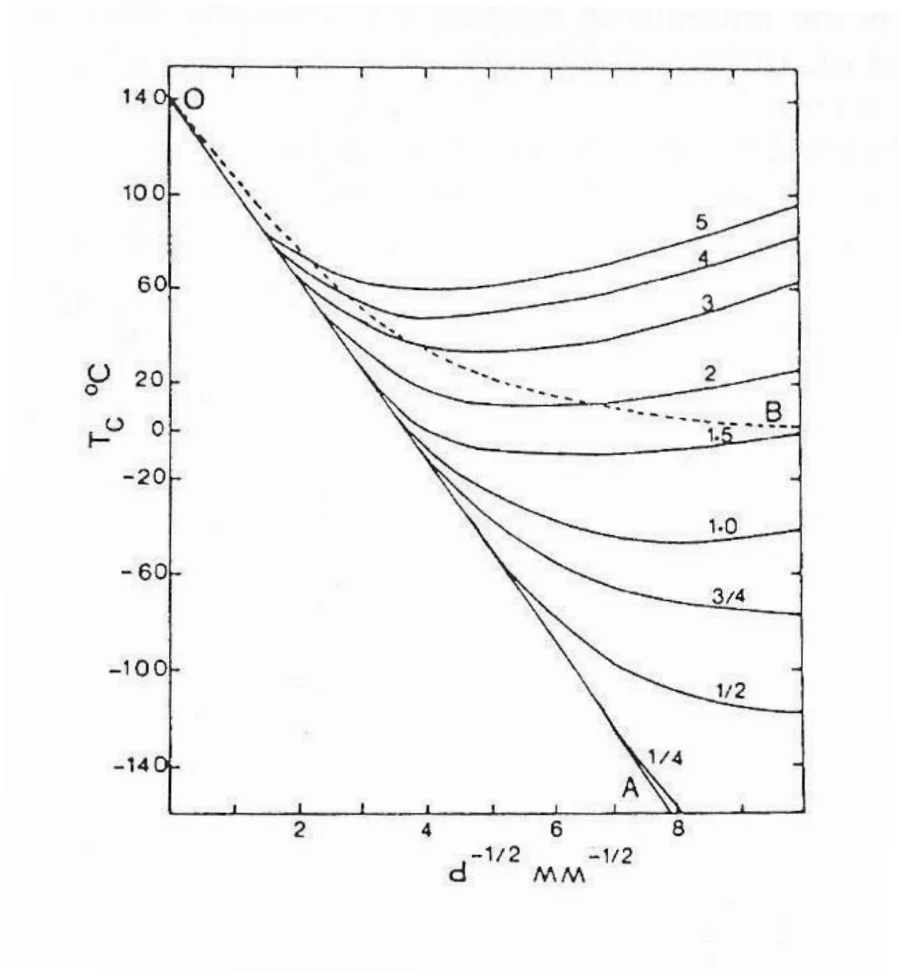

Fig 41 Calculated T_c data for various values of t and $d^{-1/2}$. [323]

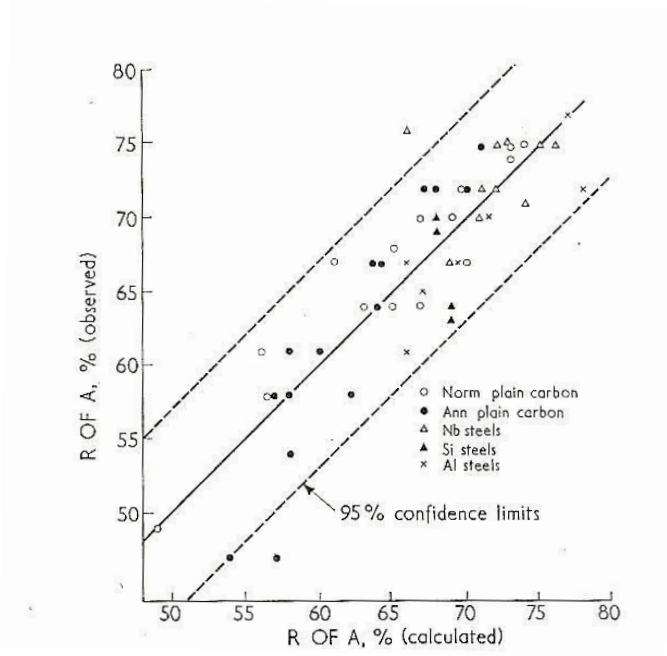

Fig 42 Observed and calculated reduction of area. [252]

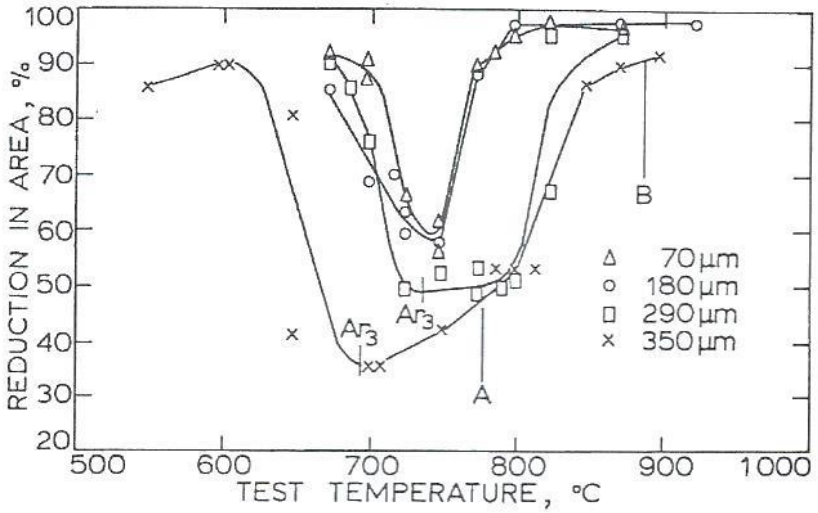

Fig 43 Hot ductility curve for 0.19%C steel with various austenite grain sizes.[331]

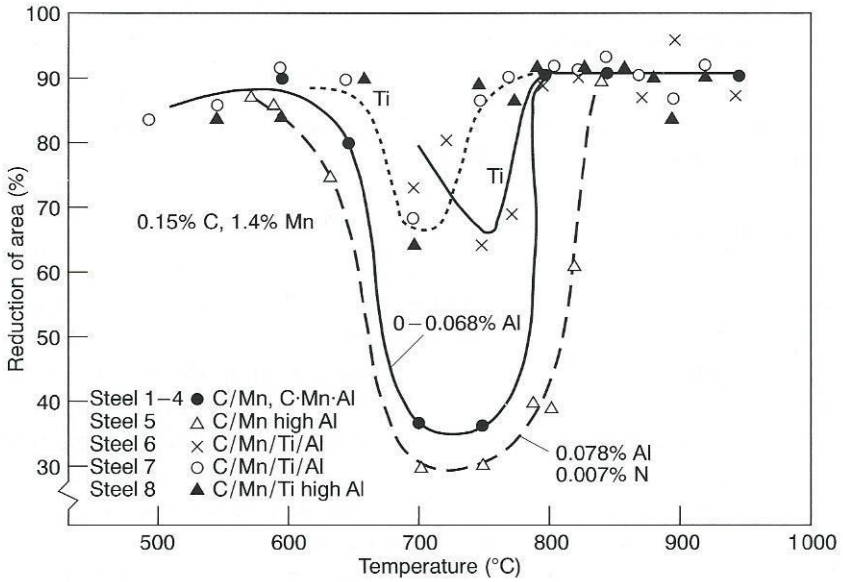

Fig 44 Influence of Al and Ti on the hot ductility of steels, with compositions given in Table 9.[334]